

NOAA Technical Memorandum NOS OMS 5

SYNTHESIS OF CURRENT MEASUREMENTS IN PUGET SOUND,
WASHINGTON - VOLUME 3: CIRCULATION IN PUGET SOUND:
AN INTERPRETATION BASED ON HISTORICAL RECORDS OF
CURRENTS

Curtis C. Ebbesmeyer, Carol A. Coomes,
Jeffrey M. Cox, Jonathan M. Helseth,
and Laurence R. Hinchey
Evans-Hamilton, Inc.
6306 21st Avenue, N.E.
Seattle, Washington 98115

Glenn A. Cannon
Pacific Marine Environmental Laboratory
National Oceanic and Atmospheric Administration
Seattle, Washington 98105

Clifford A. Barnes
Department of Oceanography
University of Washington
Seattle, Washington 98195

Rockville, Md.
May 1984

UNITED STATES
DEPARTMENT OF COMMERCE
Malcolm Baldrige, Secretary

National Oceanic and
Atmospheric Administration
John V. Byrne, Administrator

National Ocean Service
Paul M. Wolff,
Assistant Administrator



Submitted to
National Oceanic and Atmospheric Administration
National Ocean Services
Ocean Assessment Division

by

Evans-Hamilton, Inc.
Seattle, Washington 98115

Pacific Marine Environmental Laboratory, NOAA
Seattle, Washington 98115

Department of Oceanography
University of Washington
Seattle, Washington 98195

DISCLAIMER

The National Oceanic and Atmospheric Administration (NOAA), Evans-Hamilton, Inc., and The University of Washington do not approve, recommend, or endorse any proprietary product or proprietary material mentioned in this publication. No reference shall be made to NOAA or to this publication furnished by NOAA in any advertising or sales promotion which would indicate or imply that NOAA approves, recommends, or endorses any proprietary product or proprietary material mentioned herein, or which has as its purpose an intent to cause directly or indirectly the advertised product to be used or purchased because of this publication.

CONTENTS

| | |
|--|----|
| Tables | v |
| Figures | vi |
| Abbreviations | ix |
| Preface | x |
| | |
| 1. Introduction | 1 |
| 1.1 Project Overview | 1 |
| 1.2 Volume 3 Overview | 5 |
| 2. Methods | 6 |
| 2.1 Field Data | 6 |
| 2.1.1 Currents | 6 |
| 2.1.2 Winds | 6 |
| 2.1.3 Runoff | 6 |
| 2.1.4 Tides | 6 |
| 2.2 Computations | 7 |
| 2.2.1 Estimates of Volume Transport | 7 |
| 2.2.2 Variance at Selected Frequencies | 13 |
| 2.2.3 Multiple Regressions | 14 |
| 2.3 Hydraulic Tidal Model | 14 |
| 3. Variance and Mean Circulation | 15 |
| 3.1 Variance | 15 |
| 3.2 Mixing in Sill Zones | 21 |
| 3.3 Mean Circulation | 23 |
| 3.3.1 Vertical Profiles | 23 |
| 3.3.2 Plan View | 26 |
| 3.3.2.1 Inner Strait of Juan de Fuca | 28 |
| 3.3.2.2 Admiralty Inlet and Whidbey Basin | 31 |
| 3.3.2.3 Puget Sound Main Basin | 31 |
| 3.3.2.4 Southern Basin | 35 |
| 4. Temporal Variability of Transport in the Main Basin | 38 |
| 4.1 Gross Variability of Transport | 38 |
| 4.2 Dependence of Transport on Tide, Wind, and Runoff | 41 |
| 4.3 Seasonal Cycle of Transport | 53 |
| 5. Regional Variations of Transport and Temporal Scales | 56 |
| 5.1 Refluxing in Admiralty Inlet | 56 |
| 5.2 Temporal Scales of Circulation and Water Parcels | 62 |

| | |
|---|----|
| 6. Conclusions | 67 |
| 6.1 Mean Current Patterns | 67 |
| 6.2 Variance | 67 |
| 6.3 Temporal Variability in the Main Basin | 67 |
| 6.4 Variations of Transport and Time Scales | |
| Between Puget Sound's Basins | 68 |
| Acknowledgements | 70 |
| References | 71 |
| Appendix A. Vertical Profiles of Currents and Water | |
| Properties in the Following Areas | 74 |
| 1. Outer Strait of Juan de Fuca | 77 |
| 2. Rosario Strait | 78 |
| 3. West of Whidbey Island | 79 |
| 4. Admiralty Inlet | 80 |
| 5. Central Main Basin | 81 |
| 6. Northern East Passage | 82 |
| 7. Southern East Passage | 83 |
| 8. Dalco Passage | 84 |
| 9. Colvos Passage | 85 |
| 10. Rich Passage | 86 |
| 11. Agate Passage | 87 |
| 12. The Narrows | 88 |
| 13. Narrows-Nisqually Basin | 89 |
| 14. Balch Passage | 90 |
| 15. Nisqually Reach | 91 |
| 16. Nisqually-Dana Passage | 92 |
| 17. Dana Passage | 93 |
| 18. Deception Pass | 94 |
| 19. Saratoga Passage | 95 |
| 20. Port Susan | 96 |
| 21. Northern Hood Canal | 97 |
| 22. Southern Hood Canal | 98 |
| 23. Dabob Bay | 99 |

TABLES

| <u>Number</u> | | <u>Page</u> |
|---------------|---|-------------|
| 2.1 | Volume transport estimated for the upper and lower layers using data obtained across-channel at four sections in Puget Sound | 8 |
| 2.2 | Mean, median, and standard deviation of transport within 2 cm s ⁻¹ speed intervals of U ₁₀₀ in the Main Basin's lower layer | 13 |
| 3.1 | Codes designating selected sills and basins | 16 |
| 4.1 | Characteristics of the records of U ₁₀₀ | 40 |
| 4.2 | Variance of the current U ₁₀₀ within selected ranges of period | 41 |
| 4.3 | Mean, standard deviation, maximum and minimum of SETR within months during September 1975-August 1976 | 46 |
| 4.4 | Coefficients computed from the three multiple regressions | 46 |
| 4.5 | Mean, standard deviation, and variance of the observed transport and the terms in eq. (6) computed from 211 daily values during 17 September 1975-14 April 1976 | 50 |
| 4.6 | Seasonal cycle of transport estimated using eq. (6) | 55 |
| 5.1 | Estimates of volume transport at fourteen cross sections in Puget Sound | 57 |
| 5.2 | Temporal scales of the circulation in Puget Sound's basins | 63 |
| 5.3 | Monthly progression of the Main Basin's temporal scale | 63 |

FIGURES

| <u>Number</u> | | <u>Page</u> |
|---------------|---|-------------|
| 1.1 | Inland marine waters of northwestern Washington and Canada | 2 |
| 1.2 | Puget Sound and approaches | 3 |
| 2.1 | Schematic tidal cycle at Seattle showing minor and major ebb tide ranges | 7 |
| 2.2 | Sections where transport has been estimated in Puget Sound | 9 |
| 2.3 | Contours of net along-channel speed at four sections in Puget Sound | 10 |
| 2.4 | Transport (T_m) versus speed (U_{100}) in the Main Basin's lower layer | 12 |
| 3.1 | Plan view of Puget Sound and approaches showing locations of sills and basins | 17 |
| 3.2A | Variance and profile view of mid-channel depth along the major branch of Puget Sound | 18 |
| 3.2B | Variance and profile view of mid-channel depth along the branch connecting Admiralty Inlet and Whidbey Basin | 19 |
| 3.2C | Variance and profile view of mid-channel depth along the branch connecting Admiralty Inlet and Hood Canal | 20 |
| 3.3 | Time-series of salinity at selected depths illustrating vigorous tidal mixing in Deception Pass and Admiralty Inlet | 22 |
| 3.4 | Profiles of temperature, dissolved oxygen, salinity, and density made at discrete depths at two sites in and near The Narrows toward the end of a flood tide | 24 |

| <u>Number</u> | | <u>Page</u> |
|---------------|---|-------------|
| 3.5 | Representative cross-sectional areas in the three most energetic regions of Puget Sound: Admiralty Inlet, The Narrows, and Deception Pass | 25 |
| 3.6 | Contrast of the vertical profiles of net current speed in the outer Strait of Juan de Fuca, Puget Sound Main Basin, and Whidbey Basin | 27 |
| 3.7 | Plan view of net circulation in the upper layer of the inner Strait of Juan de Fuca | 29 |
| 3.8 | Perspective view of the bathymetry in the inner Strait of Juan de Fuca | 32 |
| 3.9 | Plan view of net circulation in the upper layer of Admiralty Inlet and Whidbey Basin | 33 |
| 3.10 | Plan view of net circulation in the upper layer of the Main Basin | 34 |
| 3.11 | Plan view of net circulation in the upper layer of selected regions of the Southern Basin | 36 |
| 4.1 | Histogram of current speed (U_{100}) in the Main Basin's lower layer | 39 |
| 4.2 | Current speed in Colvos Passage and Seattle tides at section 7 | 43 |
| 4.3 | Volume transport (T_m -type) in Colvos Passage at section 7 versus the summed tide range (SETR) at Seattle computed for the period 25 February-25 March 1977 | 44 |
| 4.4 | Volume above mean-lower-low water of the Southern Basin versus Seattle tide | 45 |
| 4.5 | Daily values of: net wind speed at West Point, net current in the depth range of 103-113 m at site 146, summed ebb tide range from tides observed at Seattle, and total runoff into Puget Sound | 48 |

| <u>Number</u> | | <u>Page</u> |
|---------------|---|-------------|
| 4.6 | Current speed near 100 m depth (U_{100}) in the Main Basin's lower layer versus the sum of the ebb tide range (SETR) at Seattle | 49 |
| 4.7 | Daily estimates of transport from eq. (6) compared with transport (T_m -type) observed in the Main Basin's lower layer | 52 |
| 4.8 | Monthly progression of transport | 54 |
| 5.1 | Sections where transport has been estimated in Puget Sound | 60 |
| 5.2 | Schematic vertical section of transport through Puget Sound's Main Basin | 62 |
| 5.3 | The fraction and location of a water parcel remaining in Puget Sound shown at four month intervals during a hypothetical year | 65 |
| 5.4 | The fraction of a water parcel remaining in Puget Sound during a hypothetical year | 66 |

LIST OF ABBREVIATIONS

ABBREVIATIONS

| | |
|-----------|---|
| °C | -- degrees Celsius |
| cm | -- centimeter |
| CTD | -- Conductivity-Temperature-Depth |
| km | -- kilometer |
| m | -- meter |
| MESA | -- Marine Ecosystems Analysis |
| NOAA | -- National Oceanic and Atmospheric Administration |
| NOS | -- National Ocean Survey |
| OMPA | -- Office of Marine Pollution Assessment |
| PMEL | -- Pacific Marine Environmental Laboratory |
| ‰ | -- salinity in parts per thousand |
| s | -- second |
| SETR | -- sum of the ebb tide ranges |
| | Note: The volume transports described below were computed separately in the upper and lower layers of the estuarine flow, or in some areas only for a single layer. |
| T_a | -- volume transport computed from current observations made across-channel. |
| T_m | -- volume transport equivalent to three-fourths of T_u |
| T_u | -- volume transport computed from currents observed at mid-channel. |
| U_{100} | -- current measured at section 6 near mid-channel in the Main Basin's lower layer in the depth range of 92-116 m. |

PREFACE

Puget Sound is an estuary in northwestern Washington consisting of three branches joined near their mouths to an entrance sill zone. In turn, this zone connects to the Pacific Ocean via the Strait of Juan de Fuca. The branches consist largely of basins embraced by sill zones; the largest or Main Basin accounts for half of Puget Sound's volume and the other half occurs mostly in three secondary basins. The estuarine flow is strongly modified by vertical mixing of surface and deep water over the sills as the water moves between the basins. As a result, the major portion of the surface flow is mixed downward and returned inland before exiting Puget Sound. This downwelling has raised concerns that primary fractions of municipal and industrial wastes are also refluxed inland and may be retained in the fjord complex for considerable periods.

To describe the characteristics of the circulation in Puget Sound, a synthesis of historical measurements of currents, water properties, and meteorological conditions has been undertaken. The results of this project are presented in three volumes:

- Volume 1. Index to current measurements made in Puget Sound from 1908-1980, with daily and record averages for selected measurements.
- Volume 2. Indices of mass and energy inputs into Puget Sound: runoff, air temperature, wind, and sea level.
- Volume 3. Circulation in Puget Sound: an interpretation based on historical records of currents.

Volume 1 contains the locations and statistics of the recorded currents, and describes the types of equipment used to obtain the data. Volume 2 describes indices of the mass and energy inputs into Puget Sound which influence Puget Sound's water properties and circulation.

This volume (Volume 3) contains an interpretation of the circulation based on the data contained in Volumes 1 and 2. Two aspects have been addressed: regional variability within Puget Sound's basins of mean currents, variance, and volume transport; and the temporal variability within the Main Basin. The mean circulation consists primarily of two-layer flow, but there are sizeable flows which occur as single layers in and between some sill zones. Many of the sill zones are quite energetic (variance of order $10^4 \text{ cm}^2 \text{ s}^{-2}$) compared with the basins. Two of the most energetic sill zones embrace the Main Basin and cause it to have a vigorous, rapid circulation through the year which is modulated largely by wind action.

The Main Basin's volume transport in each layer is an order of magnitude larger, and the temporal scale is sixfold larger, than in the secondary basins. The computations of volume transport show that approximately two-thirds of the Main Basin's upper layer is refluxed downward into its lower layer via the sill zone at its mouth. Because of the refluxing in this and other sill zones, and because of the mismatch of the time scales between the basins, the flushing time for a conservative substance in Puget Sound may be on the order of years.

SYNTHESIS OF CURRENT MEASUREMENTS IN
PUGET SOUND, WASHINGTON

VOLUME 3. CIRCULATION IN PUGET SOUND:
AN INTERPRETATION BASED ON
HISTORICAL RECORDS OF CURRENTS

Jeffrey M. Cox, Curtis C. Ebbesmeyer, Carol A. Coomes, Jonathan M. Helseth,
Laurence R. Hinchey, Glenn A. Cannon, and Clifford A. Barnes

1. INTRODUCTION

1.1 PROJECT OVERVIEW

Puget Sound is an estuary located in northwestern Washington (Fig. 1.1). The population near Puget Sound numbers several million people and a variety of wastes are discharged into the estuary. The dilution and distribution of these wastes is in part controlled by a complex circulation of water in Puget Sound.

In a gross perspective the estuary consists of a central or main basin, three secondary basins, and an entrance sill zone which connects to the Pacific Ocean via the Strait of Juan de Fuca (Fig. 1.2). The central axis is a chain of sills and basins. The prominent features of this chain are a seaward sill zone (Admiralty Inlet), a central basin (Main Basin), a secondary sill zone, and a terminal basin (Southern Basin). Appended to the central axis near its mouth are two other basins. One of these (Hood Canal) has a sill at its mouth; the other (Whidbey Basin) lacks an entrance sill, but contains an outlet to the Strait of Juan de Fuca at its head.

The circulation in the Main Basin is in part controlled by vigorous tidal mixing in the embracing sill zones (Ebbesmeyer and Barnes, 1980). As a consequence some of the water initially moving seaward in the estuary's upper layer is carried to depth within these zones, where it is then returned to the estuary's lower layer moving inland. This partial recycling of surface waters through Puget Sound has increased the concern regarding the fate of wastes discharged into the estuary. A common belief was that most of these wastes were rapidly removed from Puget Sound within the outflow of the upper layer. The recent study by Ebbesmeyer and Barnes (1980) suggests that these wastes will accumulate in the water column to some presently unknown

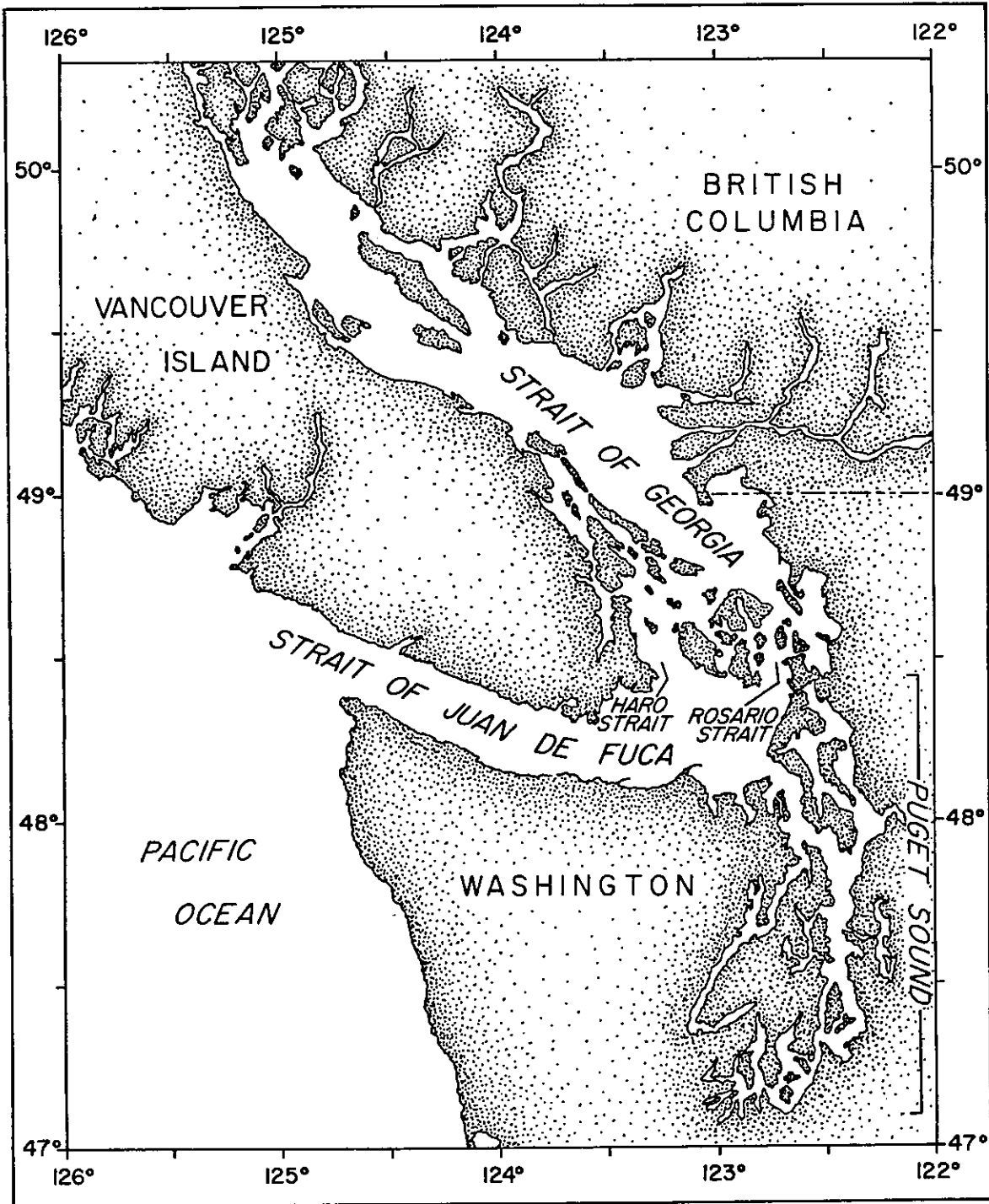


Figure 1.1. Inland marine waters of northwestern Washington and Canada.

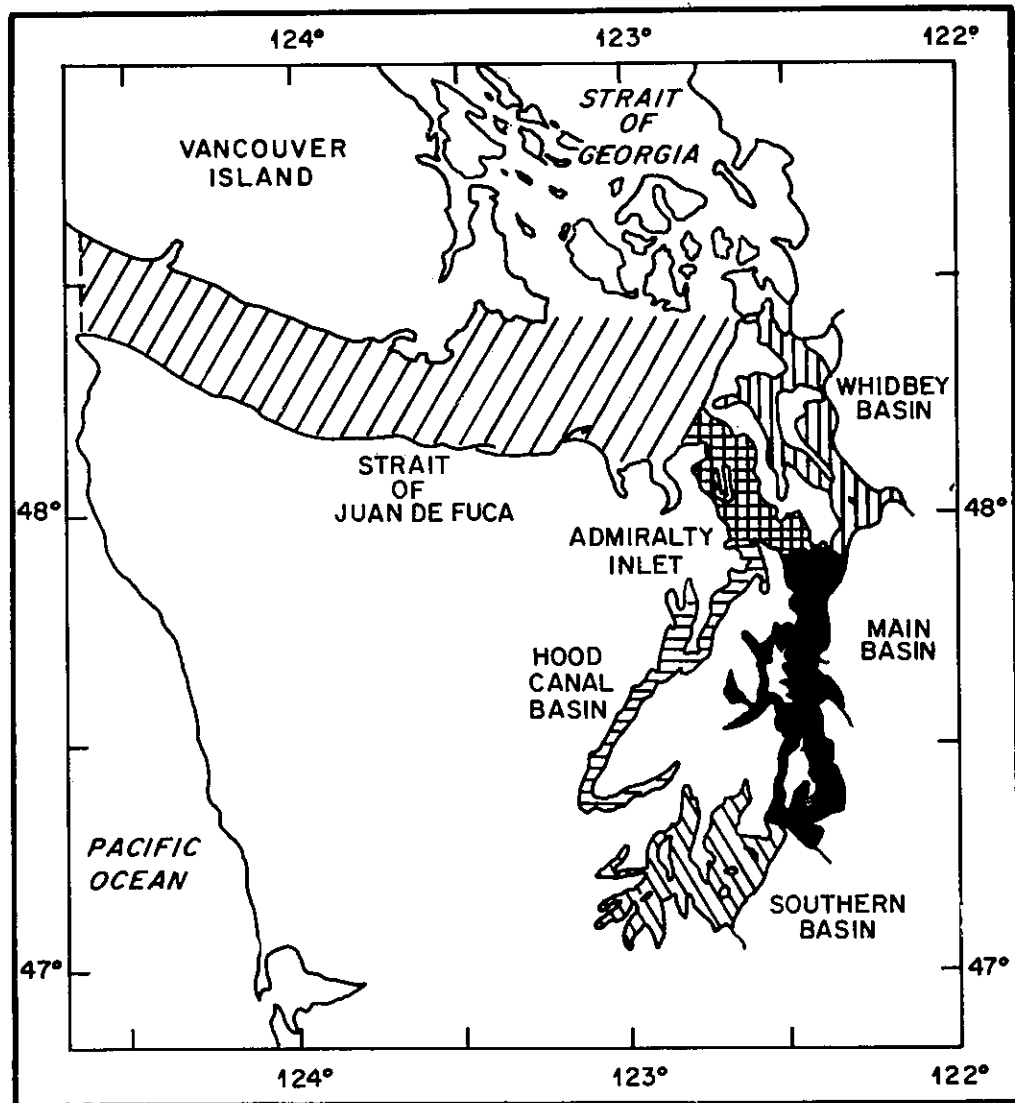


Figure 1.2. Puget Sound and approaches. The Sound consists of the Main Basin (darkened), three secondary basins (Whidbey Basin, Hood Canal Basin, and Southern Basin), and an entrance sill zone (cross-hatched) which are attached to the ocean via the Strait of Juan de Fuca.

background concentration depending upon the rate of their input to the estuary, and the rate of their removal by the combined effects of: escape to the Strait of Juan de Fuca; chemical and biological decomposition; and settling to the bottom.

To predict the background concentration of the wastes for particular rates of discharge, one needs to know the composition of the waste, its settling characteristics, and its biological and chemical removal rates. For some wastes these rates may be small compared to those associated with the physical removal of the waste from the estuary by circulatory features. Hence, an accurate estimate of the amount of surface water (and its waste content) recycled through the estuary is a primary concern.

For the Main Basin, a rough estimate of the recycled fraction is currently available; estimates for the secondary basins remain undetermined. Based upon hydrographic data taken from 1932-1975, Ebbesmeyer and Barnes (1980) estimated that approximately two-thirds of the surface water flowing seaward in Admiralty Inlet was mixed downward and returned landward within the Main Basin's lower layer.

To further describe this circulation, we have undertaken a synthesis of water property, current, and related measurements (runoff, air temperature, wind, and sea level) taken in and around Puget Sound. Observations of the water's physical characteristics (temperature, salinity, and nutrients) have been sampled at many locations and times since the 1930's. These data have been indexed by Collias (1970) and presented in atlas form by Collias, McGary and Barnes (1974). These data have also been combined and interpreted in order to deduce the quantities and patterns of water movement (Friebertshauser and Duxbury, 1972; Barnes and Ebbesmeyer, 1978; and Ebbesmeyer and Barnes, 1980).

Currents have been measured at various times and locations in Puget Sound since 1908, and although many observations were available, no systematic exploration of the various observations had been undertaken to complement the analysis of water properties. An analysis had not previously been performed because of the formidable amount of data, and because the data had been stored in various forms in scattered locations.

Specific objectives of the present synthesis are: 1) estimate the portion of surface water that is refluxed into Puget Sound; 2) examine the response of currents to inputs of mass and energy; and 3) describe seasonal variations of the circulation.

The data gathered for this project and the results of the synthesis have been organized into three volumes as follows:

- Volume 1. Index to current measurements made in Puget Sound from 1908-1980, with daily and record averages computed for selected measurements.
- Volume 2. Indices of mass and energy inputs into Puget Sound: runoff, air temperature, wind, and sea level.
- Volume 3. Circulation in Puget Sound: an interpretation based on historical records of currents and water properties.

Volume 1 contains an index to current measurements made in Puget Sound from 1908-1980. Daily and record averages and standard deviations of net currents, and water properties where available, are presented for measurements spanning at least one tidal day (approximately 25 hours).

Volume 2 provides daily and monthly averages of runoff, air temperature, wind, and sea level.

Volume 3 describes selected aspects of Puget Sound's general circulation, but also examines the variability within the Main Basin.

This study was initiated by the Marine Ecosystems Analysis (MESA) Puget Sound Project within the Office of Marine Pollution Assessment (OMPA) of the National Oceanic and Atmospheric Administration (NOAA). The MESA Puget Sound Project was established to focus scientific research on environmental problems relating to Puget Sound. The primary objective of the Project is to document the occurrence and fluxes of contaminants of special concern, the dynamic processes influencing their physical and chemical transport and fate, and their biological and ecological effects.

1.2 VOLUME 3 OVERVIEW

This volume contains an interpretation of the circulation within Puget Sound utilizing the data presented in Volumes 1 and 2. The data base which we have accumulated is large and also heterogeneous in space and time. Despite the varied texture of the data base, two general aspects have been addressed.

First, we examined regional patterns neglecting the temporal variability. Composite vertical profiles of the mean current and variance were compiled from the records obtained in 23 areas of Puget Sound. These areas cover much of Puget Sound and contain sufficient data to reveal marked regional contrasts. At some cross sections of Puget Sound there was sufficient data to examine the cross-channel variability.

Second, we examined temporal variability in the Main Basin. Many current observations have been made at one location in the Main Basin's lower layer. These observations were used to deduce the effects of tide, wind, and runoff on the net circulation.

2. METHODS

Field observations of currents, winds, runoff, tides, and water properties were collected from a variety of sources and have been described in Volumes 1 and 2. The analysis of these data using various computational techniques is described herein.

2.1 FIELD DATA

2.1.1 Currents

Measurements were made at numerous sites throughout Puget Sound during 1908 to 1980 using different kinds of equipment, primarily Aanderaa type current meters (see descriptions in Volume 1 by Cox et al., 1983). Unless stated otherwise the data utilized herein consist of net currents computed over a tidal day (called daily averages) and over an entire record as reported by Cox et al. (1983).

Generally, the current flows consist of two layers, the upper layer moving out of the fjord-complex, and the lower layer flowing inland. For clarity, the out-estuary or seaward direction has been denoted in this report by solid arrows and the in-estuary or inland direction by dashed arrows.

2.1.2 Winds

Daily (24 hours) and monthly wind speed and direction obtained at West Point during 1969-1978 are as given in Volume 2 by Coomes et al. (1983). Arrows used to denote the direction of the winds correspond to those used for current direction.

2.1.3 Runoff

The average total runoff entering Puget Sound was tabulated by Coomes et al. (1983) for individual months for the period 1930-1968 and individual days (24 hours) during 1969-1978.

2.1.4 Tides

Tidal observations as measured at Seattle and values of high and low waters were tabulated in Volume 2 by Coomes et al. (1983). As will be seen later the range of the ebb tides between the high and low waters can be used to estimate volume transport in the Main Basin. Figure 2.1 shows a tidal cycle, where R_1 and R_2 denote the ranges of the minor and major

ebb tide ranges, respectively. The sum of the ebb tide ranges (SETR) is defined as $R_1 + R_2$. Values of SETR were computed from the observed tides and assigned to the calendar day which most nearly coincided with the duration of the two ranges.

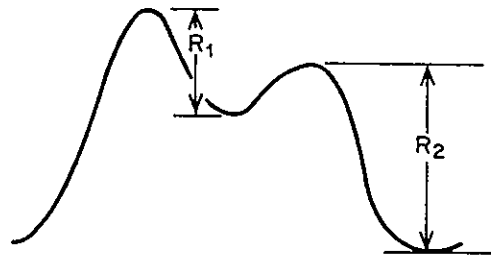


Figure 2.1. Schematic tidal cycle at Seattle showing minor (R_1) and major (R_2) ebb tide ranges.

2.2 COMPUTATIONS

2.2.1 Estimates of Volume Transport

The flow of water at various locations in Puget Sound has previously been characterized by volume transport computed separately for the upper and lower layers (Barnes and Ebbesmeyer, 1978; Cannon and Ebbesmeyer, 1978; Ebbesmeyer and Barnes, 1980; and Cannon, 1983). Herein transport was estimated using one or a combination of three methods: (1) from observations made across-channel; (2) from vertical profiles made at mid-channel; and (3) from observations made at a single depth in the Main Basin's lower layer.

Transport estimated from observations made across-channel were computed as follows. First, the cross-sectional area was divided into small rectangles and an along-channel current speed was assigned by extrapolating and/or interpolating the available observations to the center of each rectangle. Second, transport was found for each rectangle by multiplying

the area times the estimated speed. Third, transport (T_a) was computed separately in the upper and lower layers by summing the incremental values where the speeds were directed out of, or into the estuary, respectively.

Current observations have been made along four transects in Puget Sound where T_a -type transport may be estimated (Fig. 2.2): in Admiralty Inlet, sections 2, 3, and 4; and in the Main Basin section 6. Figure 2.3 shows contours of current speed and Table 2.1 shows the transport computed for the upper and lower layers across the four sections. Table 2.1 indicates that the lower-layer transport systematically exceeds upper-layer transport by approximately 20%. On the average the upper- and lower-layer transport must balance^a to maintain a constant water level. The difference indicates a systematic bias between the two layers which may be explained in part as follows. The shallowest observations of currents were obtained between depths of 5-10 meters. However the estuarine speeds are usually highest close to or at the water surface. The speeds near the surface are probably underestimated, and as a result the upper-layer transport probably also has been underestimated.

TABLE 2.1. VOLUME TRANSPORTS ESTIMATED FOR THE UPPER AND LOWER LAYERS USING DATA OBTAINED ACROSS-CHANNEL AT FOUR SECTIONS IN PUGET SOUND (SEE FIG. 2.2).

| Section | Volume Transport (T_a ; $10^4 \text{ m}^3 \text{ s}^{-1}$) | | | |
|-----------------|--|-------------|------------------------|------|
| | upper layer | lower layer | Difference upper-lower | Mean |
| Admiralty Inlet | | | | |
| 2 | 1.2 | 1.5 | 0.3 | 1.3 |
| 3 | 2.1 | 2.4 | 0.3 | 2.2 |
| 4 | 1.1 | 1.3 | 0.2 | 1.2 |
| Main Basin | | | | |
| 6 | 2.0 | 2.2 | 0.2 | 2.1 |

^aExcept for the amount of freshwater being transported seaward which is an order of magnitude smaller than the transport in the upper and lower layers.

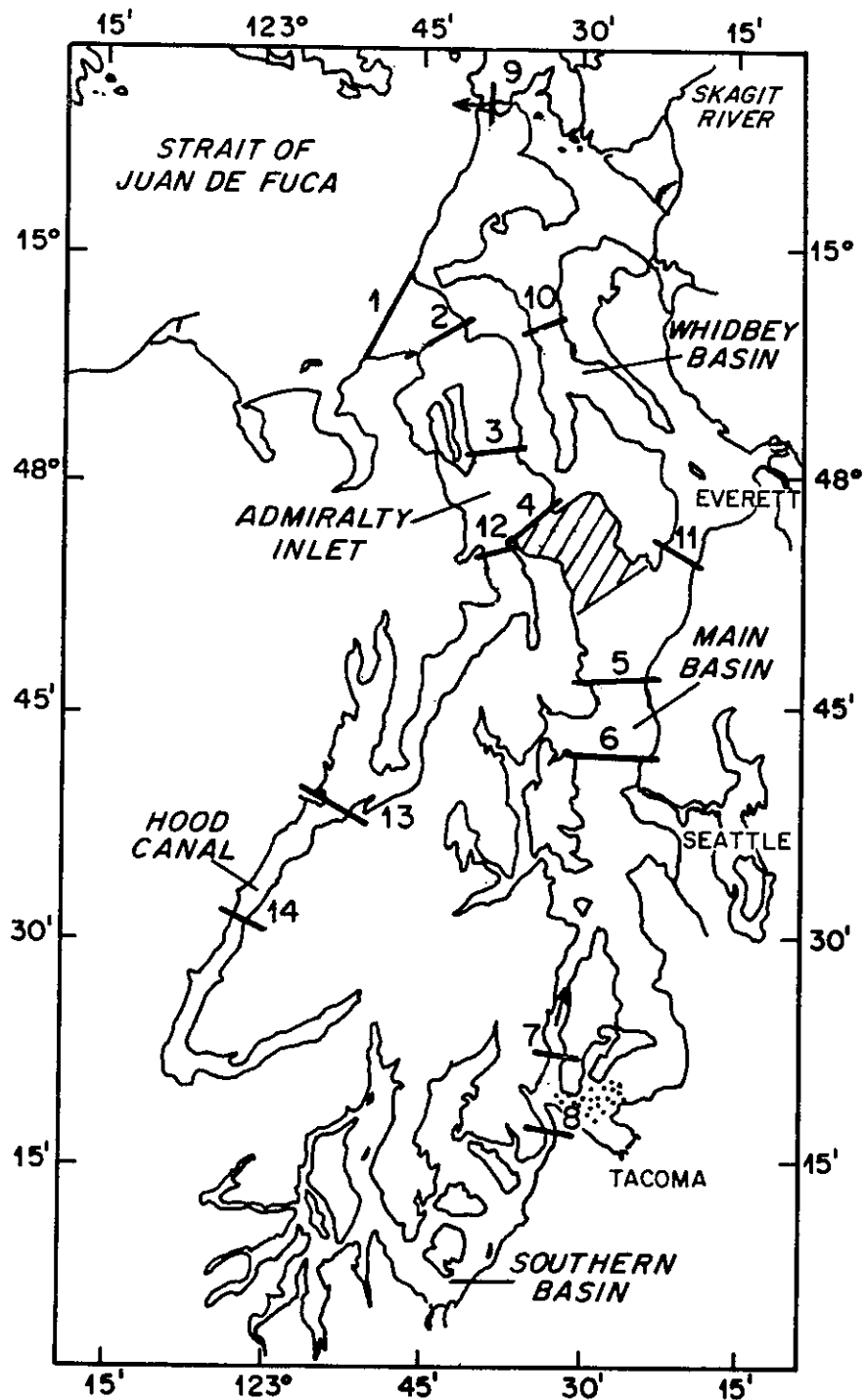


Figure 2.2. Sections (bars) where transport has been estimated in Puget Sound. The number above the bar indicates the section number. The hatched and stippled areas at the northern and southern ends of the Main Basin indicate regions of intense downwelling and upwelling, respectively. See Table 5.1 for data and methods used to estimate the transports.

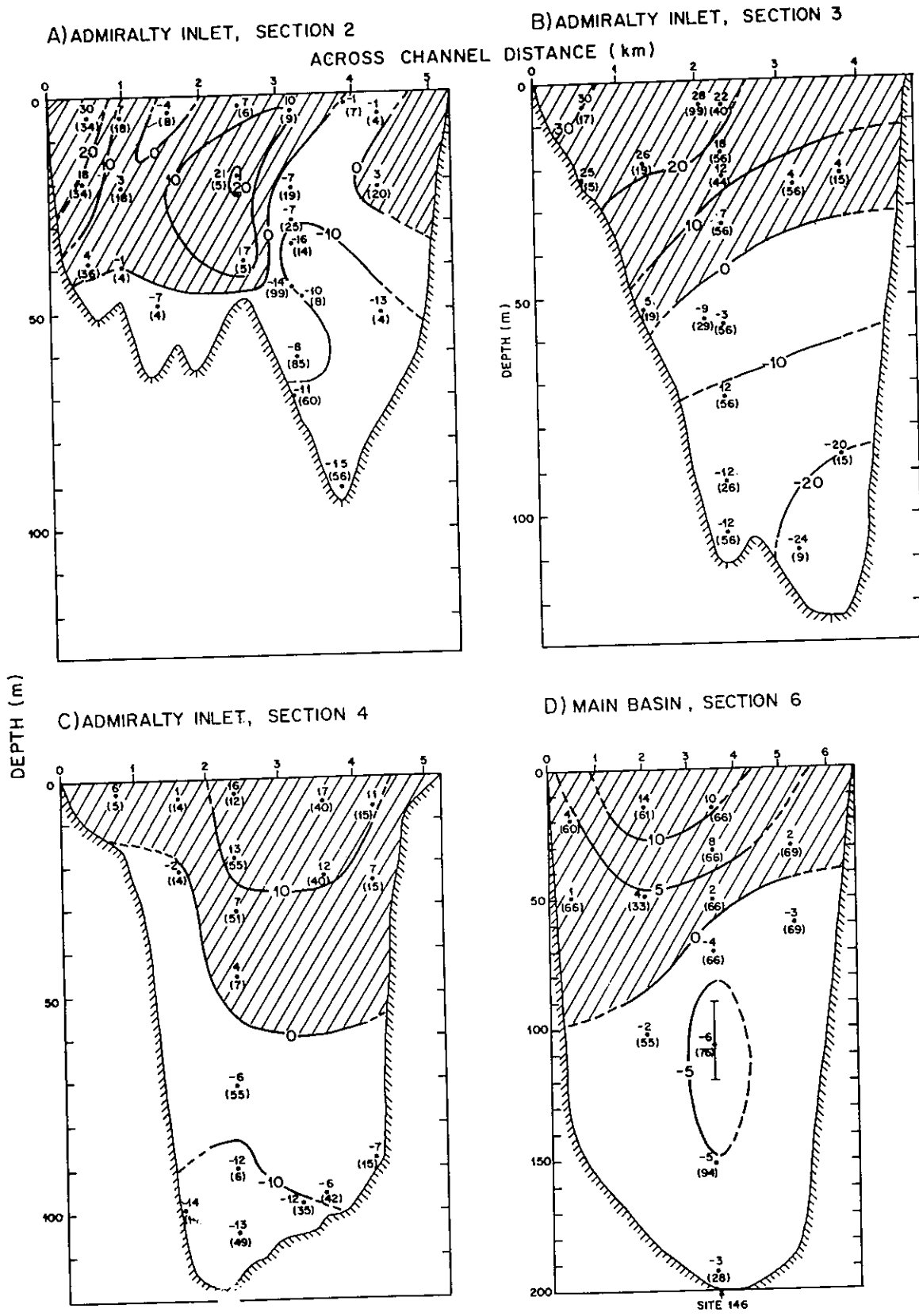


Figure 2.3. Contours of net along-channel current speed at four sections in Puget Sound (Fig. 2.2): Admiralty Inlet, sections 2 (A), 3 (B), and 4 (C); and Main Basin, section 6 (D). Notation: upper layer is denoted by hatching; lower layer is unshaded; dots represent sites of observations where the upper number denotes the net speed (cm s^{-1}) and the lower number in parenthesis indicates the record length (days); and in (D) the vertical bar denotes the depth range of U100 at site 146.

Observations made near mid-channel were used to estimate transport as follows. First, a vertical profile was made of the net along-channel speed. Second, the observed values were interpolated and/or extrapolated to a uniform set of depths. Third, cross-channel areas were determined from hydrographic charts, and incremental areas centered on the selected depths were multiplied by the current speeds to obtain transport in the selected depth ranges. Finally, the transport (T_u) was determined in each layer by summing the increments.

Transport estimates of type T_u usually exceed the actual transport because the mean flow in a channel is lower than the flow at mid-channel. To obtain a relation, transports were estimated at section 6 using T_a - and T_u -type transport estimates. The ratio (T_a/T_u) is 0.77 for both layers; this value is close to 0.74 obtained for nearby section 5 by Barnes and Ebbesmeyer (1978), close to 0.75 estimated by Ebbesmeyer and Barnes (1980) using dissolved oxygen as a tracer, and close to 0.75 reported for flows in other channels (Sverdrup, Johnson, and Fleming, 1942). As a result, the transport estimated from mid-channel observations has been multiplied by 0.75 in the remainder of this report and has been designated as T_m .

Currents often have been measured near 100 m depth at site 146^b near mid-channel along section 6. All totaled, 443 days of current meter record were obtained in the depth range of 90-116 m during 1972-1977. During portions of this period, however, only one or two current meters were deployed in the lower layer with the result that the vertical structure was inadequately resolved. It was useful to determine the extent to which the net current near 100 m depth (U_{100}) can be used alone to estimate the transport in the Main Basin's lower layer.

Figure 2.3D shows the location of U_{100} superimposed on contours of net speed across section 6. This section was constructed from observations made during 15 June-28 September 1976. In the upper layer the highest net speeds lie within a core located near mid-channel. In the lower layer the data are less extensive but indicate highest speeds near a depth of 100 m. The speed near 100 m depth decreases westward from mid-channel; data are lacking to show the speed decreasing eastward. Thus, the long time series of U_{100} occurs within the core of higher speed in the Main Basin's lower layer.

To illustrate the relation, values of U_{100} and T_m -type transport were compared for 216 individual days (Fig. 2.4). The magnitude of the vector U_{100} were used and reckoned positive if the direction lay within $\pm 90^\circ$ of the mean out-estuary direction (56° True). To find a systematic relation, transport values were placed within speed intervals of 2 cm s^{-1} and the median and standard deviation were computed within each group (Table 2.2). The median was used because of the skewness evident at lower speeds (see Fig. 2.4). Despite the simplicity of this approach it is evident that transport in the lower layer is, on the average, a linear function of U_{100} .

A linear regression of the median values of T_m and U_{100} in Table 2.2 gave the following relation

^bSite numbers for current meter records were assigned in Volume 1 by Cox et al. (1983).

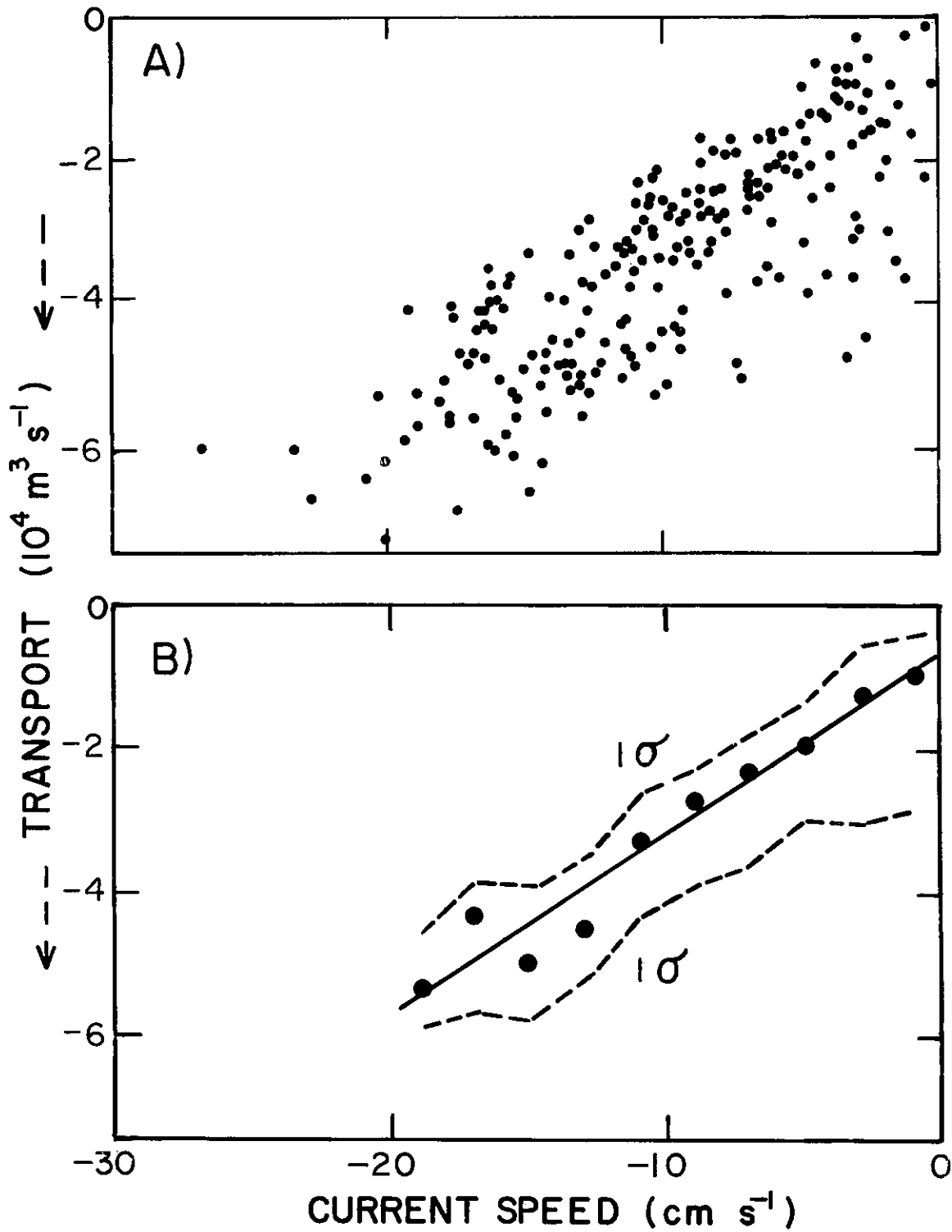


Figure 2.4. Transport (T_m) versus current speed (U_{100}) in the Main Basin's lower layer. Upper panel (A) shows values computed from daily net currents. Lower panel (B) computed from values in (A), shows median values (dots) and one standard deviation limits (dashed lines) about mean values within 2 cm s^{-1} speed intervals. Straight line is least-squares-best-fit to the median values.

$$T_m = (-0.7 + 0.26 U_{100}) 10^4 \text{ m}^3 \text{ s}^{-1}, \quad (1)$$

where U_{100} is expressed in units of cm s^{-1} . Some estimates of the uncertainty of eq. (1) can be obtained by inspection of Table 2.2. The standard deviation of the daily transports averages $0.9 \times 10^4 \text{ m}^3 \text{ s}^{-1}$ for all of the speed groups. In contrast, the estimates of transport for the upper and lower layers differ by an average of $0.3 \times 10^4 \text{ m}^3 \text{ s}^{-1}$ (Table 2.1). The sizeable uncertainty of the transport can be attributed in large part to the variability of the vertical structure on daily scales as illustrated by Cannon and Laird (1978). However, if transport is averaged over a number of days, the uncertainty decreases. Assuming that the t-statistic is applicable, then the uncertainty at the 5% level is approximately $0.3 \times 10^4 \text{ m}^3 \text{ s}^{-1}$ for a 30-day sample, or approximately 10% of the mean transport.

TABLE 2.2. MEAN, MEDIAN, AND STANDARD DEVIATION OF TRANSPORT WITHIN 2 CM S^{-1} SPEED INTERVALS OF U_{100} IN THE MAIN BASIN'S LOWER LAYER. TOTAL SAMPLE OF 216 VALUES IS SHOWN IN FIG. 2.4.

| U_{100} Speed interval (cm s^{-1}) | Transport (T_m ; $10^4 \text{ m}^3 \text{ s}^{-1}$) | | | |
|---|---|--------|-------------|--------|
| | mean | median | Std. dev. | sample |
| 0-2 | -1.7 | -1.0 | 1.2 | 10 |
| -2-4 | -1.8 | -1.3 | 1.2 | 25 |
| -4-6 | -2.2 | -2.0 | 0.8 | 24 |
| -6-8 | -2.7 | -2.4 | 0.9 | 26 |
| -8-10 | -3.1 | -2.8 | 0.8 | 32 |
| -10-12 | -3.5 | -3.3 | 0.9 | 32 |
| -12-14 | -4.4 | -4.6 | 0.9 | 22 |
| -14-16 | -4.9 | -5.0 | 0.9 | 21 |
| -16-18 | -4.8 | -4.4 | 0.9 | 19 |
| -18-20 | -5.3 | -5.4 | 0.7 | 5 |
| mean = 0.9 | | | total = 216 | |

2.2.2 Variance at Selected Frequencies

In order to determine the variance at selected frequencies, fast-fourier-transforms were computed for U_{100} . The time series consisted of 256 (0.70 years) values computed daily between 17 September 1975 and 29 May 1976. The variance was summed over all frequencies and the variance at each harmonic determined as a percentage of the total variance.

2.2.3 Multiple Regressions

Multiple regressions were used to find empirical relations between the observations of U_{100} and three variables: tide (i.e., SETR), wind, and runoff. The 1% level of significance of the correlation coefficient (r) was determined from Table A-11 of Snedecor and Cochran (1967).

2.3 HYDRAULIC TIDAL MODEL

The University of Washington's hydraulic tidal model has vertical and horizontal scales of 1:1152 and 1:40,000, respectively. Salinity is regulated by a salt pump apparatus and maintained at 16⁰/oo. Tides are generated by a tide computer which is able to reproduce representative tides of specific time periods or repeating tides. Freshwater is added proportionate to the discharge of major rivers (Barnes et al., 1957) and can be adjusted according to high and low runoff seasons. Wind effects are not represented. Operating characteristics of the model have compared favorably with selected field observations (Rattray and Lincoln, 1955).

3. VARIANCE AND MEAN CIRCULATION

The Strait of Georgia, Strait of Juan de Fuca, and Puget Sound form a dendritic pattern of waterways. A key feature within this system is the location of sills and basins. A differentiation utilizing this feature consists of two classes: (1) basins embraced by sills; and (2) basins with sills at their mouths and shorelines at their heads.

Table 3.1 lists the sills and basins in Puget Sound and its approaches. Figures 3.1 and 3.2 show, in plan and profile views, respectively, the sequence of sills and basins along the three primary branches of the system. The Major branch lies along a line connecting the Strait of Juan de Fuca, the Main Basin, and Southern Basin and consists primarily of basins embraced by sills. The second branch (Whidbey Branch) lies along a line through Admiralty Inlet, Saratoga Passage, and Deception Pass. Finally, the third branch (Hood Canal Branch) lies along a line through Admiralty Inlet and Hood Canal. The basins and sills can be distinguished by the variance of the local fluctuating currents which are superimposed on the mean circulation.

3.1 VARIANCE

The total variance of the oscillating currents has been presented by Cox et al. (1983) for measurements in Puget Sound. The data for the Strait of Juan de Fuca were obtained from various sources both published and unpublished. Appendix A shows total variance versus depth for 23 locations; and Figure 3.2 shows the total variance averaged over the water column at selected locations throughout Puget Sound. It can be seen that the variance over the sills greatly exceeds that in the basins.

Three of the sill zones have large variances of approximately $10^4 \text{ cm}^2 \text{ s}^{-2}$: Admiralty Inlet (S2a); The Narrows (S3); and Deception Pass (S6). A closer inspection shows that the variance over Admiralty Inlet's outer sill ($\sim 1.2 \times 10^4 \text{ cm}^2 \text{ s}^{-2}$) exceeds by a third the variance in both Deception Pass and The Narrows ($\sim 0.9 \times 10^4 \text{ cm}^2 \text{ s}^{-2}$). A distinguishing characteristic of Puget Sound's Main Basin is that it is embraced by two of the three most energetic regions in Puget Sound.

Total variance in the Main Basin averages approximately $0.02 \times 10^4 \text{ cm}^2 \text{ s}^{-2}$, or on the order of twenty- to thirtyfold less than the variance in The Narrows and Admiralty Inlet. These results based upon several hundred current records agree with comparisons of tidal kinetic energy for these same areas presented by Ebbesmeyer and Barnes (1980). They computed kinetic energy associated with average tidal currents using tidal elevations and prisms, and found that the kinetic energy in the embracing sill zones exceeded that in the Main Basin by one to two orders of magnitude.

TABLE 3.1. CODES DESIGNATING SELECTED SILLS AND BASINS (SEE FIGS. 3.1 AND 3.2 FOR LOCATIONS).

1. Sills

| Code | Name | Max. Depth (m) |
|------|--|-------------------|
| S0 | Sill in Juan de Fuca Canyon ¹ | 227 |
| S1 | Victoria-Dungeness | 115 |
| S2a | Admiralty Inlet (outer sill) | 64 |
| S2b | Admiralty Inlet (inner sill) | 106 |
| S3 | The Narrows | 44 |
| S4 | Nisqually Reach | 31 |
| S5 | Dana Passage | 33 |
| S6 | Deception Pass | 11 |
| S7 | Hood Canal | 53 |
| S8 | Dabob Bay | 123 |
| S9 | Port Susan | 97 |

2. Basins

| Code | Name | Embracing Sills | Max. Depth (m) |
|-------------------------------------|---|---------------------|-------------------|
| a. Basins Embraced by Sills | | | |
| B1 | Outer Strait of Juan de Fuca | S0 ^a -S1 | 370 |
| B2 | Inner Strait of Juan de Fuca ² | S1 -S2 | 342 |
| B3 | Puget Sound Main Basin | S2 -S3 | 284 |
| B4 | Narrows-Nisqually Basin | S3 -S4 | 167 |
| B5 | Nisqually-Dana Basin | S4 - S5 | 110 |
| B6 | Whidbey Basin | S2 - S6 | 161 |
| b. Basins with a Single Sill | | | |
| B7 | Hood Canal | S7 | 177 |
| B8 | Dabob Bay | S8 | 187 |
| B9 | Port Susan | S9 | 123 |

¹Sill S0 in the Juan de Fuca Canyon not shown in Figs. 3.1 and 3.2; see Ebbesmeyer and Barnes (1980).

²Embracing sills S1-S2 are shown herein; other embracing sills in Haro and Rosario Straits are not shown.

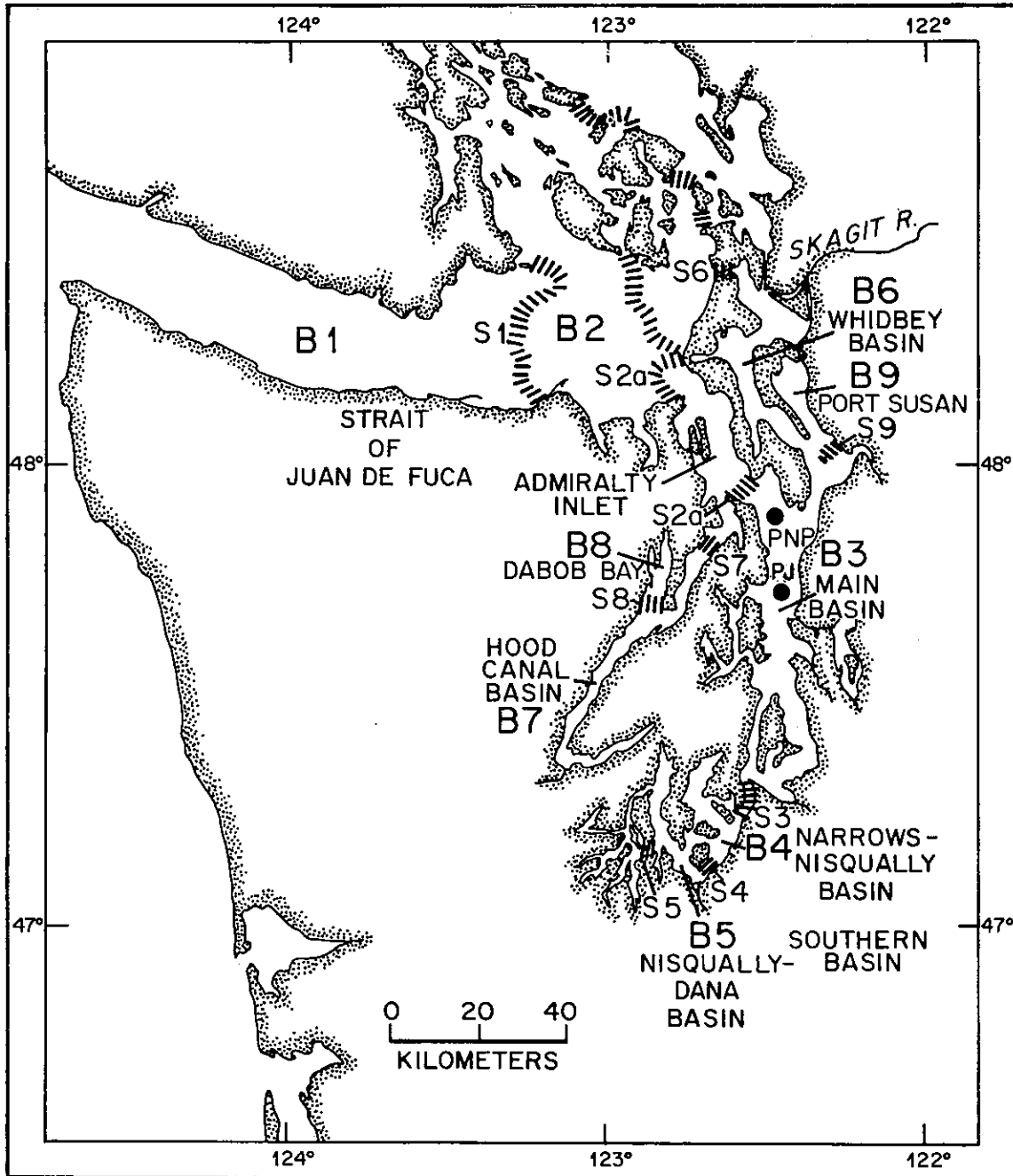


Figure 3.1. Plan view of Puget Sound and approaches showing locations of sills (hatched) and basins. See Table 3.1 for explanation of codes for sills (S1-S9) and basins (B1-B9). The two dots in the Main Basin denote hydrographic stations: PNP, Point No Point; and PJ, Point Jefferson.

A) MAJOR BRANCH

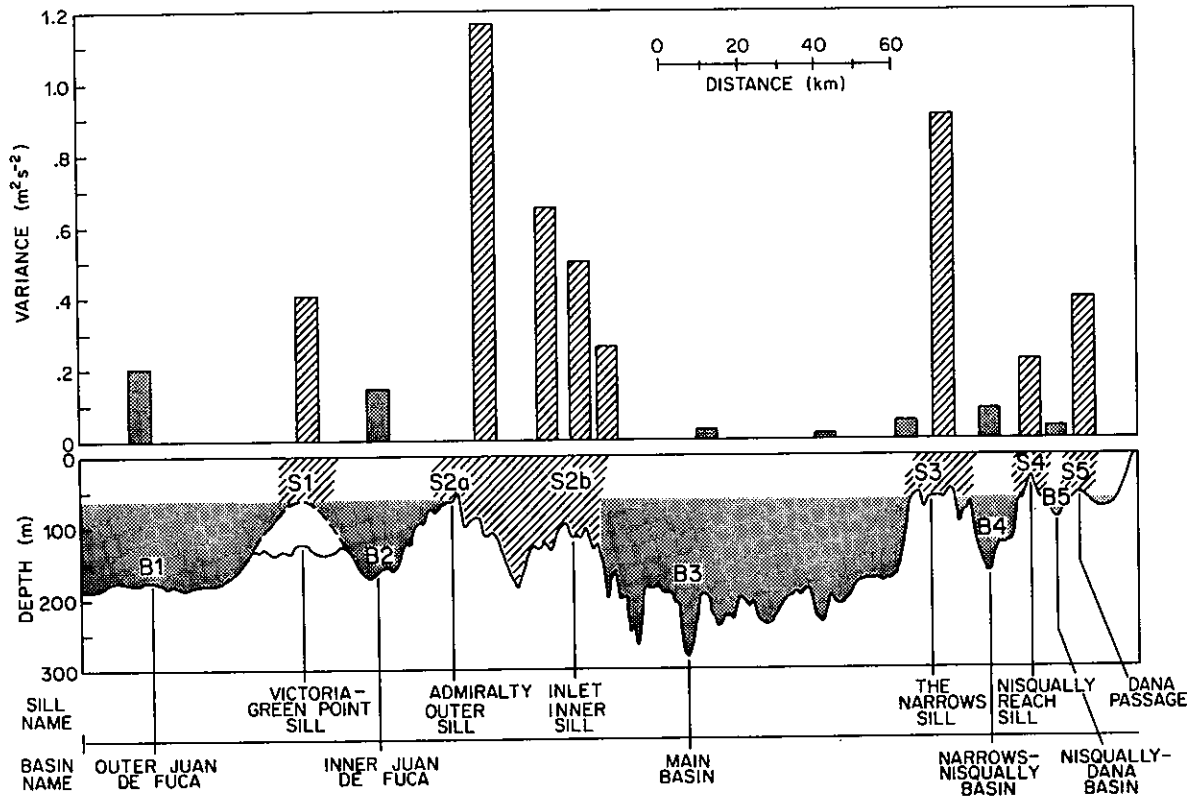


Figure 3.2A. Variance (top) and profile view of mid-channel depth (bottom) along the major branch of Puget Sound. Notation: sills (hatched; S1-S5) and basins (stippled; B1-B5).

B) WHIDBEY BRANCH

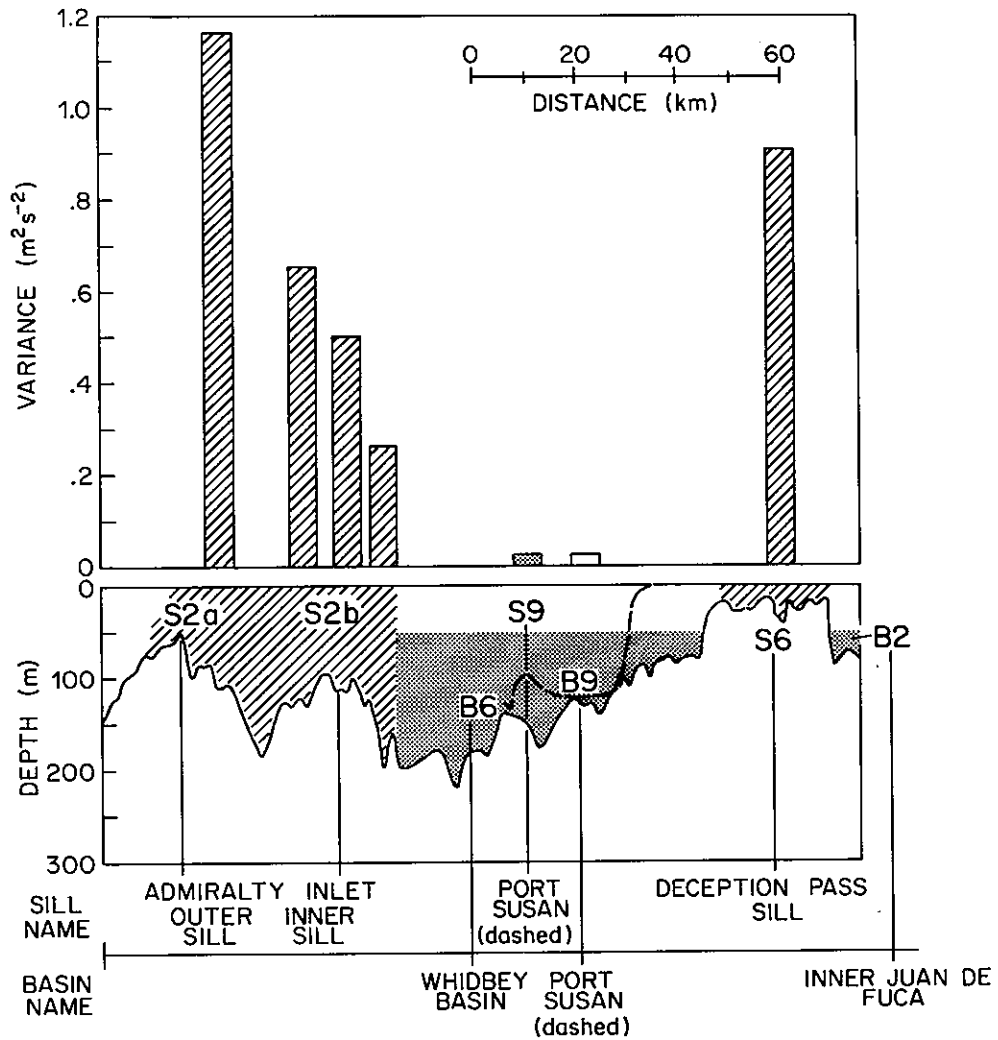


Figure 3.2B. Variance (top) and profile view of mid-channel depth (bottom) along the branch connecting Admiralty Inlet and Whidbey Basin. Notation: sills (hatched; S2 and S6) and basins (stippled; B2, B6, and B9).

C) HOOD CANAL BRANCH

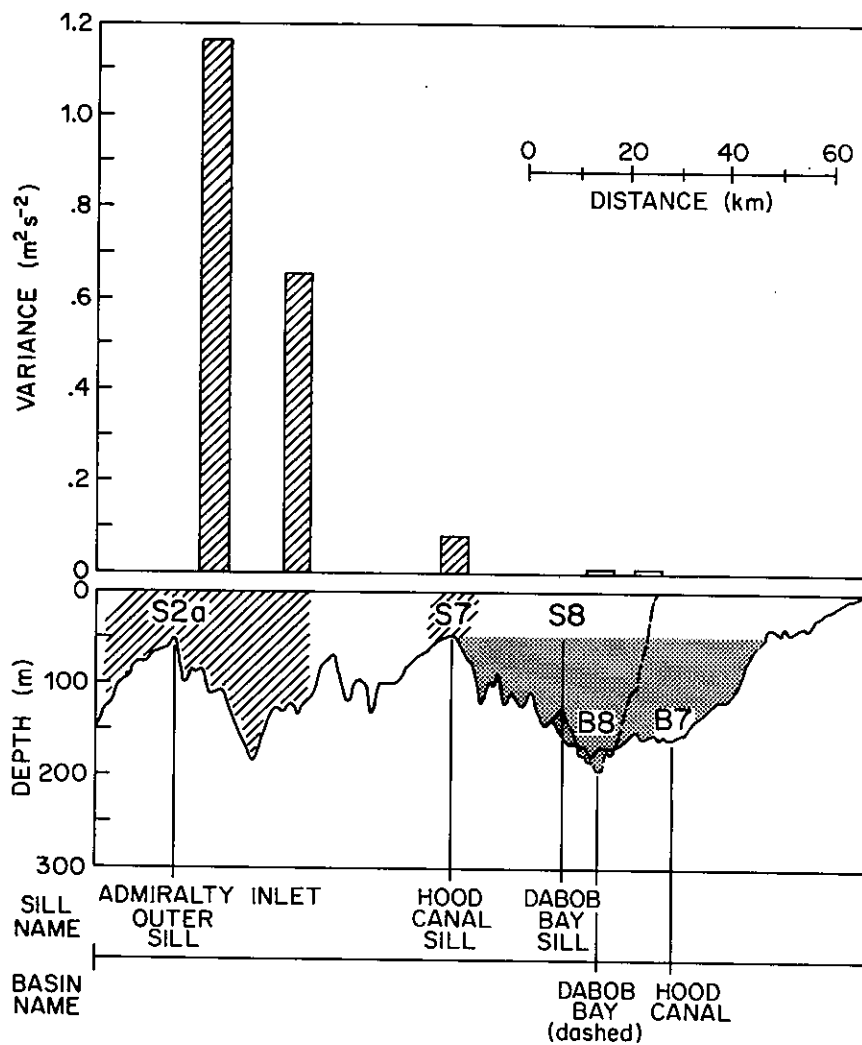


Figure 3.2C. Variance (top) and profile view of mid-channel depth (bottom) along the branch connecting Admiralty Inlet and Hood Canal. Notation: sills (hatched; S2, S7, and S8) and basins (stippled; B7 and B8).

The ratio of variance over the sills to variance in the basins is less elsewhere. In The Narrows-Nisqually Basin (B4, Fig. 3.2A), which is embraced by sills in The Narrows (S3) and Nisqually Reach (S4), the variance is two- to tenfold smaller than in those two sill zones. In the Nisqually-Dana Basin (B5, Fig. 3.2A) embraced by the sills in Nisqually Reach (S4) and Dana Passage (S5), the variance is five- to tenfold smaller. In Saratoga Passage and Port Susan (B6 and B9; Fig. 3.2B) the variance is about thirtyfold smaller than in Deception Pass, and fortyfold smaller than over the outer sill in Admiralty Inlet. Finally, in Hood Canal and Dabob Bay (B7 and B8; Fig. 3.2C) the variance is about eightfold smaller than over the Hood Canal sill (S7).

3.2 MIXING IN SILL ZONES

Barnes and Ebbesmeyer (1978) and Ebbesmeyer and Barnes (1980) examined the longitudinal distributions of surface and bottom salinity, dissolved oxygen, and temperature along the Major and Whidbey branches. They found that the water traversing the basins near surface and bottom changes moderately in temperature, salinity, and oxygen whereas there were sharp changes in crossing the highly energetic sill zones. This contrast indicated that vigorous mixing of surface and deep waters occurred primarily in the sill zones and secondarily in the basins.

To examine mixing in the sill zones and basins, it is useful to examine time series of water properties at selected locations in and near the sill zones. Observations have been made near the three most energetic zones (S2, S3, S6).

Mixing in Deception Pass was examined by Collias, Barnes, and Lincoln (1973) using a two-day series of hourly observations of salinity taken at a location between Deception Pass and the north fork of the Skagit River (Fig. 3.3C). Observations were made at depths of 0, 10, and 20 m (Fig. 3.3A). The striking features are the intervals when the difference in salinity between depths decreases sharply to small values on the order of $0.1^{\circ}/\text{oo}$. These intervals occur during flood currents, and correspond to the arrival of water which has been vigorously mixed in Deception Pass. During ebb currents the well-mixed water is replaced by unmixed, stratified water arriving from the north fork of the Skagit River.

The mixing in Admiralty Inlet can be illustrated by examining a site off Bush Point (Fig. 3.3C) lying between the energetic outer sill zone in Admiralty Inlet and the major source of freshwater, Whidbey Basin. Salinity observations at selected depths were reported by Barnes and Collias (1956) for the period 1-5 June 1954 at approximately two-hour intervals. Figure 3.3B shows time-series of salinity observed at depths of 0, 10, 40, 70, and 108-110 m. The pattern is comparable to that observed between Deception Pass and the Skagit River, but the vertical differences are not as small. During flood currents the water, which has been mixed over the outer sill in Admiralty Inlet, arrives at the site and has a vertical salinity difference of approximately $0.4^{\circ}/\text{oo}$. During ebb currents the water at the site is replaced by more highly stratified water originating from Whidbey Basin.

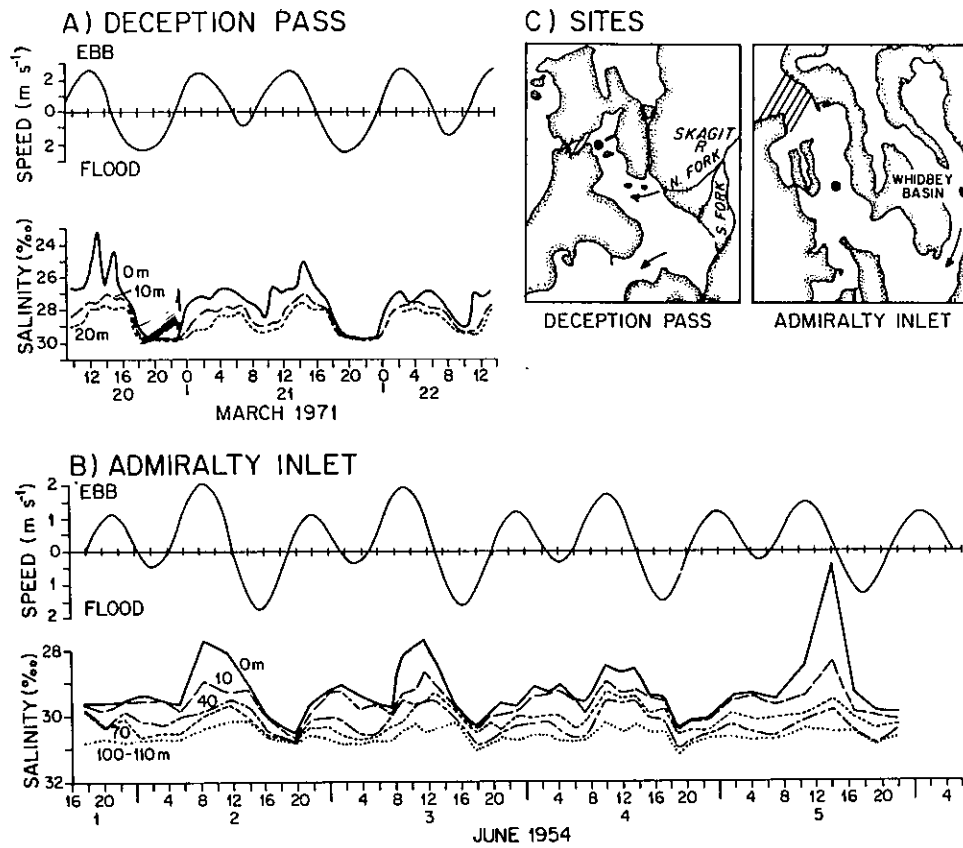


Figure 3.3. Time-series of salinity at selected depths illustrating vigorous mixing in Deception Pass (A; from Collias et al., 1973) and Admiralty Inlet (B). Also shown are predicted tidal currents by the U.S. Coast and Geodetic Survey for Deception Pass (a; 1971) and Bush Point (B; 1954). Chart (C) shows sites of the time-series (●), mixing zones (hatched), and flow from freshwater sources (arrows).

To illustrate the mixing in The Narrows, Ebbesmeyer and Barnes (1980) showed a vertical section of salinity obtained during a flood tide on 3-4 March 1949. On the flood tide, water stratified from surface to bottom feeds from East Passage into the northern end of The Narrows and mixes to nearly vertical homogeneity near the southern end of The Narrows. These observations were made with an early model of a conductivity-temperature-depth (CTD) probe having an accuracy of approximately $0.1^{\circ}/\text{oo}$. To examine the mixing of the other water properties, additional observations were utilized which were made using water bottles and reversing thermometers. During 19 December 1960 two casts were made near the end of a flood tide in The Narrows and southern East Passage. Figure 3.4 shows vertical profiles of temperature, salinity, sigma-t, and dissolved oxygen at the two sites. The contrast in stratification at each site is evident; the vigorous mixing in The Narrows has reduced the top-to-bottom differences in temperature, salinity, oxygen, and density.

The preceding examples indicate that tidal currents in the three most energetic sill zones are sufficient to mix the waters to near vertical homogeneity. Water within the basins initially stratified by $1-5^{\circ}/\text{oo}$, can be mixed such that the vertical difference is reduced to less than $0.1^{\circ}/\text{oo}$ in Deception Pass and The Narrows. In Admiralty Inlet the initial stratification of $1-2^{\circ}/\text{oo}$ was reduced to approximately $0.4^{\circ}/\text{oo}$. After mixing, the larger vertical difference in Admiralty Inlet probably occurs in part because the cross-sectional area of Admiralty Inlet is much larger than those in The Narrows and Deception Pass (Fig. 3.5).

3.3 MEAN CIRCULATION

Puget Sound is appended to the larger fjord system consisting of the Strait of Juan de Fuca and the Strait of Georgia. The major freshwater source is the Fraser River which discharges into the Southern Strait of Georgia. Most of the Fraser River discharge exits to the Pacific Ocean via the inner Strait of Juan de Fuca. Since Puget Sound also joins the inner Strait of Juan de Fuca it is necessary to examine the current patterns which may lead from the Strait of Georgia to Puget Sound as well as the patterns within Puget Sound itself.

The mean circulation has been examined in profile and plan views.

3.3.1 Vertical Profiles

Vertical profiles of net currents were constructed for 23 areas in Puget Sound and its approaches (Appendix A). These profiles consist of net vector speeds computed for individual records which have been tabulated in Volume I by Cox et al. (1983). The vector net direction of each record has been grouped into two general directions: either in or out of the estuary.

The profiles can be classified within three categories: single-layer flow; two-layer flow; and unresolved because of low speeds or lack of observations. Areas showing predominantly single layer flow consist of: Rosario Strait (2); western shore of Whidbey Island (3); Colvos Passage (9);

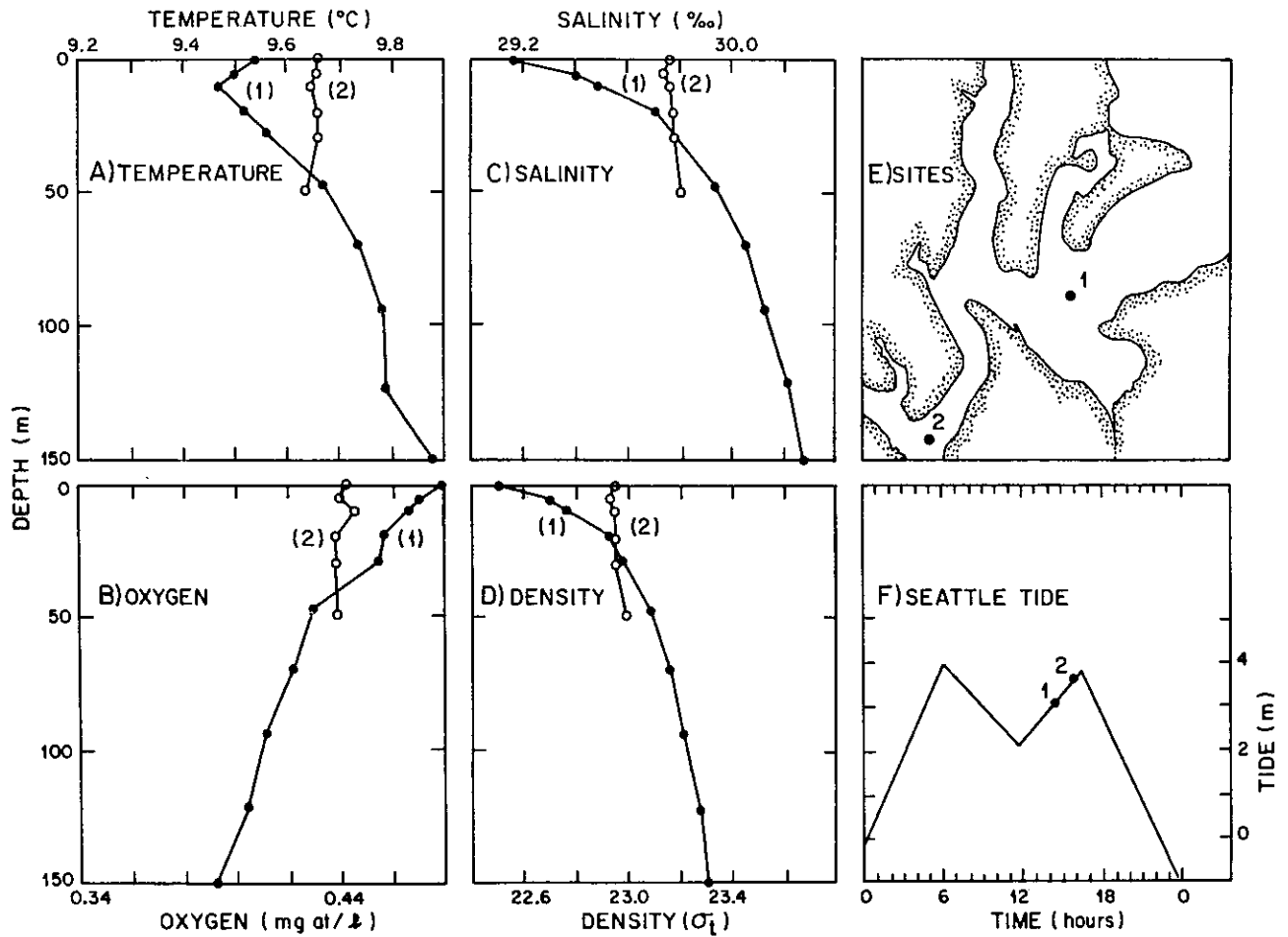


Figure 3.4. Profiles of temperature (A), dissolved oxygen (B), salinity (C), density (D), made at discrete depths (dots) at two sites in and near The Narrows (site 1 and 2 in C) near the end of a flood tide (F). Dots denote profiles made in East Passage at site 1 and circles denote profiles made at the southern end of The Narrows at site 2 after vigorous tidal mixing.

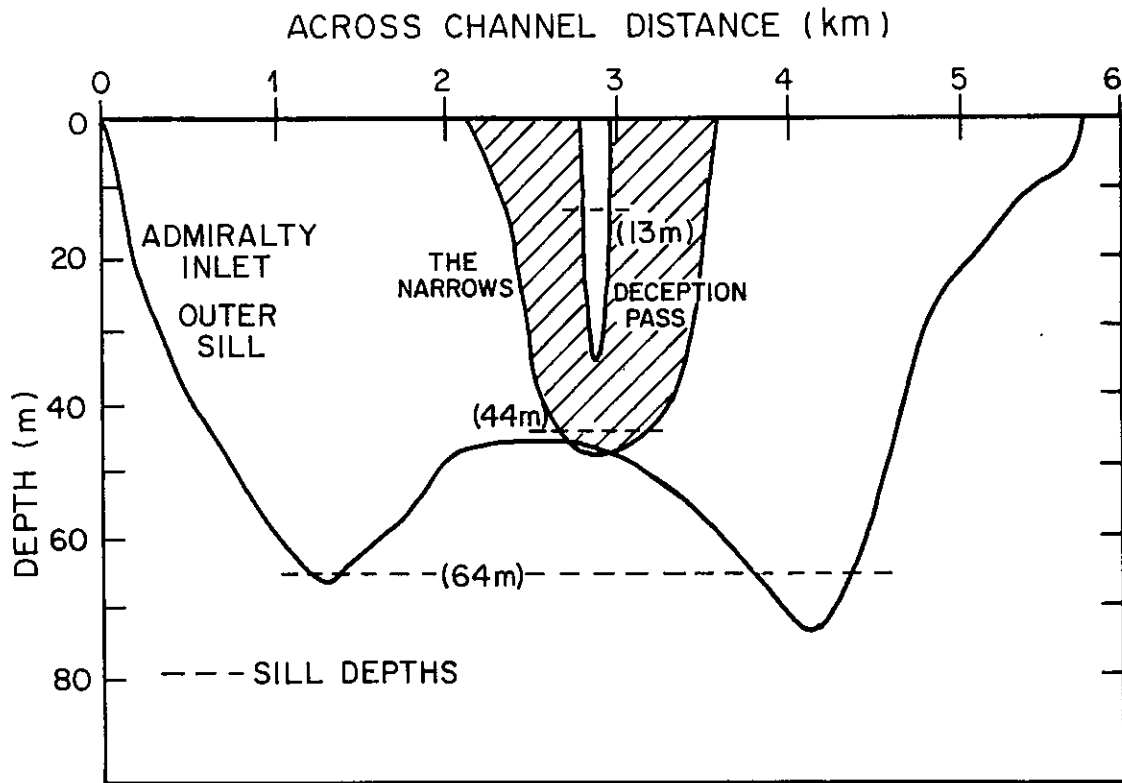


Figure 3.5. Representative cross sectional areas in the three most energetic regions of Puget Sound: Admiralty Inlet, The Narrows (hatched), and Deception Pass. Sill depths are denoted by dashed lines.

northern and southern East Passage (6.7); Dalco Passage (8); and Balch Passage (14); where the numbers in parenthesis indicate the area designated in Appendix A. The flows over the sills and within the basins generally are two-layered; in Dabob Bay and Hood Canal the speeds are too low to reveal a distinct pattern.

Within the category of two-layer flow there are three areas where a large number of observations have been made and the vertical structure appears reasonably well resolved (Fig. 3.6). In the Main Basin and the outer Strait of Juan de Fuca the outflow occurs above approximately 50 m depth, whereas in Whidbey Basin the outflow is confined to depths less than 20 m and the currents are much weaker except at the water surface. The difference between the Main and Whidbey basins confirms the earlier contrast made by Barnes and Ebbesmeyer (1978) which was based on a much smaller number of observations. The flow in Whidbey Basin resembles that in a classical fjord, Silver Bay, where most runoff enters near the head with a deep sill at its mouth (Barnes and Ebbesmeyer, 1978). In contrast, the Main Basin and the outer Strait of Juan de Fuca both have vigorous vertical mixing at their heads (i.e., in The Narrows and the inner Strait of Juan de Fuca, respectively). Barnes and Ebbesmeyer (1978) and Ebbesmeyer and Barnes (1980) demonstrated that the vigorous flow in the Main Basin was due primarily to tidal pumping associated with The Narrows; we speculate that the vertical structure in the outer Strait of Juan de Fuca occurs in large part because of vigorous tidal mixing at its head in the inner Strait of Juan de Fuca and surrounding sill zones (in Rosario Strait, Haro Strait, Deception Pass, and Admiralty Inlet).

3.3.2 Plan View

Net currents computed for each site have been combined regardless of the period and length of the measurements to determine the pattern of the horizontal flow in the upper layers of four areas: the inner Strait of Juan de Fuca, Admiralty Inlet, Main Basin, and a portion of the Southern Basin. The maps are based on data collected over many years by various investigators using different kinds of equipment. The data used to construct the maps for Admiralty Inlet and the Main and Southern basins have been presented in Volume 1 by Cox et al. (1983); data used to construct the map of the inner Strait of Juan de Fuca was gathered from many sources^c. Some of the sources include: 1) data obtained by the National Ocean Survey (NOS) over many years (1940-1977), portions of which have been discussed by Mofjeld (see Cannon, ed., 1978), Ebbesmeyer et al. (1979), and Parker (1977); 2) measurements made by the Pacific Marine Environmental Laboratory (PMEL), described by Holbrook et al. (1980).

The maps were constructed in several stages. First, the net vector from each current meter record was plotted using an arrow, scaled according to speed and designated according to record length. Because of the large amount of data all of the vectors could not be presented; therefore, the data was smoothed in the following way. At locations where many observations were obtained a single net vector was computed. Second, the direction of each

^cThe data from these sources will be tabulated at a future date.

vector was represented by a stick pointing in the vector's direction but not scaled according to speed because our primary concern was to determine flow pattern. Third, arrows were inserted in areas between the observations to represent the inferred flow pattern. Finally, to give some indication of the current strength near the water surface, net speeds were inserted at selected locations.

The patterns of flow at greater depth were not examined in as great detail as those toward the water surface. However, the flows at mid-channel near the bottom have been indicated at selected locations; the supporting data are shown in Appendix A.

Despite the simplicity of our approach some patterns were evident.

3.3.2.1 Inner Strait of Juan de Fuca

Figure 3.7 shows the patterns of net currents within the inner Strait of Juan de Fuca in approximately the upper 30 m. The key elements of the flow pattern have been coded in Figure 3.7 with the following letters:

A. Southerly outflow from the Strait of Georgia through Rosario Strait: The vertical profile of net currents (Appendix A; area 2) indicates a pre-dominantly net outflow over the water column. A net southward flow through Rosario Strait has been predicted using a hydrodynamic-numerical model of tidal flow. The model has been described by Crean (1978). Based on additional, unpublished computations Crean (personal computation) used a 2 km mesh model and computed a net southerly flow of approximately 5 cm s^{-1} . The present map probably represents an annual average, whereas Thomson (1981) has indicated a net northerly flow through Rosario Strait at surface during spring and summer.

B. Westward outflow from Puget Sound through Deception Pass: Collias, Barnes, and Lincoln (1973) deduced this flow based on intensive surveys of currents and water properties (see also currents shown for area 18 in Appendix A).

C. Southerly flow along the western shore of Whidbey Island: A portion of the water discharged from Rosario Strait continues southward past Deception Pass and along the western shore of Whidbey Island to the entrance of Admiralty Inlet. The vertical profile of net currents (area 3; Appendix A) suggests a single-layer flow; there is thus single-layer flow connecting the Strait of Georgia and both entrances to Puget Sound (i.e., via Deception Pass and Admiralty Inlet).

D & E. Westward outflow from Puget Sound through Admiralty Inlet: Water discharged from Puget Sound flows most northward and entrains a certain fraction of the southward flow along the westward shore of Whidbey Island.

F. Clockwise eddy in the northeastern section: Waters from Rosario Strait and Admiralty Inlet are partially recirculated in a clockwise circulating gyre centered in the northeastern portion of the inner Strait of Juan de Fuca.

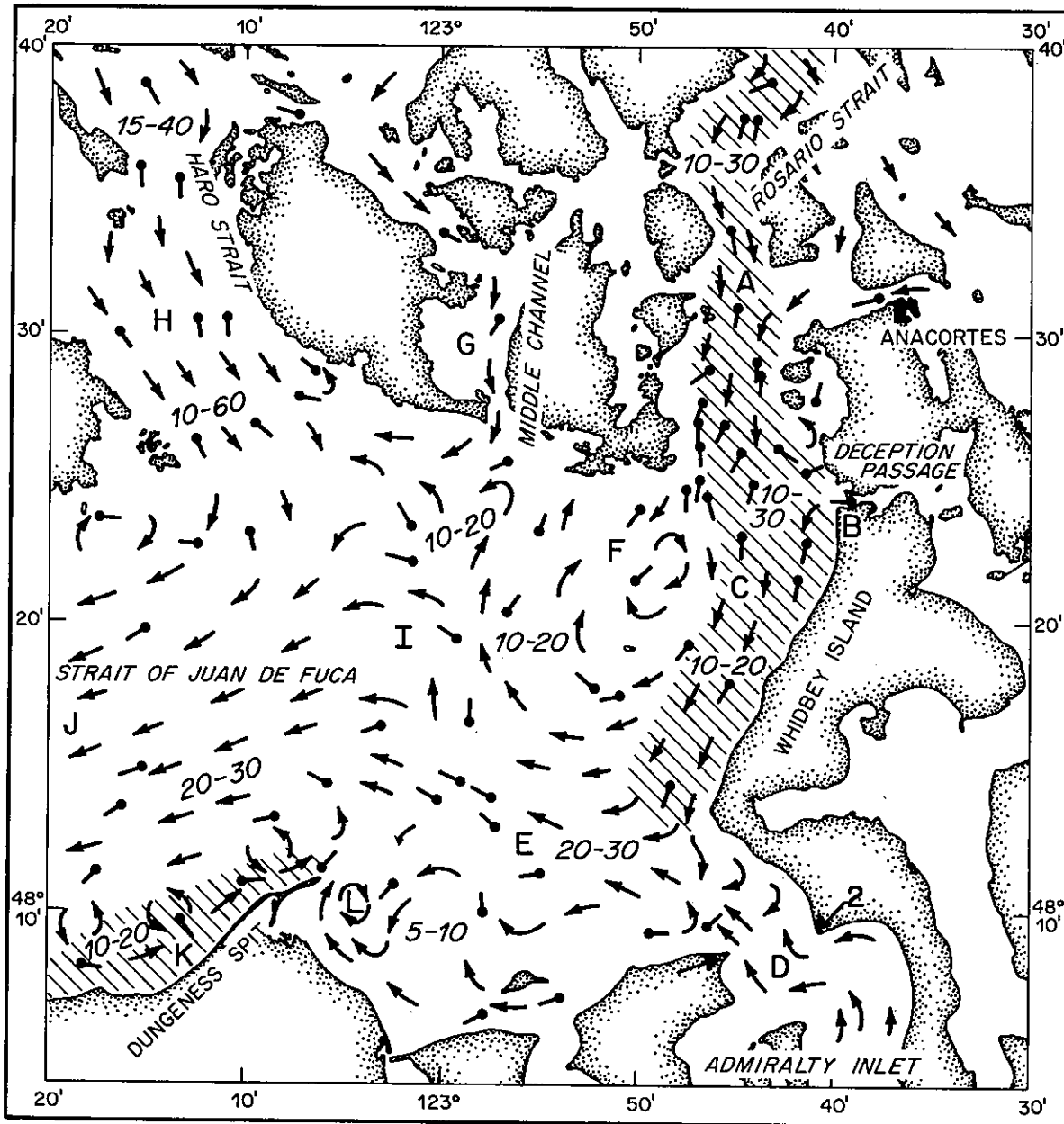


Figure 3.7. Plan view of net circulation in the upper layer (30 m) of the inner Strait of Juan de Fuca. Dots with sticks denote sites of measured currents and current direction. Numbers denote approximate current speed (cm s^{-1}) near the water surface. The arrows represent the flow pattern inferred from the observations. Hatched areas denote single layer net flow. See text for explanation of letter codes.

G. Southerly outflow through Middle Channel: Some water from the Strait of Georgia exits southward into the inner Strait of Juan de Fuca through the small constriction in Middle Channel.

H. Southerly outflow from the Strait of Georgia through Haro Strait: Outflow from the Strait of Georgia exits southward through Haro Strait turning counterclockwise around the southern end of Vancouver Island.

I. Divergence of northwestward flow in the central inner Strait of Juan de Fuca: some water from Admiralty Inlet and Rosario Strait diverges to enter the recirculating eddy (F) with some water continuing westward to the outer Strait of Juan de Fuca (J).

J. Westerly flow into the outer Strait of Juan de Fuca: The combined flows from Haro Strait, Rosario Strait, Middle Channel, Deception Pass, and Admiralty Inlet exit westward into the outer Strait of Juan de Fuca

K. Eastward flow from Port Angeles Harbor to Dungeness Spit: Patterns of sulphite waste liquor made over many years and historical current meter records indicate a single layer flowing eastward and counter to the prevailing westward flow toward mid-channel (Ebbesmeyer et al., 1979).

L. Clockwise eddy eastward of Dungeness Spit: Experiments made in an hydraulic model and current meter records show a net clockwise rotating gyre immediately eastward of Dungeness Spit (Ebbesmeyer et al., 1979).

Many elements of the pattern of net flow in the upper layer of the inner Strait of Juan de Fuca were evident in observations shown by Mofjeld (see Cannon ed., 1978). Recently Frisch (1980) computed net currents near the water surface during a 5½ day period in July 1979 using a high frequency Doppler radar system (CODAR) developed by Barrick et al. (1977). The area encompassed by Frisch's (1980) map includes approximately the regions coded C, D, E, F, I, and L in Figure 3.7. Comparison of the two maps indicates that they are in substantial agreement.

Figure 3.7 indicates a net flow of water connecting the Strait of Georgia and the outer reaches of the two entrances to Puget Sound (Deception Pass and Admiralty Inlet; A, B, C, and D). Because of the large tidal excursions some of the southward flowing water will be carried into the entrances to Puget Sound. Thus, there is a pathway to Puget Sound for freshwater originating from the Strait of Georgia; the quantity of freshwater remains unknown.

This pathway also provides a route connecting the location of a number petroleum refineries (immediately to the north of Rosario Strait) with the energetic mixing zones in the entrances to Puget Sound. As we have shown before, in these highly turbulent and constricted passages surface and bottom waters are vigorously mixed. In the mixing process a significant amount of surface water is refluxed downward into the lower layer that flows inland into Puget Sound.

An example illustrative of the connection between the Strait of Georgia and Deception Pass has been described by Prof. Clifford A. Barnes (see Ebbesmeyer et al., 1979) following the 1971 spill of diesel oil at the Texaco refinery near Anacortes (see Fig. 3.7 for location). In that situation

oil was carried westward and then southward out of Rosario Strait to Deception Pass where a fraction was mixed downward and carried inland. Some oil may have been transported further southward to Admiralty Inlet, but observations necessary to document that pathway were not obtained.

Figure 3.8 shows the pattern of net flow in the upper layer (from Fig. 3.7) superimposed on a representation of the complex bathymetry in the inner Strait of Juan de Fuca. The pathway of the dense water feeding landward is shown passing through the deeper accesses to the Strait of Georgia and Puget Sound.

3.3.2.2 Admiralty Inlet and Whidbey Basin

Figure 3.9 shows the flow patterns in Admiralty Inlet and Whidbey Basin. The key elements of the flow in the upper layer are:

- A, B, C. Nearshore inflow and mid-channel outflow between Admiralty Inlet and the inner Strait of Juan de Fuca: Flow directed inland occurs along the northern (C) and southern (A) shores with outflow (B) toward mid-channel. At (C) the inflow may contain some water from Rosario Strait.
- D & E. Recirculation near section 2: Near section 2 the flow turns counterclockwise causing a significant flow component directed westward along section 2. The abrupt change in flow direction generates a gyre having a diameter comparable to the width of the channel and possibly generates secondary gyres near E.
- F. Outflow from Hood Canal into Admiralty Inlet: Water from Hood Canal enters Admiralty Inlet between sections 3 and 4.
- G, H, I, J. Outflow from the Main and Whidbey basins enters Admiralty Inlet: Immediately south of section 4 the flow turns counterclockwise. The confluence (H) of transport from the Main Basin (J) and Whidbey Basin (I) occurs near (G).
- K. Southward flow in Saratoga Passage: The shallow surface layer containing freshwater from Puget Sound's largest rivers flow southward to the Main Basin and then to Admiralty Inlet.
- L. Divergence between the Skagit River North and South Forks: The surface waters diverge between the two forks of the Skagit River, however the deep water flows northward toward Deception Pass. The northward divergence carries approximately 60% of the Skagit River's discharge through Deception Pass.
- M. Outflow through Deception Pass: The net flow top-to-bottom exits from Whidbey Basin into the inner Strait of Juan de Fuca.

3.3.2.3 Puget Sound Main Basin

Figure 3.10 shows the pattern of net currents in the upper and lower layers of Puget Sound's Main Basin. The key elements of the flow pattern in the upper layer are as follows:

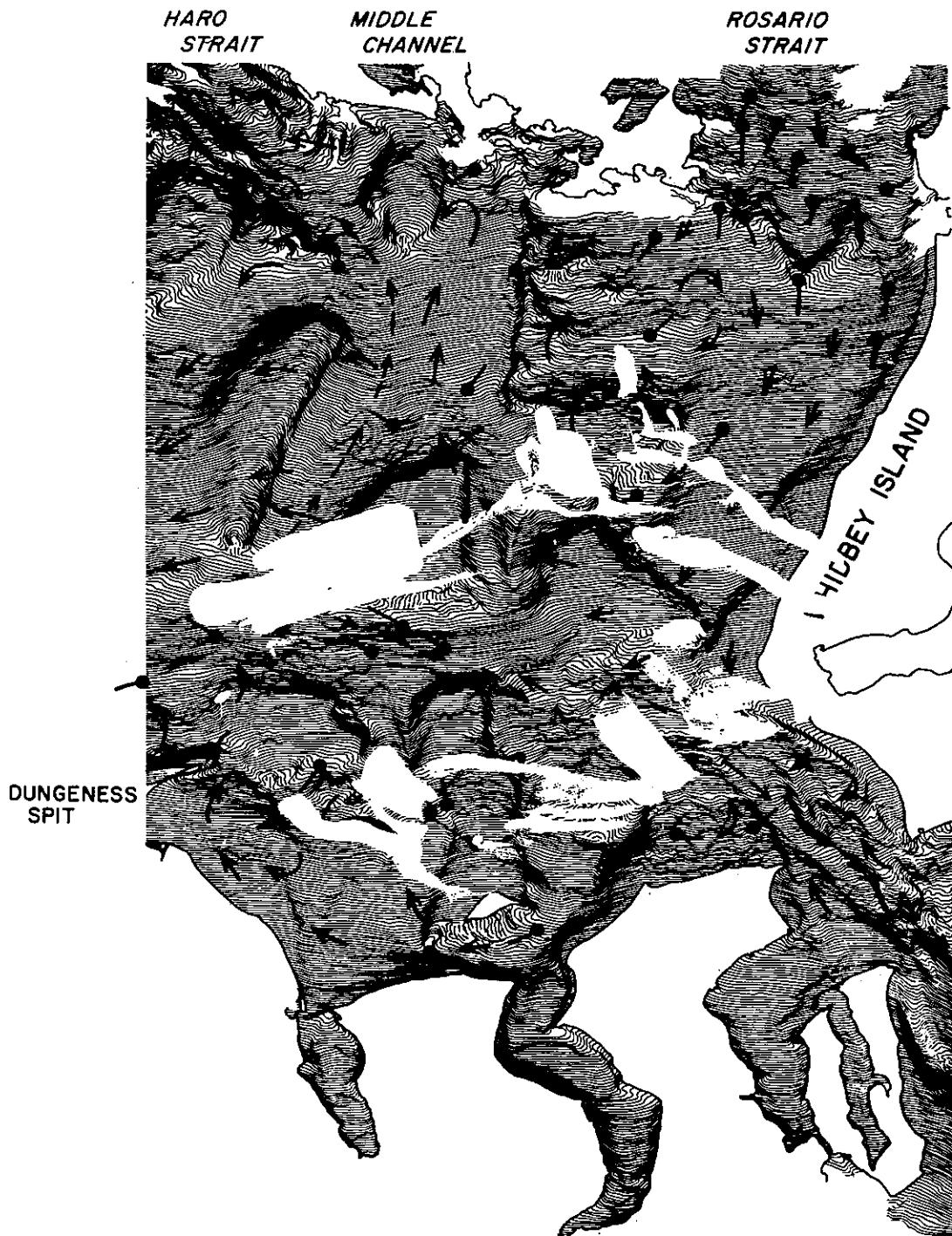


Figure 3.8. Perspective view of the bathymetry in the inner Strait of Juan de Fuca constructed by Noel McGary. The solid arrows represent the net flow pattern from Fig. 3.7 in the upper layer, and the dashed arrows represent the inflow in the lower layer.

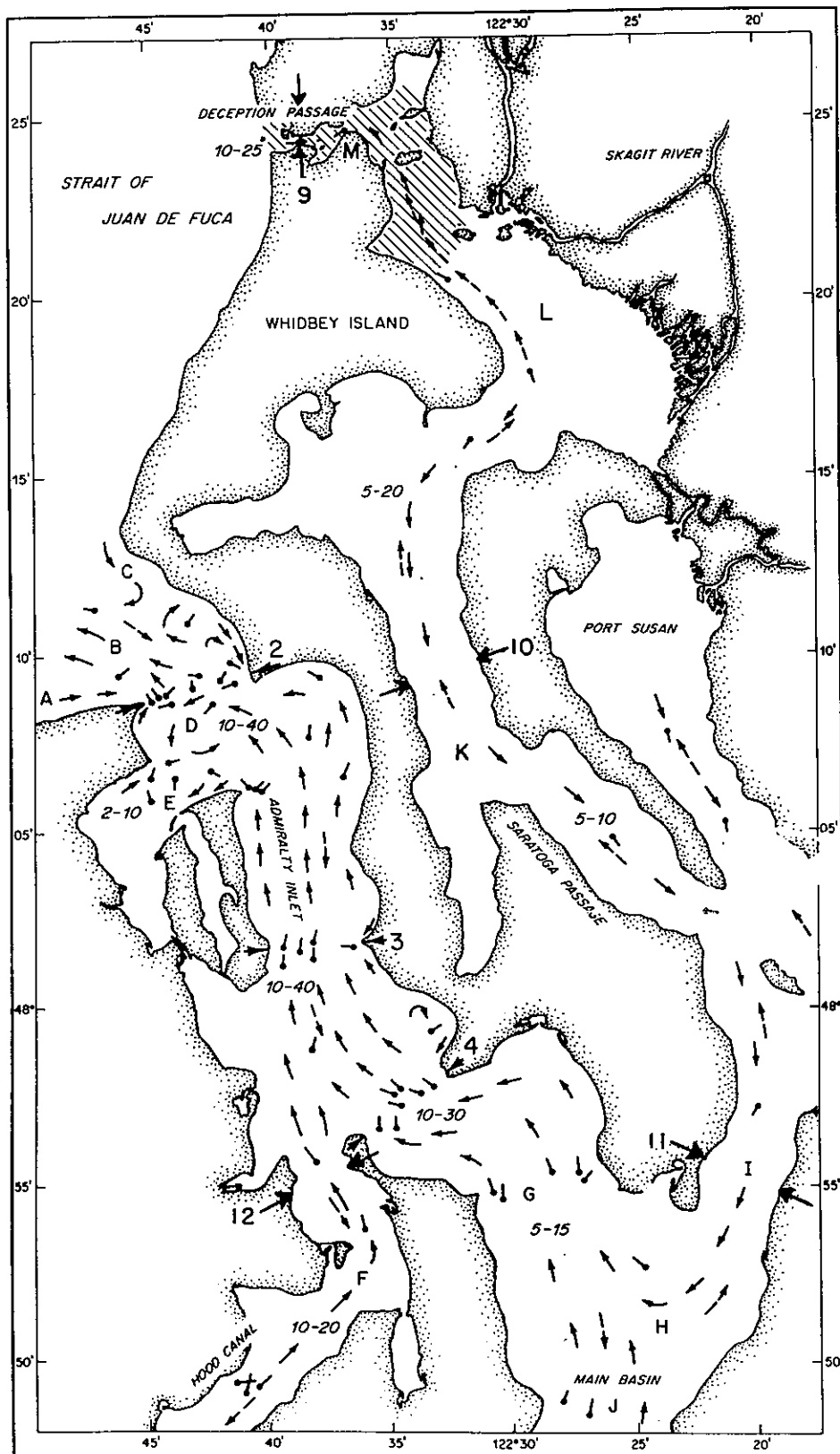


Figure 3.9. Plan view of net circulation in Admiralty Inlet and Whidbey Basin. The dots with sticks denote sites of currents observed in the upper layer (30 m depth) and the current direction; the solid arrows represent the flow pattern inferred from these observations. The numbers in the water area represent the net speed (cm s^{-1}) in the upper layer toward the water surface. The dashed arrows represent the flow in the lower layer. The numbers along the shore indicate sections where transports have been computed. The hatched area near Deception Pass denotes single layer flow. See text for explanation of letter codes.

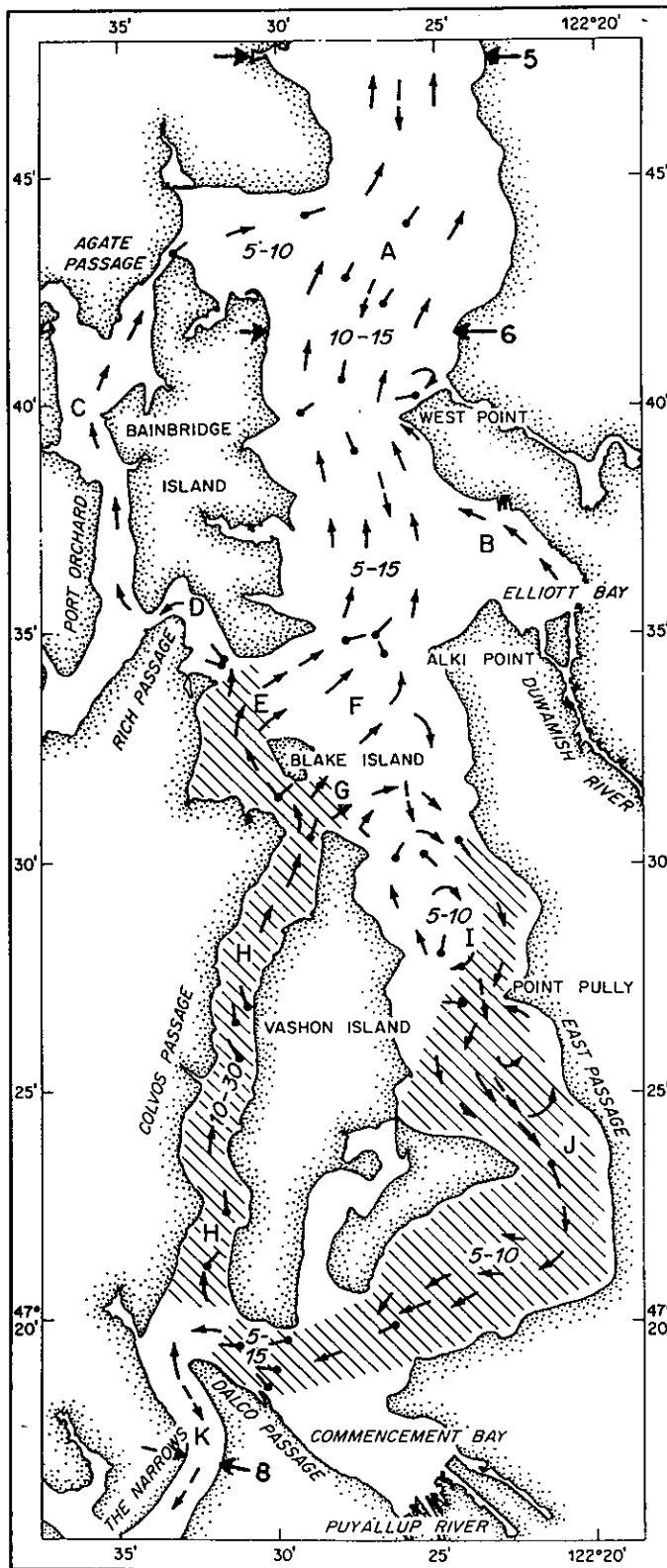


Figure 3.10. Plan view of net circulation in the Main Basin. The sticks and solid arrows represent the flow in the upper layer, and the dashed arrows represent the flow at depth. The dots with sticks denote sites of currents observed toward the water's surface and the current direction; the solid arrows represent the flow pattern inferred from the observations. The numbers in the water areas represent the net speed (cm s^{-1}) toward the water surface. Hatching denotes areas of single layer flow. The numbers (5,6) along the shore indicate sections where transport has been computed (see Fig. 2.2). See text for explanation of letter codes.

- A. Northerly flow in the northern Main Basin: Water from Colvos Passage exits to Admiralty Inlet via passages surrounding Bainbridge Island.
- B. Outflow from Elliott Bay: Flow near the surface containing mostly Duwamish River water enters the main flow seaward near West Point.
- C. Northerly flow through Port Orchard: A small fraction of the discharge from Colvos Passage flows northward via Port Orchard re-entering the Main Basin through Agate Passage.
- D. Outflow through Rich Passage: A portion of the flow from Colvos Passage flows through Rich Passage to feed the northerly flow in Port Orchard.
- E. Outflow from Colvos Passage between Blake and Bainbridge islands: The northward flow from Colvos Passage enters the Main Basin over a 53 m sill opposite Alki Point.
- F. Divergence of outflow from Colvos Passage: Region of unresolved flows where a major fraction of the flow from Colvos Passage flows northward and a secondary portion flows southward in East Passage.
- G. Outflow in Colvos Passage between Blake and Vashon islands: Northward flow in Colvos Passage diverges to flow around Blake Island with part flowing northeastward over the sill (24 m) between Blake and Vashon islands. An unknown portion of this flow continues northward while some feeds back into East Passage.
- H. Northerly flow in Colvos Passage: From surface to bottom there is a net northerly flow in Colvos Passage.
- I. Gyre in northern East Passage: Some effluent from Colvos Passage (at G) flows eastward then southward along the eastern shore to Point Pully where some water recirculates northward along the western shore to close a net clockwise rotating gyre. To investigate this feature, dye was released near the water surface in the hydraulic model off Point Pully. After several tidal cycles some dye was observed to travel around the gyre.
- J. Net flow continuing southward in East Passage: South of the gyre the mean flow is generally southward, but with a sinuous pattern and back-eddies within the convoluted channel.
- K. Net northward flow in The Narrows: The water discharged northward from The Narrows is directed primarily into Colvos Passage.

3.3.2.4 Southern Basin

The available observations indicate the net flow pattern for only a portion of the Southern Basin as shown in Figure 3.11. The elements in the upper layer are:

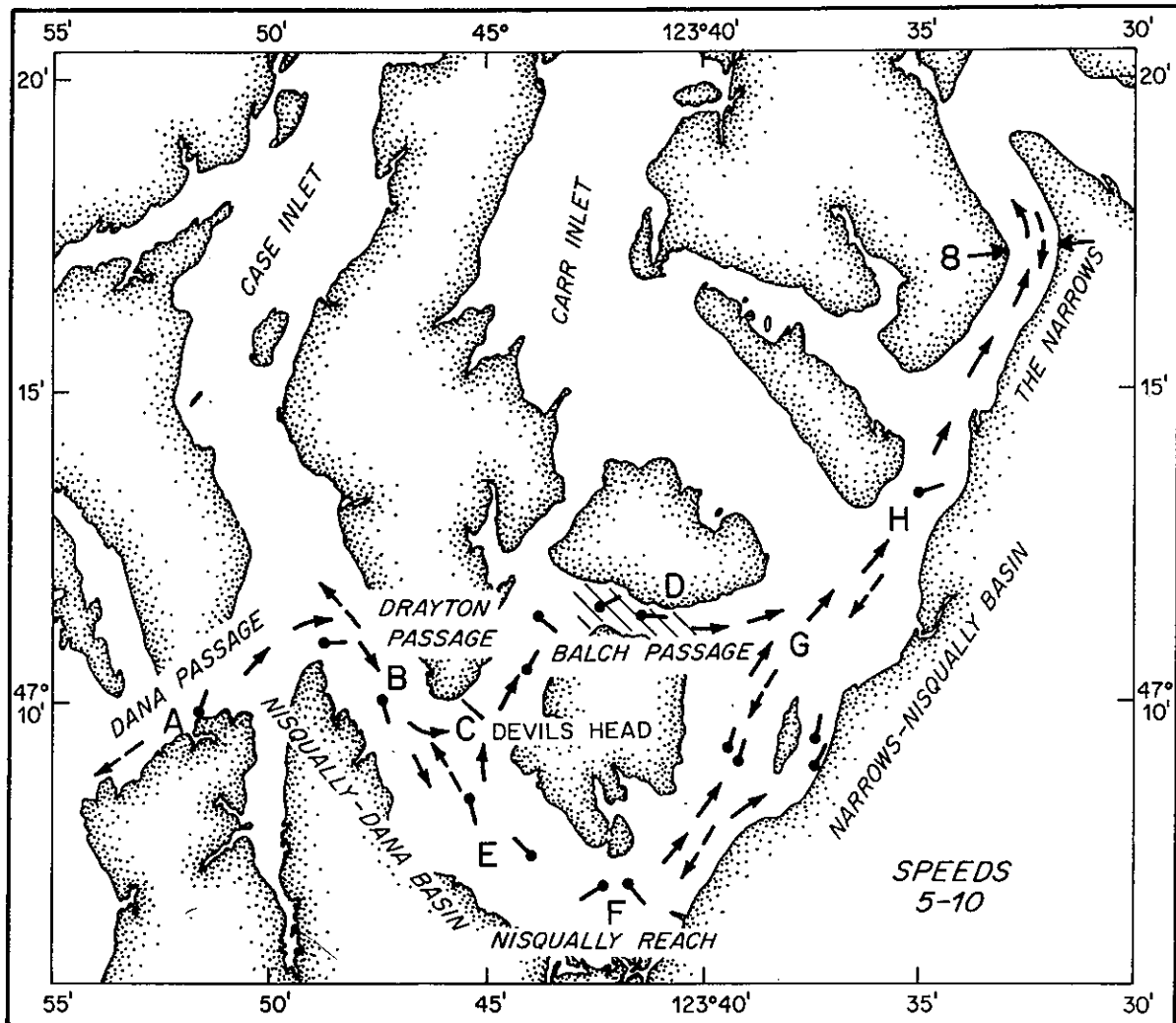


Figure 3.11. Plan view of net circulation in selected regions of the Southern Basin: The sticks and solid arrows represent the flow in the upper layer, and the dashed arrows represent the flow in the lower layer. The dots with sticks denote sites of currents observed in the upper layer toward the water surface and the current direction; the solid arrows represent the flow pattern inferred from the observations. The numbers in the water area represent the net speed (cm s^{-1}) toward the water surface. Hatching denotes areas of single layer flow. The number (8) along the shore indicates the section where transport has been computed (see Fig. 2.2). See text for explanation of letter codes.

A. Outflow in Dana Passage: A portion of the outflow from Dana Passage turns clockwise into the Nisqually-Dana Basin.

B, C, E. Divergence of outflow opposite Devil's Head: The net outflow from (B) partly diverges with some continuing southward to (E) and some turning northward into Drayton Passage (C).

D & G. Eastward flow in Balch Passage: The flow in the constricted Balch Passage (D) is, from the surface to the bottom, directed eastward re-entering the major axis of the Southern Basin near (G).

F. Divergence off the Nisqually River delta: The outflow from the Nisqually River apparently diverges eastward and westward near (F). A geometrically similar flow pattern occurs off the Skagit River delta where water from the north and south forks diverges northward and southward, respectively (Collias, Barnes, and Lincoln, 1973).

H. Net outflow from Southern Puget Sound: The combined streams from the island matrix exit through The Narrows continuing northward through Colvos Passage.

4. TEMPORAL VARIABILITY OF TRANSPORT IN THE MAIN BASIN

In many fjords the renewal of the water below sill depth occurs between periods of stagnation. The quiescent periods may last from months to years. Occasionally the renewal of water in the Main Basin has been described as occurring during the fall in association with upwelling off the Washington coast, the implication being that there were also quiescent periods in the Main Basin. To investigate this aspect, the temporal variability of transport in the Main Basin's lower layer was explored in several ways. First, the histogram and variance of the current representative of transport were examined; second, statistical experiments were performed using daily observations to investigate the dependence of transport on tides, wind, and runoff; and third, monthly averages were computed to reveal the seasonal cycle of transport.

4.1 GROSS VARIABILITY OF TRANSPORT

The gross variability of transport in the Main Basin's lower layer was investigated using daily values of U_{100} since this current is representative of the transport (see section 2). Figure 4.1 contains the histogram of daily net speeds constructed from the available records listed in Table 4.1. The histogram shows that the speeds are distributed over a broad range of approximately 35 cm s^{-1} , where 93% of the speeds are directed inland and 7% are directed seaward. The histogram resembles a Gaussian distribution, so that it seems reasonable to expect that the mean (8.3 cm s^{-1} directed inland) and standard deviation 5.8 cm s^{-1} will provide an adequate description of the variability. Assuming that the t-distribution is applicable, the mean value has an uncertainty of approximately 0.5 cm s^{-1} at the 5% level. Using eq. (1), the mean speed is equivalent to a transport of $2.9 \times 10^4 \text{ m}^3 \text{ s}^{-1}$ with an uncertainty of $0.2 \times 10^4 \text{ m}^3 \text{ s}^{-1}$ (at the 5% level) or approximately 7% of the mean value.

To examine the variance at selected frequencies, Fast-Fourier Transforms of U_{100} were computed. The variance was calculated for observations made during 16 September 1975-4 June 1976 when a long record of U_{100} divided into eight period ranges: nearly half (46%) of the variance occurs with less than fortnightly (shorter than 12.2 days) periods; most of the other half (41%) occurs with fortnightly to monthly (12.8-32.0 days) periods; and a small remainder (14%) occurs with seasonal (36.6-256 days) periods.

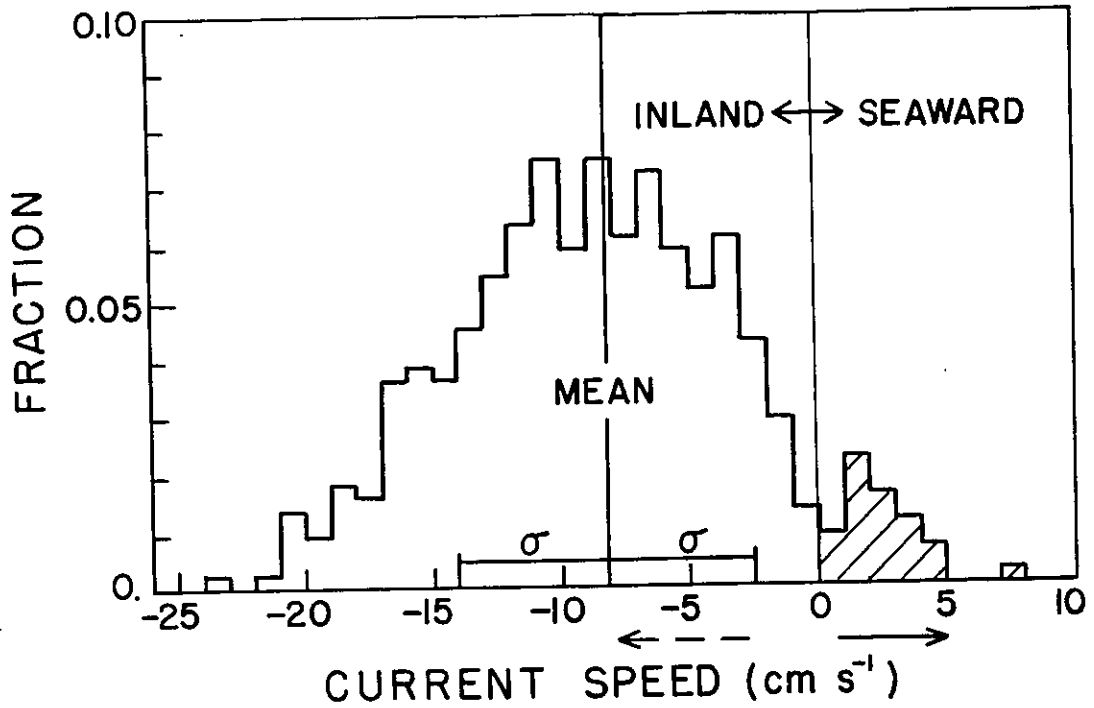


Figure 4.1. Histogram of current speed (U_{100}) in the Main Basin's lower layer (see Figs. 2.2 and 2.3 for locations). At bottom, arrows denote out-estuary (solid) and in-estuary (dashed) directions.

TABLE 4.1. CHARACTERISTICS OF THE RECORDS OF U_{100} . SHOWN FOR EACH RECORD ARE: DATE, DEPTH, DURATION, NET SPEED AND DIRECTION, AND TRANSPORT COMPUTED FROM EQ. (1).

| Date | Year | Depth (m) | Duration (days) | Net Current Speed (cm s^{-1}) | Direction ($^{\circ}\text{True}$) | Transport ($10^4 \text{ m}^3 \text{ s}^{-1}$) |
|---------------|------|--------------|--------------------|--|--|--|
| <u>Winter</u> | | | | | | |
| 1/1-1/27 | 1976 | 113 | 27 | 9.6 | 244 | -3.20 |
| 1/28-2/23 | 1976 | 113 | 27 | 11.2 | 243 | -3.61 |
| 1/9-2/13 | 1973 | 116 | 36 | 10.5 | 242 | -3.43 |
| 1/31-3/2 | 1972 | 90 | 30 | 12.9 | 244 | -4.05 |
| 2/25-3/20 | 1976 | 103 | 25 | 9.0 | 248 | -3.04 |
| 2/23-3/28 | 1977 | 113 | 32 | 6.0 | 244 | -2.26 |
| mean | | 108.0 | 29.5 | 9.9 | 244 | -3.27 |
| Std. dev. | | 9.9 | 4.0 | 2.3 | 2 | 0.61 |
| <u>Spring</u> | | | | | | |
| 3/21-4/14 | 1976 | 103 | 25 | 8.3 | 254 | -2.86 |
| 4/16-5/9 | 1976 | 107 | 24 | 9.2 | 247 | -3.09 |
| 5/10-6/3 | 1976 | 107 | 25 | 7.7 | 250 | -2.70 |
| mean | | 105.7 | 24.7 | 8.4 | 250 | -2.88 |
| Std. dev. | | 2.3 | 0.6 | 0.8 | 4 | 0.20 |
| <u>Summer</u> | | | | | | |
| 6/21-7/20 | 1976 | 105 | 28 | 7.7 | 249 | -2.70 |
| <u>Autumn</u> | | | | | | |
| 9/10-10/11 | 1977 | 92 | 32 | 4.6 | 258 | -1.90 |
| 9/17-10/13 | 1975 | 110 | 27 | 8.7 | 242 | -2.96 |
| 10/12-11/9 | 1977 | 92 | 27 | 6.5 | 240 | -2.39 |
| 10/14-11/9 | 1975 | 110 | 27 | 8.7 | 236 | -2.96 |
| 11/11-12/6 | 1975 | 113 | 26 | 4.7 | 243 | -1.92 |
| 12/7-12/31 | 1975 | 113 | 25 | 8.5 | 243 | -2.91 |
| mean | | 105.0 | 27.3 | 7.0 | 244 | -2.51 |
| Std dev. | | 10.2 | 2.4 | 2.0 | 8 | 0.51 |

TABLE 4.2. VARIANCE OF THE CURRENT U_{100} WITHIN SELECTED RANGES OF PERIOD.

| Period (days) | Description | Current | |
|------------------|-------------|---|---------------------------------|
| | | Variance ($\text{cm}^2 \text{s}^{-2}$) | Percentage of total variance |
| 2.0- 3.0 | | 0.71 | 2.1 |
| 3.0- 5.8 | | 3.92 | 11.6 |
| 6.0- 7.8 | Weekly | 2.67 | 7.9 |
| 8.0-12.2 | | 8.11 | 24.0 |
| 12.8-15.1 | Fortnightly | 4.12 | 12.2 |
| 16.0-23.3 | | 3.92 | 11.6 |
| 25.6-32.0 | Monthly | 5.78 | 17.1 |
| 36.6-256. | Seasonal | 4.56 | 13.5 |

4.2 DEPENDENCE OF TRANSPORT ON TIDE, WIND, AND RUNOFF

To investigate the sources of the variability it was necessary to consider the processes which might influence the transport. Herein the processes were viewed as perturbing the mean circulation.

The mean circulation in the Main Basin and embracing sill zones has been diagrammed by Ebbesmeyer and Barnes (1980) following Barnes and Ebbesmeyer (1978). Briefly, the pattern consists of upwelling and downwelling which occurs primarily in or near the sill zones embracing the Main Basin. The upwelling occurs northward of The Narrows in East Passage, and the downwelling occurs in Admiralty Inlet. During the downwelling process the major fraction of the Main Basin's upper layer is refluxed downward and into the lower layer. Because of the strong upwelling and downwelling the Main Basin's circulation resembles a convective cell. Some of the processes which modify the mean circulation have been previously investigated as discussed below.

The currents and water properties near the bottom in the Main Basin were investigated by Cannon and Ebbesmeyer (1978), Cannon and Laird (1978), and Geyer and Cannon (1982). They found that the bottom water was often renewed at fortnightly intervals when dense water flowed inland along bottom from Admiralty Inlet. In many instances bottom water renewal occurred in association with flood tides having ranges larger than 3.5 m. When the flood range exceeds 3.5 m, Farmer and Rattray (1963) have shown that the flood tide excursion exceeds the length of Admiralty Inlet. Moreover, the deep exterior water immediately seaward of Admiralty Inlet always exceeds the density of Main Basin bottom water. It appears that on the occasions of large flood tides, the exterior water may enter the Main Basin with least mixing and thus displace water in the Main Basin near the bottom.

Barnes and Ebbesmeyer (1978) and Ebbesmeyer and Barnes (1980) used experiments in the hydraulic tidal model to investigate the sensitivity of transport in the Main Basin to tidal pumping in The Narrows and its approaches. The tidal pumping process can be summarized briefly as follows. Immediately northward of The Narrows in East Passage, lower-layer Main Basin water is drawn upward on flood tides, mixed with surface water over the sill (44 m) in The Narrows, and the mixture is discharged into the Southern Basin. The returning ebb contains variable amounts of Southern Basin resident and river water, as well as refluxing Main Basin water. These are again mixed vertically, and then directed northward through Colvos Passage. The mixture enters the Main Basin opposite Alki Point and above the level of no-net-motion (approximately 50 m). Experiments in the hydraulic model showed that the net transport in the Main Basin's upper layer was proportional to the tidal prism in the Southern Basin.

Some effects of the wind have been mentioned by several investigators. Cannon and Ebbesmeyer (1978) observed large currents near the water surface during a ten-day period when the winds were southerly at a mean speed of approximately 6 m s^{-1} . Ebbesmeyer and Barnes (1980) suggested that winds were effective in transporting surface water from the Main Basin into the energetic sill zones. Because of the strong upwelling and downwelling in the sill zones and the prevalence of moderate to strong winds during winter, it appeared that winds could be effective in modulating the rate of water movement in the convective cell.

Finally, Friebertshauser and Duxbury (1972) computed budgets of salt and freshwater for sub-regions of Puget Sound, and found the monthly progression of transport in the sill zones embracing the Main Basin.

From the earlier investigations it appeared useful to compare measurements of tide, wind, and runoff with the Main Basin's transport. To perform the comparisons, observations were selected for which daily averages could be computed during 1969-1978. The wind was represented by observations made at West Point. This location was chosen because of its open exposure midway along the Main Basin's longitudinal axis. The authors' experience has indicated that measurements made at West Point are representative of winds occurring elsewhere along the Main Basin. Runoff was taken as the total discharge which exits Puget Sound through Admiralty Inlet. To represent the tidal influences several aspects were considered as described below.

Experiments performed by Ebbesmeyer and Barnes (1980) using the hydraulic tidal model indicated that much of the Main Basin's upper-layer transport originates in Colvos Passage. In Colvos Passage the tidal currents set northward nearly all of the time; usually there are two periods of maximum northerly currents which occur during the major and minor ebb tides of each day (Fig. 4.2). A dependence on the ebb tide range was evident from a correlation of SETR with daily net transport computed from current measurements made at mid-channel in southern Colvos Passage during 25 February-25 March 1977 (Fig. 4.3). The correlation of transport with SETR in Colvos Passage is striking; computation of the linear regression gave

$$T_m = (-0.32 + 0.58 \text{ SETR}) 10^4, \quad (2)$$

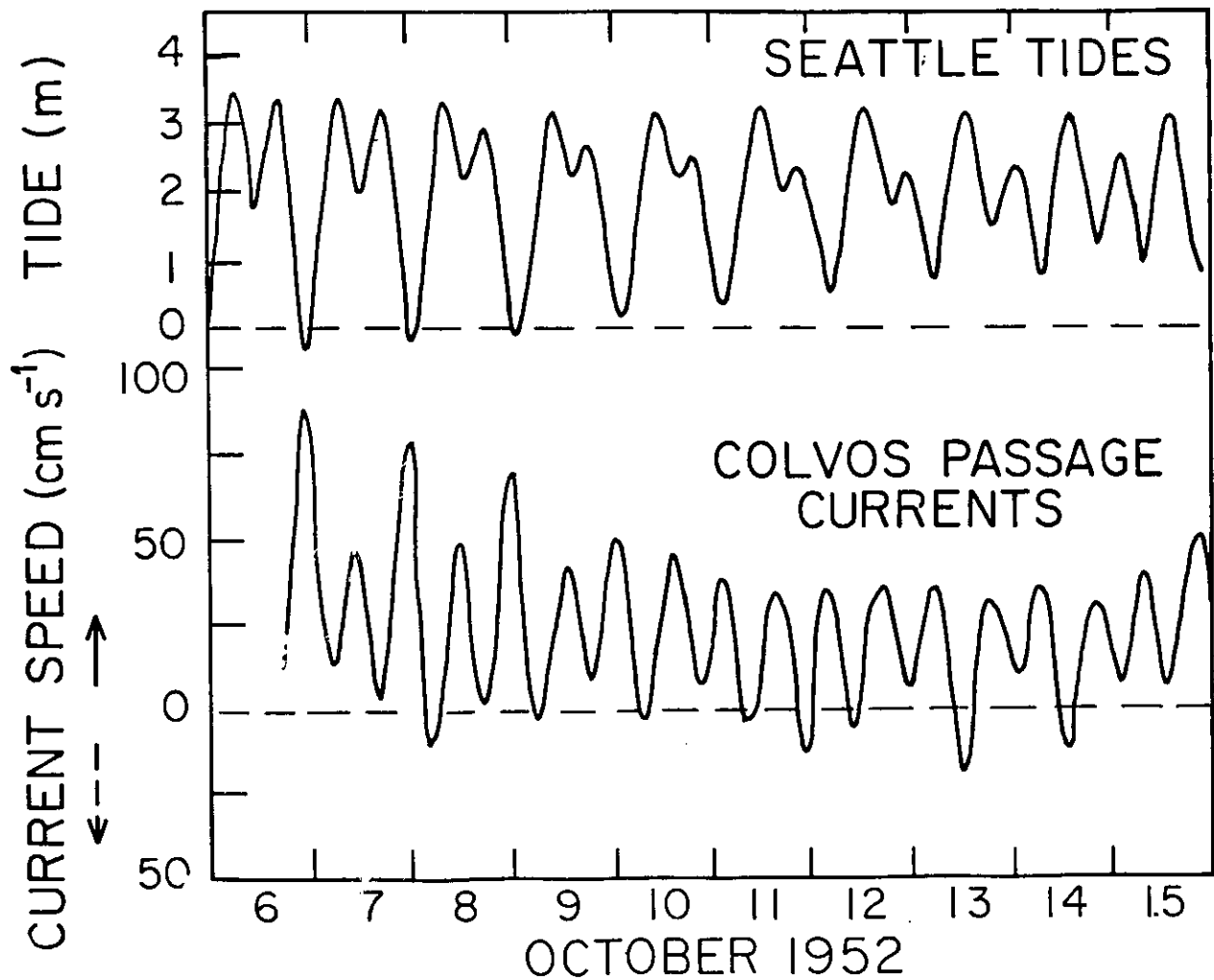


Figure 4.2. Current speed (vertically averaged) in Colvos Passage and Seattle tides (6-15 October 1952) at section 7 (see Fig. 2.2; from Ebbesmeyer and Barnes, 1980). At lower left arrows denote northward (solid) and southward (dashed) flow.

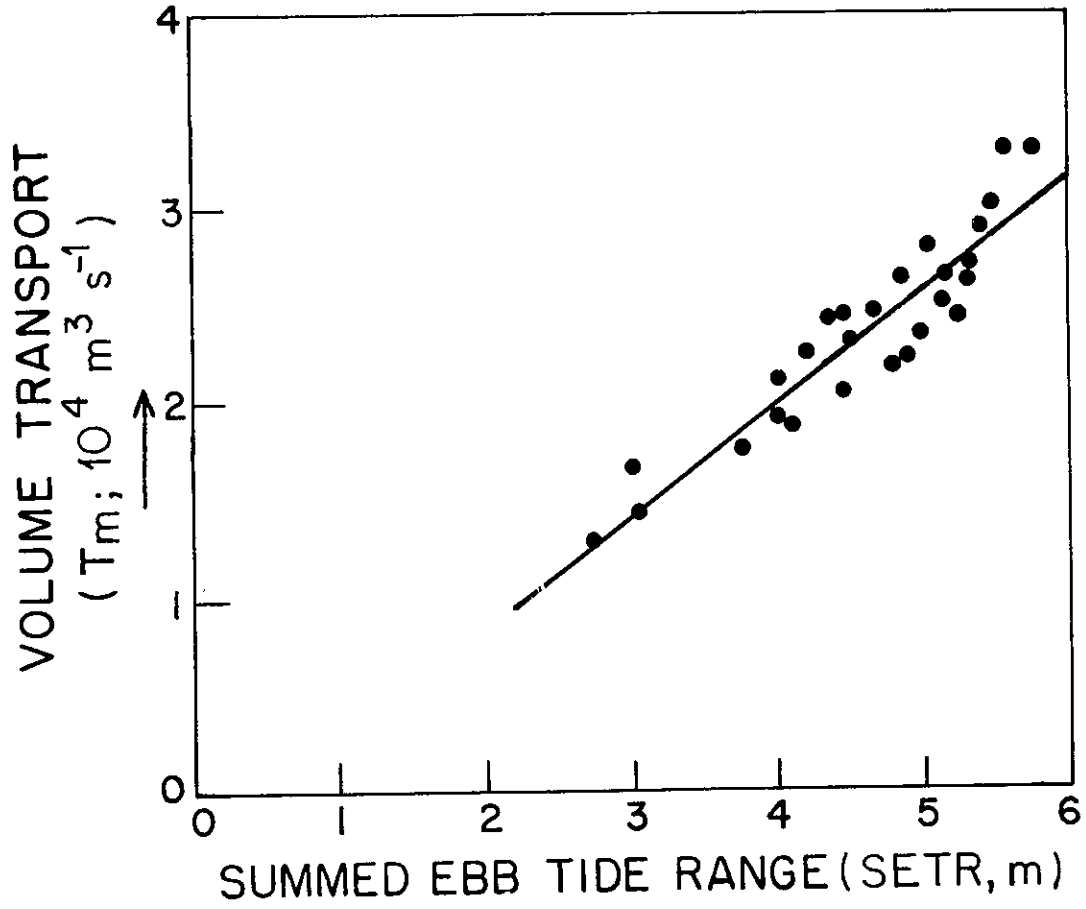


Figure 4.3. Volume transport (T_m -type) in Colv Passage at section 7 (see Fig. 2.2) versus the summed ebb tide ranges (SETR) at Seattle computed for the period 25 February-25 March 1977. The solid line represents the least-squares-best-fit eq. (1).

where SETR is expressed in meters, T is expressed in $m^3 s^{-1}$, and the regression coefficient ($r = 0.93$) is significant at the 1% level.

The coefficient in eq. (2) multiplying SETR may be compared with a value deduced from the tidal prism of the Southern Basin. For this computation the volume of the Southern Basin was graphed as a function of tide at Seattle using volumetric data of McLellan (1954; Fig. 4.4). Within the range of normal tides the relation is nearly linear. Assuming that the volume equivalent to SETR is completely expelled through Colvos Passage during a tidal day, then the slope in Figure 4.4 is equivalent to a coefficient of approximately $0.56 \times 10^4 m^3 s^{-1}$ per meter of SETR. The agreement with the coefficient in eq. (2) suggests that most of the Southern Basin's tidal prism is expelled through Colvos Passage.

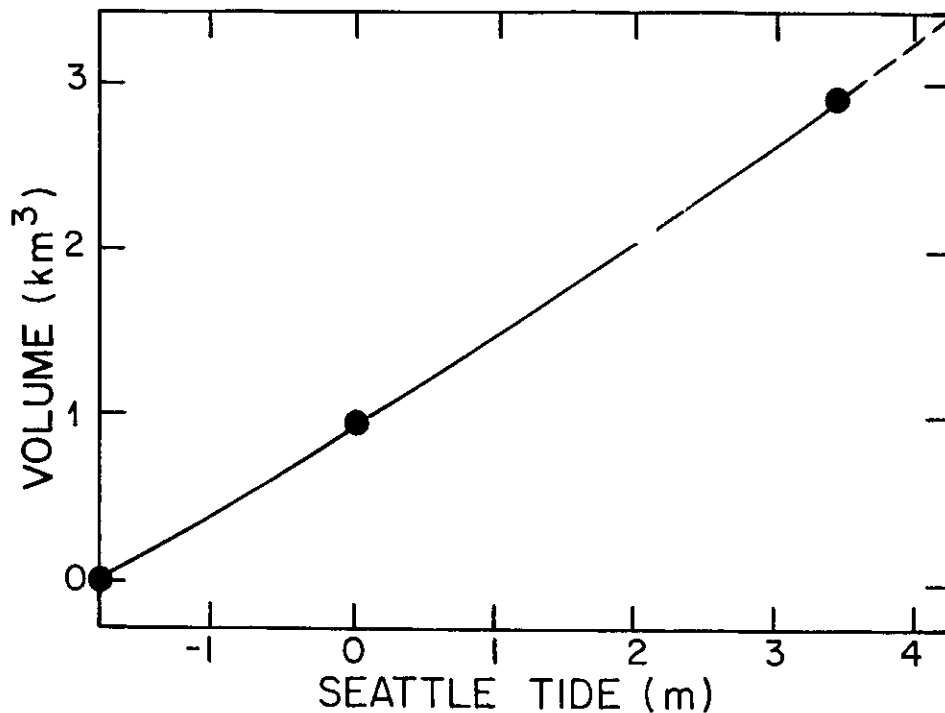


Figure 4.4. Volume above mean-lower-low water of the Southern Basin versus Seattle tide. Dots indicate computations of McLellan (1954) and the line indicates a nearly linear relation of tide and volume.

TABLE 4.3. MEAN, STANDARD DEVIATION, MAXIMUM, AND MINIMUM OF SETR WITHIN MONTHS DURING SEPTEMBER 1975-AUGUST 1976.

| Month | Summed Ebb Tide Range (SETR; m) | | | |
|-----------|---------------------------------|-----------|---------|---------|
| | Mean | Std. dev. | Maximum | Minimum |
| September | 4.72 | 0.95 | 6.67 | 3.42 |
| October | 4.71 | 0.90 | 6.57 | 3.50 |
| November | 4.66 | 0.83 | 6.16 | 3.29 |
| December | 4.61 | 0.90 | 6.19 | 2.43 |
| January | 4.61 | 0.82 | 5.88 | 3.16 |
| February | 4.50 | 0.90 | 6.04 | 2.93 |
| March | 4.54 | 0.93 | 6.22 | 3.04 |
| April | 4.56 | 0.90 | 6.43 | 3.29 |
| May | 4.63 | 0.84 | 6.31 | 3.42 |
| June | 4.74 | 0.78 | 6.13 | 3.32 |
| July | 4.85 | 0.87 | 5.94 | 3.14 |
| August | 4.78 | 0.92 | 6.19 | 2.93 |
| Mean | 4.66 | 0.88 | 6.23 | 3.16 |

TABLE 4.4. COEFFICIENTS COMPUTED FROM THE THREE MULTIPLE REGRESSIONS.

| Regression | r | Coefficient | | | | Sample |
|------------|------|-------------|-------|------|-----------------------|--------|
| | | a | b | c | d | |
| 1 | 0.30 | -1.57 | -0.22 | 0.16 | -1.2×10^{-4} | 48 |
| 2 Mean | 0.66 | -0.75 | -0.38 | 0.15 | - | 32 |
| Std. dev. | 0.10 | 1.65 | 0.37 | 0.05 | - | |
| 3 | 0.84 | -1.30 | -0.29 | - | - | 8 |

Figure 4.5 shows the seasonal progression of SETR for the period September 1975-August 1976. The SETR exhibits a fortnightly periodicity where the mean lowest and highest values which occur during each month are 3.2 and 6.2 m, respectively (Table 4.3). The annual mean value corresponds to a transport of $2.4 \times 10^4 \text{ m}^3 \text{ s}^{-1}$ or approximately 85% of the transport computed at sections 5 and 6 in the Main Basin. In contrast, bottom water renewal apparently occurs below 150 m depth, where on the average approximately 20% of the transport occurs in the Main Basin's lower layer. Because the transport in Colvos Passage apparently accounts for much of the Main Basin's upper-layer transport, the effect of the tide was characterized by SETR.

Figure 4.5 shows daily values of transport computed for the Main Basin's lower layer together with tide, wind, and runoff during a year (September 1975-August 1976). Inspection of Figure 4.5 suggested that some of the transport variance could be explained by fluctuations of SETR, wind, and runoff. To explore the co-variations, three statistical experiments were performed using multiple regressions.

In the first regression transport (T) was expressed in terms of a constant, SETR, wind (W), and runoff (R),

$$T = a + b \text{ SETR} + c W + d R, \quad (3)$$

where the four coefficients (a, b, c, d) are constant; transport is expressed in $\text{m}^3 \text{ s}^{-1}$ and reckoned positive toward the north; SETR is expressed in meters; W is expressed in m s^{-1} and reckoned positive toward the south; and runoff is expressed in $\text{m}^3 \text{ s}^{-1}$. The regression was computed from 5-day averages of transport during 9 January-6 February 1973 and 17 September 1975-14 April 1976. All totaled the regression was computed from 48 sets of T, SETR, W, and R.

In the second regression the current (U_{100}) was expressed in terms of a constant, SETR, and wind,

$$U_{100} = a_1 + b_1 \text{ SETR} + c_1 W_1, \quad (4)$$

where the coefficients are constant, the units of SETR and W are the same as in eq. (3), and the effect of runoff was neglected because its contribution was found to be small based on eq. (3). A separate regression was computed using an average of 28 daily values within each of the 14 intervals listed in Table 4.1. The result was the mean and standard deviation of the coefficients based on 14 samples.

Table 4.4 lists the coefficients obtained from the first two regressions, where the coefficients in eq. (4) were transformed using the relation between U_{100} and transport in eq. (1). The correlation coefficient for each computation was found to be significant at the 1% level. These two experiments gave coefficients for wind dependence which were nearly identical,

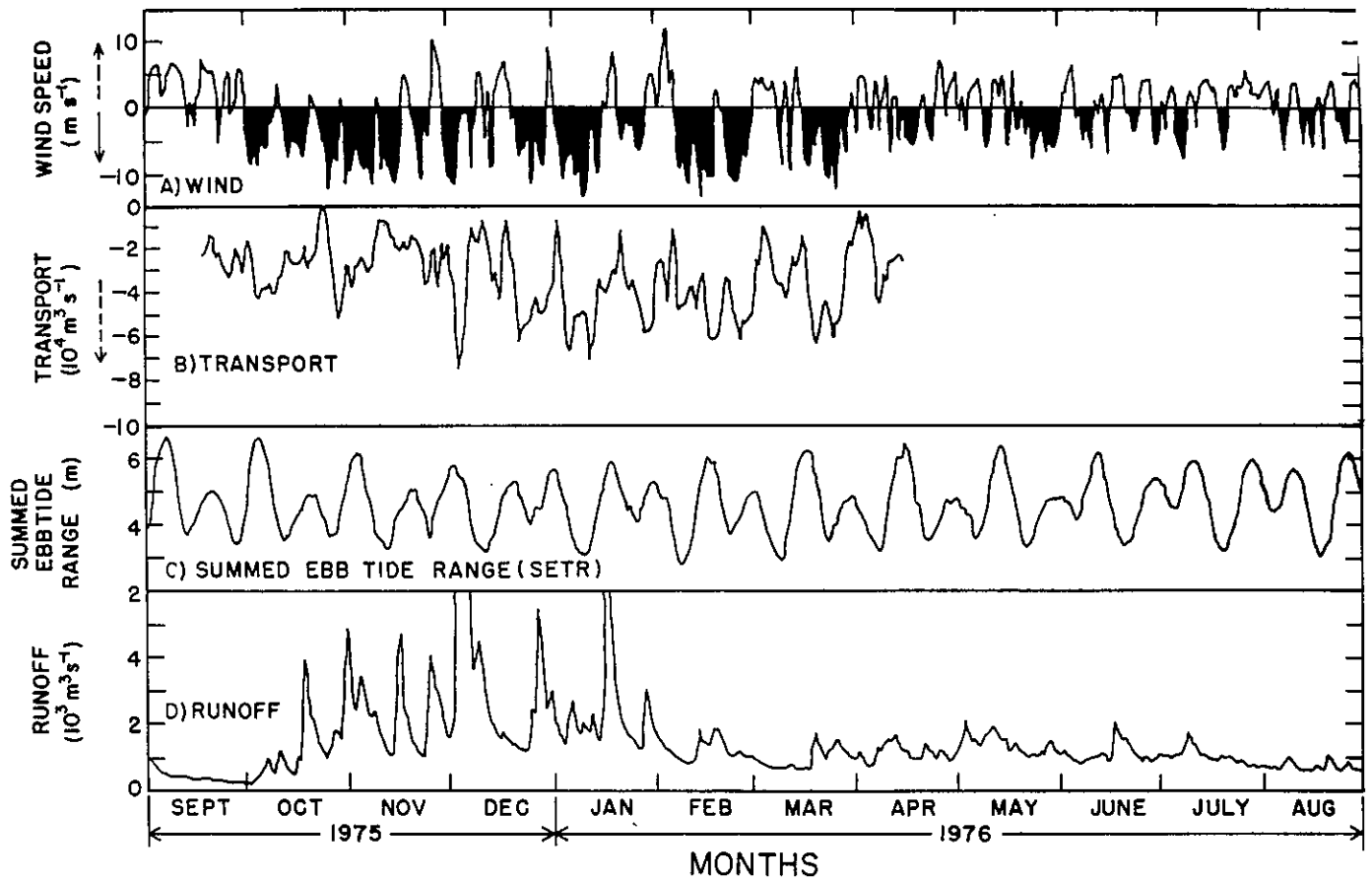


Figure 4.5. Daily values of: a) Net wind speed at West Point where darkened areas represent southerly winds; b) Net current in the depth range of 103-113 m at site 146 where negative represents currents directed toward $156\text{-}336^\circ\text{True}$, and hatching represents currents with values exceeding speeds of -10 cm s^{-1} ; c) summed ebb tide range (SETR) from tides observed at Seattle; and d) total runoff into Puget Sound. Data in panels (b) from Cox et al. (1983) and panels (a), (c), and (d) from Coomes et al. (1983). At left, the arrows denote the out-estuary (solid) and in-estuary (dashed) directions.

whereas there were large uncertainties for the constant and the dependence on SETR. To resolve the uncertainties the effects of wind and runoff were subtracted from the daily values of U_{100} using the coefficients listed in Table 4.3 and eq. (1). Then the remainders were grouped within 0.5 m intervals of SETR and the mean and 95% confidence intervals were computed in each group based on the t-distribution (Fig. 4.6).

The third regression was performed using the mean values of U_{100} versus SETR shown in Figure 4.6. The result was

$$U_{100} = (-2.3 - 1.1 \text{ SETR}). \quad (5)$$

where SETR is expressed in meters, U_{100} is expressed in cm s^{-1} , and the correlation coefficient ($r = 0.84$) is significant at the 1% level. Although the regression line does not pass through one of the 95% confidence limits, it appears that the dependence of U_{100} on SETR can be represented by the regression eq. (5).

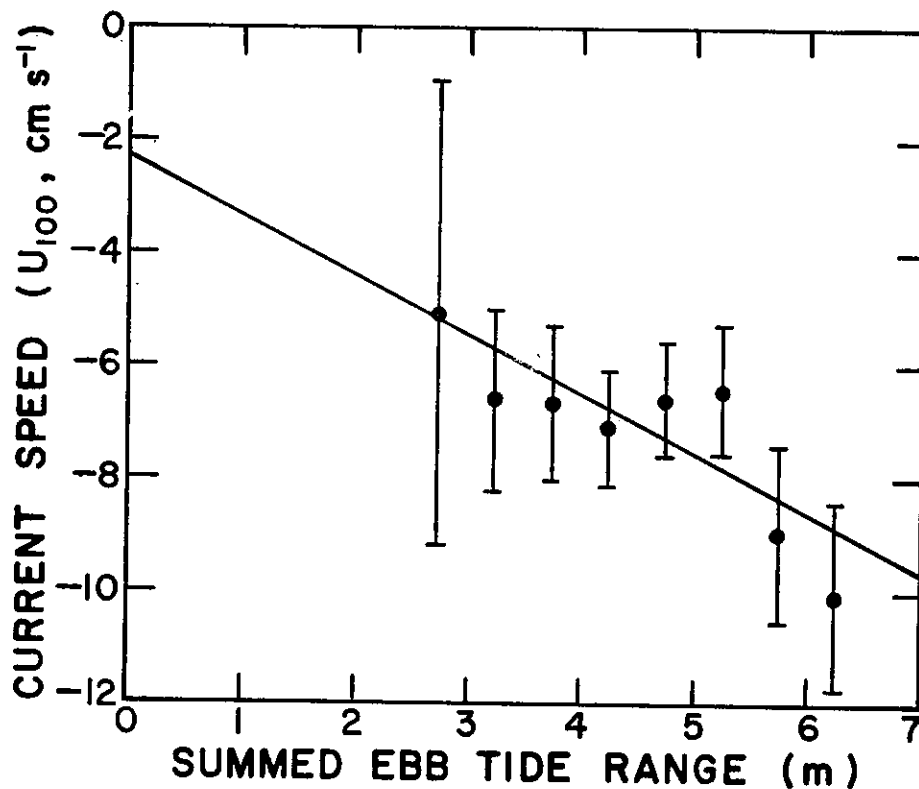


Figure 4.6. Current speed near 100 m depth (U_{100}) in the Main Basin's lower layer versus the sum of the ebb tide ranges (SETR) at Seattle. The bars represent the 95% confidence limits, and the line is the least-square-best-fit given by eq. (5).

The three experiments show that U_{100} and transport can be expressed as linear functions of SETR, wind, and runoff. The best estimates of the coefficients were combined in the following expression,

$$T = (-1.3 - 0.29 \text{ SETR} + 0.15 W - 1.2 \times 10^{-4} R) 10^4 \text{ m}^3 \text{ s}^{-1} \quad (6)$$

To compare the observed and model variance, eq. (6) was evaluated for 211 days during 17 September 1975-14 April 1976 and compared with the transports shown in Figure 4.5. Table 4.5 shows that the mean values of the model and observed transport are nearly identical, whereas the model variance equals only 38% of the observed variance. The remaining 62% of the variance may be compared with the uncertainty of estimating type- T_m transport as described below.

During 9 January-7 February 1973, Cannon and Ebbesmeyer (1978) estimated T_m -type transport at section 6 in both the upper and lower layers of the Main Basin (see Fig. 2.2). During this interval seven current meters were deployed between approximately the water surface (2 m depth; AMF current meter) and the bottom (193 m). The uncertainty may be found

TABLE 4.5. MEAN, STANDARD DEVIATION, AND VARIANCE OF THE OBSERVED TRANSPORT AND THE TERMS IN EQ. (6) COMPUTED FROM 211 DAILY VALUES DURING 17 SEPTEMBER 1975-14 APRIL 1976.

| Terms in eq. (6) | Mean ($10^4 \text{ m}^3 \text{ s}^{-1}$) | % of LHS total | Transport Std. dev. ($10^4 \text{ m}^3 \text{ s}^{-1}$) | Variance ($10^8 \text{ m}^6 \text{ s}^{-2}$) | % of LHS total |
|--------------------------------------|---|-------------------|---|---|-------------------|
| <u>Left hand side (LHS)</u> | | | | | |
| Total transport | -3.33 | | 0.97 | 0.94 | |
| <u>Right hand side</u> | | | | | |
| Constant | -1.30 | (39) | 0 | 0 | |
| Tidal pumping | -1.33 | (40) | 0.25 | 0.06 | (6) |
| Wind | -0.47 | (14) | 0.87 | 0.76 | (81) |
| Runoff | -0.22 | (7) | 0.20 | 0.04 | (4) |
| Total | -3.32 | (100) | 1.32 | 0.86 | (91) |
| <hr/> | | | | | |
| Observed transport (T_m -type) | -3.28 | | 1.57 | 2.46 | |

by comparing the transport in each layer with the average of the upper and lower layers. The difference computed each day had a variance of $0.08 \times 10^6 \text{ m}^6 \text{ s}^{-2}$, or approximately 5% of the variance unaccounted for by the regression model. Therefore most of the variance unaccounted for by eq. (6) cannot be explained by the uncertainty in estimating the transport.

The correlation coefficients obtained in the three statistical experiments were all significant at the 1% level; consequently it was of some interest to examine the coefficients, as well as determine the relative importance of the terms in eq. (6). The first term in eq. (6) is a constant transport in the Main Basin's lower layer which is directed inland. This term represents the transport associated with effects other than those of tide, wind, and runoff. The constant value may be deduced from experiments in the hydraulic model. Ebbesmeyer and Barnes (1980) found the transport in the Main Basin's upper layer in the absence of wind as well as tidal pumping by completely blocking The Narrows. They estimated a transport of $0.8 \times 10^4 \text{ m}^3 \text{ s}^{-1}$ which may be compared to the constant value of $1.3 \times 10^4 \text{ m}^3 \text{ s}^{-1}$. We speculate that this constant represents the transport associated with the classical estuarine mechanism wherein the mean circulation is driven only by mixing in the Main Basin.

The second term in eq. (6) represents the transport associated primarily with tidal pumping at The Narrows. The negative coefficient indicates that as SETR increases the transport directed inland also increases.

The third term in eq. (6) indicates that winds from the south act to increase the flow directed inland in the lower layer, whereas northerly winds act to retard the inland flow. The ratio of wind speed to the speed of U_{100} is 0.0057, i.e., a wind blowing from the south induces a steady southward current equal in speed to approximately 0.6% of the wind speed. Thus, winds induce appreciable currents at depth in the Main Basin, a result which is in qualitative agreement with a prediction from theoretical considerations by Rattray (1967) that appreciable currents due to winds extend to appreciable depths in fjords.

The fourth term in eq. (6) indicates that increased runoff acts so as to increase the flow inland in the Main Basin's lower layer.

Table 4.5 illustrates the relative importance of the four terms based on transport computed during 17 September 1975-14 April 1976. The computed mean transport consists of nearly equal contributions from the constant term (39%) and tidal pumping (40%), with minor contributions associated with wind (14%) and runoff (7%). In striking contrast, the computed variance consists primarily of the contribution associated with wind (81%), with minor contributions associated with tidal pumping (6%), runoff (4%), and 9% due to co-variations among the terms. Thus, whereas the constant and tidal terms dominate the mean transport, the wind dominates the fluctuations of the transport.

Figure 4.7 illustrates many of the results deduced earlier from the statistical computations. Shown are the terms from eq. (6) computed daily and compared with their sum and the observed transport. It is evident that

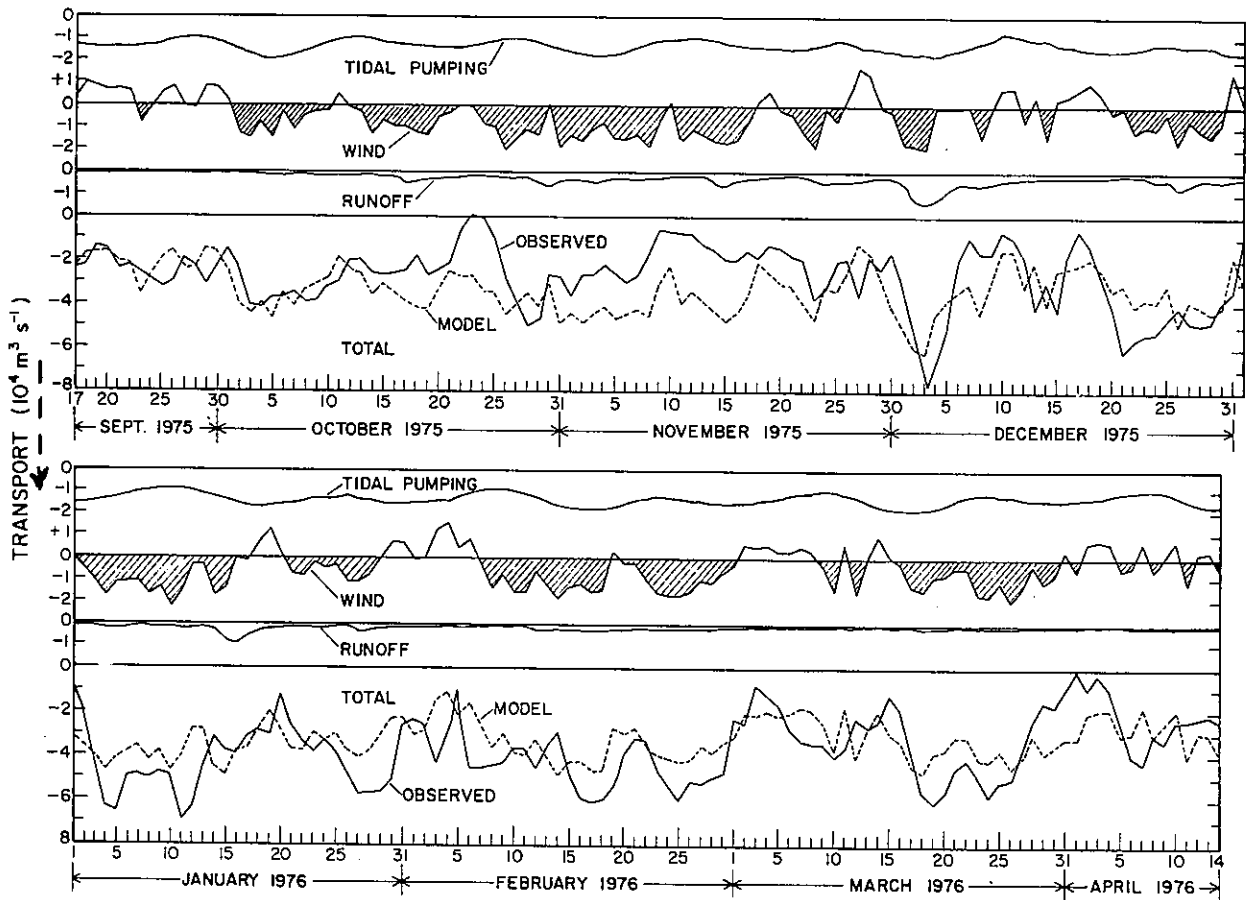


Figure 4.7. Daily estimates of transport computed from eq. (6) compared with transport (T_m -type) observed in the Main Basin's lower layer: top, September-December, 1975; bottom, January-April, 1976. Shown are the transport components associated with each term of eq. (6): on the right hand side of eq. (6), the terms associated with tidal pumping, wind, and runoff; and on the left hand side of eq. (6), the total transport (dashed) compared with the observed transport. Hatching denotes times when winds were directed from the south. Dashed arrow at left denotes inland direction.

the observed transport contains considerably more variance than the model transport, and that the two curves depart markedly at times. Despite these deficiencies, the correlation with wind is evident, and there are times when the two curves show reasonable agreement. However, the dependence on SETR is largely obscured within the overall variability.

4.3 SEASONAL CYCLE OF TRANSPORT

Earlier it was shown that approximately 14% of the transport variance occurs with seasonal periodicity. To examine the progression of transport through the year, monthly average values were computed from 16 records of U_{100} spanning an average of 28 days. Table 4.1 shows that the monthly average transport varies twofold between $1.9-4.1 \times 10^4 \text{ m}^3 \text{ s}^{-1}$ with a mean value of $2.8 \times 10^4 \text{ m}^3 \text{ s}^{-1}$. These observations indicate that the Main Basin's lower layer remains active through the year.

Figure 4.8 shows the values of monthly average transport combined into a composite year. The highest transport occurs during the winter (mean = $3.3 \times 10^4 \text{ m}^3 \text{ s}^{-1}$), and the lowest during the autumn (mean = $2.5 \times 10^4 \text{ m}^3 \text{ s}^{-1}$). The annual range between autumn and winter is $0.8 \times 10^4 \text{ m}^3 \text{ s}^{-1}$ which is significant at the 5% level and equivalent to approximately 28% of the annual average transport.

The seasonal progression of transport may be compared with a prediction based on eq. (6). To obtain the predicted values, monthly averages of SETR, wind speed, and runoff were substituted into eq. (6). Table 4.6 and Figure 4.8 shows the seasonal progression of the transport components associated with tide, wind, and runoff as well as the total transport. The predicted annual range is $0.7 \times 10^4 \text{ m}^3 \text{ s}^{-1}$, which is close to the observed range of $0.8 \times 10^4 \text{ m}^3 \text{ s}^{-1}$. Figure 4.8 shows that the range of the predicted seasonal cycle is largely controlled by the seasonal cycle of the wind.

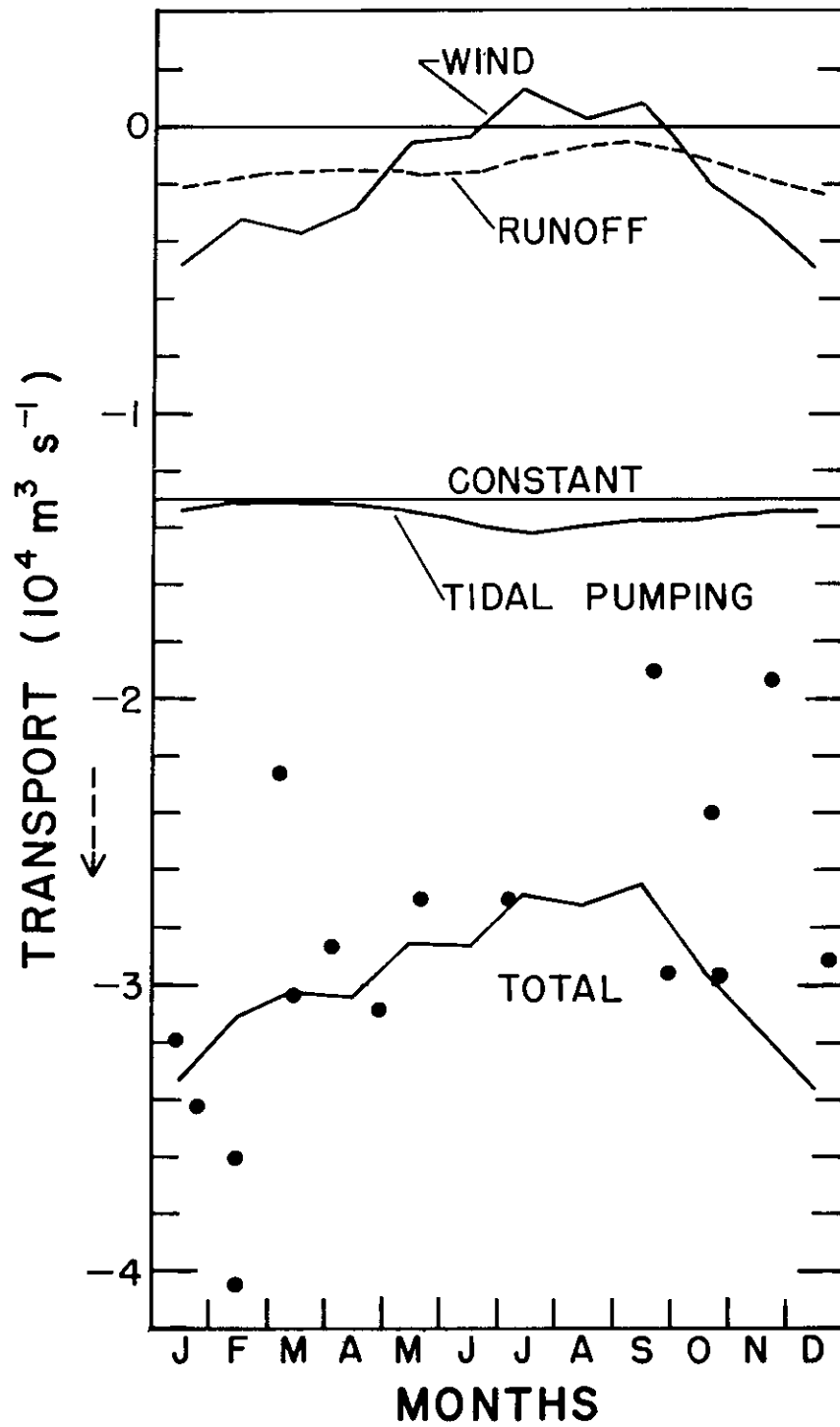


Figure 4.8. Monthly progression of transport. Dots show transport computed from observed currents (from Table 4.1), and lines show transport computed using eq. (6) (from Table 4.6). Dashed arrow at left indicates the inland direction.

TABLE 4.6. SEASONAL CYCLE OF TRANSPORT ESTIMATED USING EQ. (6). FROM LEFT TO RIGHT ARE THE FOUR COMPONENTS ASSOCIATED WITH: CONSTANT, TIDAL PUMPING, WIND, AND RUNOFF. SEE FIG. 4.8 FOR GRAPHICAL DISPLAY.

| Month | Constant ($10^4 \text{ m}^3 \text{ s}^{-1}$) | | Tidal Pumping ($10^4 \text{ m}^3 \text{ s}^{-1}$) | | Wind (m s^{-1}) | | Runoff ($10^4 \text{ m}^3 \text{ s}^{-1}$) | | Total Transport ($10^4 \text{ m}^3 \text{ s}^{-1}$) | |
|-----------|---|-------------|--|-------------|-------------------------------|-------------------|---|-------------------|---|--------------------|
| | Constant | SETR (m) | Mean Transport | SETR (m) | Mean wind | Mean Transport | Mean runoff | Mean Transport | Mean runoff | Total Transport |
| January | -1.3 | 4.61 | -1.34 | 4.61 | -3.0 | -0.48 | 1710 | -0.21 | 1710 | -3.33 |
| February | -1.3 | 4.50 | -1.31 | 4.50 | -2.0 | -0.32 | 1453 | -0.17 | 1453 | -3.10 |
| March | -1.3 | 4.54 | -1.32 | 4.54 | -2.3 | -0.37 | 1238 | -0.15 | 1238 | -3.02 |
| April | -1.3 | 4.56 | -1.32 | 4.56 | -1.7 | -0.27 | 1245 | -0.15 | 1245 | -3.04 |
| May | -1.3 | 4.63 | -1.34 | 4.63 | -0.3 | -0.05 | 1340 | -0.16 | 1340 | -2.85 |
| June | -1.3 | 4.74 | -1.38 | 4.74 | -0.2 | -0.03 | 1280 | -0.15 | 1280 | -2.86 |
| July | -1.3 | 4.85 | -1.41 | 4.85 | 0.8 | 0.13 | 809 | -0.10 | 809 | -2.68 |
| August | -1.3 | 4.78 | -1.39 | 4.78 | 0.2 | 0.03 | 464 | -0.06 | 464 | -2.72 |
| September | -1.3 | 4.72 | -1.37 | 4.72 | 0.5 | 0.08 | 478 | -0.06 | 478 | -2.65 |
| October | -1.3 | 4.71 | -1.37 | 4.71 | -1.2 | -0.19 | 805 | -0.10 | 805 | -2.96 |
| November | -1.3 | 4.66 | -1.35 | 4.66 | -2.0 | -0.32 | 1445 | -0.17 | 1445 | -3.14 |
| December | -1.3 | 4.61 | -1.34 | 4.61 | -3.1 | -0.50 | 1818 | -0.22 | 1818 | -3.36 |
| Mean | -1.3 | 4.66 | -1.35 | 4.66 | -1.2 | -0.19 | 1174 | -0.14 | 1174 | -2.98 |
| Range | 0 | 0.35 | 0.10 | 0.35 | 3.9 | 0.63 | 1354 | 0.16 | 1354 | 0.71 |

Monthly average data from: SETR - 1975-1976.
 Wind - 1969-1978.
 Runoff - 1930-1978.

5. REGIONAL VARIATIONS OF TRANSPORT AND TEMPORAL SCALES

Volume transport has been estimated at a number of locations in Puget Sound by several investigators (Friebertshauser and Duxbury, 1972; Cannon and Ebbesmeyer, 1978; Barnes and Ebbesmeyer, 1978; Hinchey, 1978; Ebbesmeyer and Barnes, 1980; and Cannon, 1983), as well as in section 4 of this study. Two useful perspectives, not previously available, can be obtained by summarizing the various estimates. First, the summary provides some indication of the regional variability of the transport. Second, the temporal scales of the circulation in the basins may be contrasted. Earlier, Barnes and Ebbesmeyer (1978) contrasted the transport in the Main and Whidbey basins; herein the contrast is extended to include Hood Canal and the Southern Basin.

5.1 REFLUXING IN ADMIRALTY INLET

In section 3, the observations of variance and water properties showed that strong vertical mixing occurs in Admiralty Inlet. One effect of the mixing is a net exchange of water between the upper and lower layers, i.e., some of the water flowing seaward in Admiralty Inlet's upper layer is mixed downward into its lower layer (Ebbesmeyer and Barnes, 1980). The mixing and refluxing in Admiralty Inlet provides a mechanism for recycling a fraction of the Main Basin's upper-layer water downward into its lower layer. The fraction can be estimated from an examination of water properties and volume transports as described below, keeping in mind that the volumes of the upper and lower layers are nearly equal.

Barnes and Ebbesmeyer (1980) estimated the fraction in two ways using historical observations of water properties. First, they examined temperature-salinity diagrams from hydrographic stations embracing Admiralty Inlet. The diagrams indicated that the Main Basin's lower layer consisted of approximately one-third exterior water from the lower layer in the inner Strait of Juan de Fuca and two-thirds water from the Main Basin's upper layer. Second, they examined the fraction using freshwater as a tracer. This computation appeared feasible because, on the average, the salinity in the Main Basin's lower layer changed inversely with the amount of freshwater exiting Puget Sound via Admiralty Inlet. A proportionality was evident between month-to-month changes in runoff and salinity, and between deviations of runoff and salinity from their long-term norms. Both approaches showed that approximately two-thirds of the Main Basin's upper layer was refluxed downward in Admiralty Inlet.

A third estimate can be obtained from an examination of the volume transports. Table 5.1 lists 23 estimates of transport made at 14 sections

TABLE 5.1. ESTIMATES OF VOLUME TRANSPORTS AT FOURTEEN CROSS SECTIONS IN PUGET SOUND (SEE FIG. 5.1).

| Cross-channel Section No. | Volume ^a transport (10 ⁴ m ³ s ⁻¹) | Data duration/type | Method ^b | Reference |
|---------------------------|---|---|---------------------|-----------------------------------|
| <u>Admiralty Inlet</u> | | | | |
| 1 | 1.3 | Historical water properties and runoff | 2 | Friebertshauer and Duxbury (1972) |
| 2 | 1.3 | Historical current measurements | 1,4 | Volume I Cox et al. (1983) |
| 3 | 2.0 ^c | 0.3 month/current measurements | 4 | Barnes and Ebbesmeyer (1978) |
| 3 | 2.0 ^c | ~1 month/current measurements | 4 | Cannon (1983) |
| 3 | 2.2 | Historical current measurements | 1,4 | Volume I Cox et al. (1983) |
| 4 | 1.2 | Historical current measurements | 1,4 | Present study |
| <u>Main Basin</u> | | | | |
| 5 | 2.8 | 1 day/current measurements | 4 | Barnes and Ebbesmeyer (1978) |
| 6 | 3.2 ^c | ~1 month/current measurements | 5 | Barnes and Ebbesmeyer (1978) |
| 6 | 3.2 ^c | ~1 month/current measurements | 5 | Cannon and Ebbesmeyer (1978) |
| 6 ^c | 2.7 | Historical dissolved oxygen measurements | 3 | Ebbesmeyer and Barnes (1980) |
| 6 | 2.9 | Historical current measurements | 1,4 | Volume I Cox et al. (1983) |
| <u>Colvos Passage</u> | | | | |
| 7 | 1.9 ^d | 0.3 month/current measurements | 1,5 | Barnes and Ebbesmeyer (1978) |
| 7 | 2.4 ^d | Historical measurements of currents and tides | 1,4 | Volume I Cox et al. (1983) |
| <u>The Narrows</u> | | | | |
| 8 | 0.3 | Historical water properties and runoff | 2 | Friebertshauer and Duxbury (1972) |
| 8 | 0.3 | Historical current measurements | 5 | Volume I Cox et al. (1983) |

TABLE 5.1 (CONTINUED).

| Cross-channel Section No. | Volume transport ($10^4 \text{ m}^3 \text{ s}^{-1}$) | Data duration/type | Method | Reference |
|---------------------------|--|--|--------|---|
| <u>Whidbey Basin</u> | | | | |
| 11 | 0.8 | Historical water properties and runoff | 2 | Friebertshauser and Duxbury (1972) |
| 10 | 0.2 | 0.6 months/current measurements | 5 | Barnes and Ebbesmeyer (1978) |
| 11 | 0.3 | Historical current measurements | 1,5 | Volume I Cox et al. (1983) |
| <u>Hood Canal</u> | | | | |
| 12 | 0.2 | Historical water properties and runoff | 2 | Friebertshauser and Duxbury (1972) |
| 12 | 0.5 | Historical current measurements | 1,5 | Present study |
| 13 | 0.2 | Historical dissolved oxygen measurements | 3 | Hinchey ^e (1978, unpublished) |
| 14 | 0.1 | Historical dissolved oxygen measurements | 3 | Hinchey ^e (1978, unpublished) |
| <u>Deception Pass</u> | | | | |
| 9 | 0.1 ^d | ~ 1 month/water level and current meter measurements | 6 | Collias et al. (1973) |

a Average transport in the upper and lower layers.

b Methods

- 1 Analysis of historical current meter measurements in Volume I.
- 2 Water budget study using historical water property data during 1965-1968.
- 3 Transport in the lower layer estimated using dissolved oxygen as a timed tracer. Analysis based on historical data collected during 1932-1975.
- 4 Transport estimated from at least three current meter stations across-channel made synoptically.
- 5 T_m -type transport estimate.
- 6 Estimate based on water level and current meter measurements.

c Data also used in present analysis.

d The flow top to bottom is directed out of the estuary.

e Unpublished analysis of historical measurements of dissolved oxygen in Hood Canal using method of Ebbesmeyer and Barnes (1980).

in Puget Sound based on this and previous investigations. If transport was estimated for both layers at a given section the average of the two values has been listed in Table 5.1. Figure 5.1 shows where the 23 transport estimates were made. If more than one estimate was available at a section, the average of the values listed in Table 5.1 has been shown in Figure 5.1.

The uncertainty of the transport estimates can be obtained from an examination of the individual estimates made at the same section. In Admiralty Inlet six estimates have been made at four cross sections (Table 5.1). In outer Admiralty Inlet, sections 1 and 2 are located sufficiently close together that the transport should be comparable. At section 1, Friebertshausen and Duxbury (1972) estimated the transport at monthly intervals using budgets of salt and freshwater; Table 5.1 shows the annual average value. At section 2, the transport was estimated from many observations of currents. Both methods gave an identical transport of $1.3 \times 10^4 \text{ m}^3 \text{ s}^{-1}$. At section 3, three estimates have been made; the range is $0.2 \times 10^4 \text{ m}^3 \text{ s}^{-1}$. Finally, at section 4, only a single estimate is available from the present study. The intercomparisons in Admiralty Inlet indicate that the uncertainty in transport is approximately $0.1 \times 10^4 \text{ m}^3 \text{ s}^{-1}$, or less than 10% of the mean transport.

At section 3, in central Admiralty Inlet, the transport is approximately $2.0\text{-}2.2 \times 10^4 \text{ m}^3 \text{ s}^{-1}$ which is anomalously large compared with values of $1.2\text{-}1.3 \times 10^4 \text{ m}^3 \text{ s}^{-1}$ to the north (sections 1, 2) and south (section 4). Section 3 lies immediately seaward of Hood Canal's entrance where the transport has been estimated to be $0.2\text{-}0.5 \times 10^4 \text{ m}^3 \text{ s}^{-1}$. Moreover, section 3 also lies in the basin located between Admiralty Inlet's inner and outer sills which are separated by a distance of approximately 35 km, or about one-third the Main Basin's length. We speculate that the anomalous value at section 3 is associated with the outflow from Hood Canal and with refluxing over Admiralty Inlet's sills.

Midway on the Main Basin's longitudinal axis five estimates of transport have been made at sections 5 and 6. At section 6, the transport computed in this study from the historical current meter records has an annual average of $2.9 \times 10^4 \text{ m}^3 \text{ s}^{-1}$ (Table 4.1). Ebbesmeyer and Barnes (1980) obtained an annual average transport of $2.7 \times 10^4 \text{ m}^3 \text{ s}^{-1}$ using differences in dissolved oxygen between the ends of the Main Basin. At section 5, a third estimate^a ($2.8 \times 10^4 \text{ m}^3 \text{ s}^{-1}$) was computed by Barnes and Ebbesmeyer (1978) using current observations made at three stations across-channel during a tidal day. The three estimates vary between $2.7\text{-}2.9 \times 10^4 \text{ m}^3 \text{ s}^{-1}$; the difference is less than 10% of the mean transport.

The transport has also been estimated at sections located in the junction between the Main and secondary basins (section 8, Southern Basin; section 11, Whidbey Basin; and section 12, Hood Canal). The estimates were made in two ways: first, Friebertshausen and Duxbury (1972) used

^aAt section 6, two other estimates were made by Barnes and Ebbesmeyer (1978); their data were included in the present analysis, and thus do not provide independent assessment of transport.

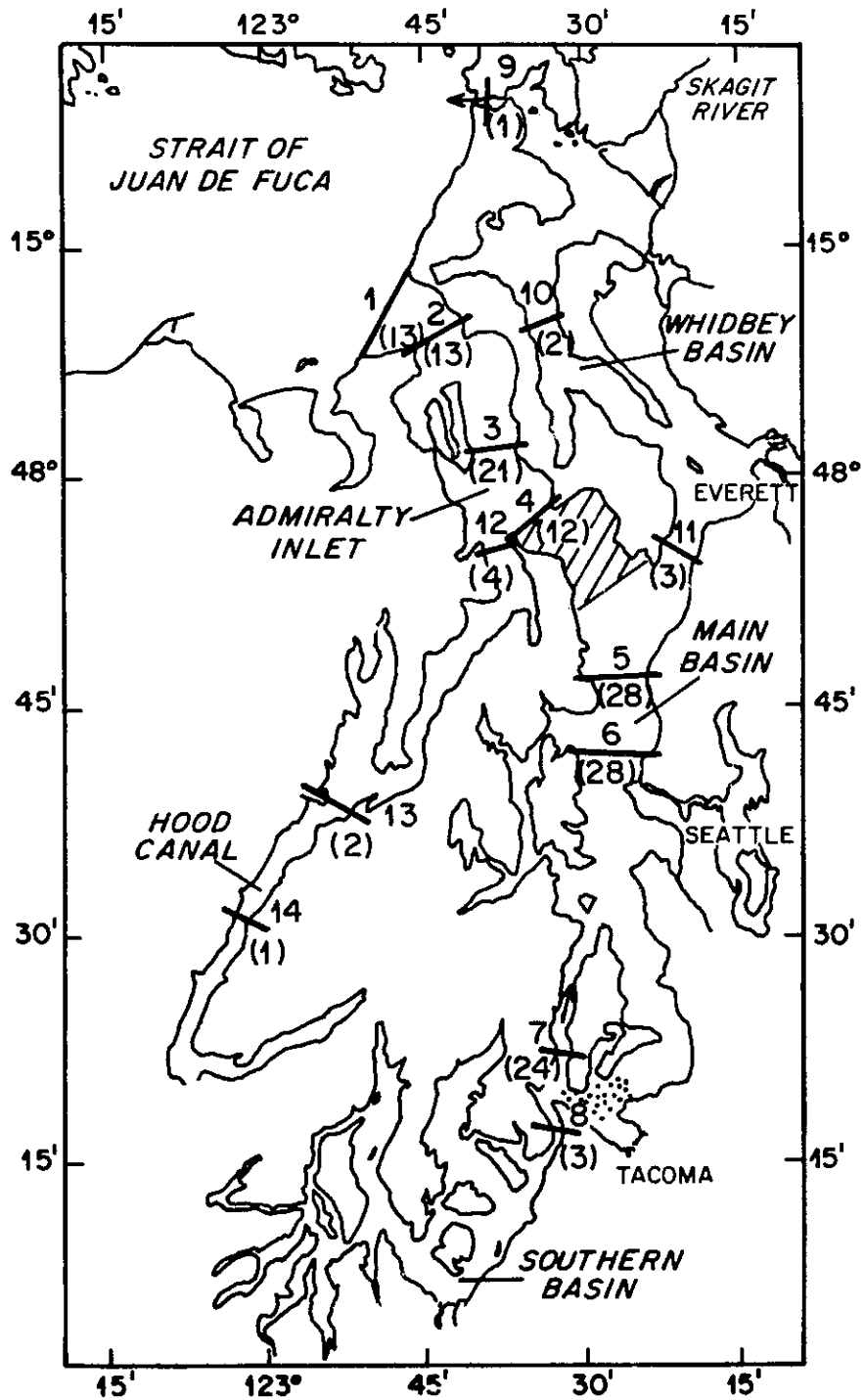


Figure 5.1. Sections (bars) where transport has been estimated in Puget Sound. The number above the bar indicates the section number, and the number below the bar in parenthesis indicates the transport in units of $10^3 \text{ m}^3 \text{ s}^{-1}$. The hatched and stippled areas at the northern and southern ends of the Main Basin indicate regions of intense downwelling and upwelling, respectively. See Table 5.1 for data and methods used to estimate the transport.

budgets of salt and freshwater; and second, the present study utilized the historical current meter records. The estimates lie in the range between $0.2-0.5 \times 10^4 \text{ m}^3 \text{ s}^{-1}$ except for an apparently large value of $0.8 \times 10^4 \text{ m}^3 \text{ s}^{-1}$ at the entrance to Whidbey Basin made by Friebertshauer and Duxbury (1972). They did not allow for freshwater exiting Whidbey Basin via Deception Pass, and as this loss is appreciable, it probably accounts for the larger estimate of transport. As a result, this value has not been used in further considerations.

Figure 5.1 and Table 5.1 show that within Puget Sound the transport is largest in the Main Basin. Earlier Barnes and Ebbesmeyer (1978) noted the order of magnitude difference in transport between the Main and Whidbey basins. Additional data show that in two^b of the secondary basins (Hood Canal and Whidbey Basin) and in the entrances to each of the secondary basins, the transport is an order of magnitude larger than in the Main Basin. It appears that the Main Basin's transport is tenfold longer than many other locations in Puget Sound.

The fraction of the water in the Main Basin's upper layer which is refluxed into its lower layer via Admiralty Inlet may be estimated using the transport computed across the following sections: at section 4 in Admiralty Inlet; section 6 in the Main Basin; and section 11 at the entrance to Whidbey Basin. The transport which enters Admiralty Inlet from the Main and Whidbey basins is approximately the sum of the transport through sections 6 and 11, or $3.2 \times 10^4 \text{ m}^3 \text{ s}^{-1}$. However, at section 4 in southern Admiralty Inlet a transport of only $1.2 \times 10^4 \text{ m}^3 \text{ s}^{-1}$ escapes seaward; the difference of $2.0 \times 10^4 \text{ m}^3 \text{ s}^{-1}$, or 0.63 apparently is refluxed downward and inland. This fraction is close to the previous estimate of 0.67 obtained by Ebbesmeyer and Barnes (1980).

Ebbesmeyer and Barnes (1980) did not differentiate where the refluxing might occur in Admiralty Inlet, whereas in the present study the transport estimates suggest that the refluxing takes place southward of section 4, or in the southern quarter of Admiralty Inlet (Fig. 5.1). In the center of this segment many hydrographic data have been taken. Observations reported by Ebbesmeyer and Barnes (1980) at this location showed a column of less dense water extending from surface to bottom; similar patterns have been noted by the authors in other observations. The repeated occurrence of this downwelling signature suggests a dynamic process in which surface water is carried to bottom in the southern end of Admiralty Inlet.

The summary of transport also leads to some refinement of the circulation diagram previously drawn by Ebbesmeyer and Barnes (1980). Figure 5.2 shows their diagram revised in two ways. First, the geometry of the pattern has remained essentially unchanged except for the downwelling in Admiralty Inlet; this has been redrawn to reflect the localized downwelling at the southern end of Admiralty Inlet. Second, the arrows have been revised so as to be roughly scaled according to transport. The result is a circulation in which the water moves vertically near the sill zones and horizontally between the sill zones.

^bNo estimate is available within the third secondary basin (Southern Basin).

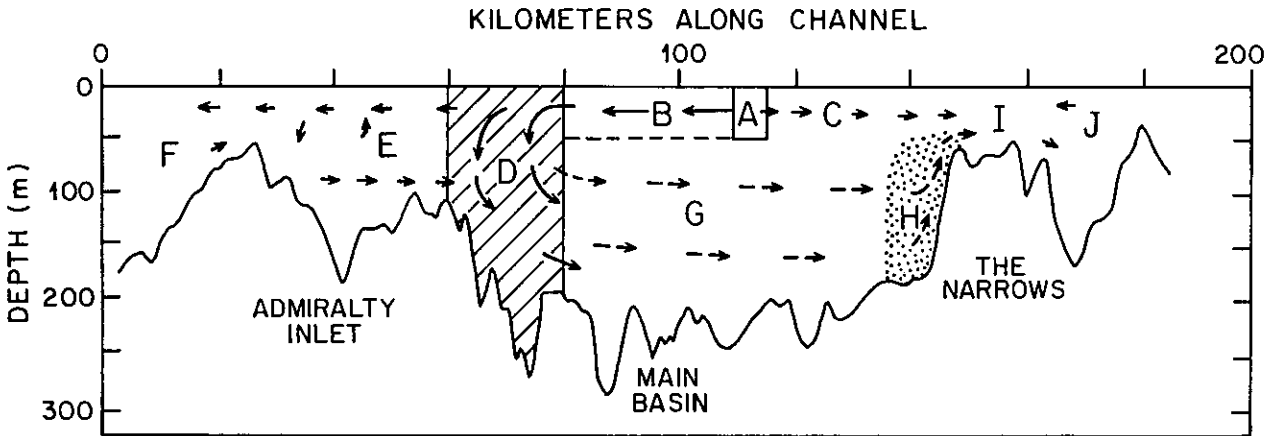


Figure 5.2. Schematic view of transport through Puget Sound's Main Basin. Arrows have been roughly scaled according to transport. Letter code: A, B, C, divergence from Colvos Passage (A) mostly into the Main Basin's upper layer (B) with some transport into East Passage (C); D, (hatched) zone of intense downwelling within inner Admiralty Inlet where most of Main Basin's upper layer (B; above dashed line) is refluxed into the lower layer (G); E, F, net transport in Admiralty Inlet (E) connecting to the Strait of Juan de Fuca (F); G, net transport in the Main Basin's lower layer; H, (stippled) zone of strong upwelling near The Narrows; I, J, intense vertical mixing (I) but small net transport through The Narrows connecting to the Southern Basin (J).

5.2 TEMPORAL SCALES OF CIRCULATION AND WATER PARCELS

The transport can be used to estimate the temporal scale associated with the circulation in Puget Sound's basins as well as the time that a water parcel might remain in Puget Sound.

The temporal scale of circulation was defined as a basin's volume divided by the transport in each layer. Table 5.2 lists the scales for the Main and secondary basins. These scales were computed using transport from near the mid-section of each basins except for the Southern Basin, where transport near its entrance was used. These computations show that the temporal scale in the Main Basin is approximately one month, whereas the scale for the secondary basins varies from 1.9 months (Southern Basin), to 5.4 months (Whidbey Basin), and to 9.3 months (Hood Canal). On the average, the temporal scale of the secondary basins is five to sixfold longer than for the Main Basin.

In the Main Basin the seasonal cycle of the temporal scale may be computed from the monthly estimates of transport (see section 4). Table 5.3 shows that the scale varies between 27 and 35 days with a mean value of 31 days, i.e., the scale fluctuates by approximately 13%. Thus, the Main Basin's temporal scale remains short throughout the year.

TABLE 5.2. TEMPORAL SCALES OF THE CIRCULATION IN PUGET SOUND'S BASINS. THE TEMPORAL SCALE EQUALS THE VOLUME DIVIDED BY THE TRANSPORT WHERE THE VOLUMES WERE COMPUTED BY MCLELLAN (1954); THE TRANSPORT FOR THE BASINS IS T_m -TYPE TRANSPORT ESTIMATED FROM TABLE 5.1.

| Basin | (1) Volume (km^3) | (2) Transport ($10^4 \text{ m}^3 \text{ s}^{-1}$) | (1/2) Temporal scale (months) |
|----------------|------------------------------------|---|--|
| Main Basin | 76.2 | 2.8 | 1.0 |
| Hood Canal | 24.4 | 0.1 | 9.3 |
| Whidbey Basin | 28.2 | 0.2 | 5.4 |
| Southern Basin | 15.0 | 0.3 ^a | 1.9 |

^aEstimated at the entrance to the Southern Basin.

TABLE 5.3. MONTHLY PROGRESSION OF THE MAIN BASIN'S TEMPORAL SCALE. THE SCALE EQUALS THE MAIN BASIN'S VOLUME DIVIDED BY TRANSPORT IN THE UPPER AND LOWER LAYERS. TRANSPORT IS FROM TABLE 4.6.

| Month | Transport ($10^4 \text{ m}^3 \text{ s}^{-1}$) | Temporal scale (days) |
|-----------|--|-----------------------------|
| January | -3.33 | 27.3 |
| February | -3.10 | 30.0 |
| March | -3.02 | 29.6 |
| April | -3.04 | 30.7 |
| May | -2.85 | 32.9 |
| June | -2.86 | 32.2 |
| July | -2.68 | 35.1 |
| August | -2.72 | 35.3 |
| September | -2.65 | 36.4 |
| October | -2.96 | 31.6 |
| November | -3.14 | 29.2 |
| December | -3.36 | 27.0 |
| Mean | -2.98 | 31.4 |

An important consideration is the time interval during which a substance may remain within Puget Sound. Estimating this scale is difficult because a substance can migrate through physical, chemical, biological, and geological cycles. While it was beyond the scope of this report to consider all these pathways, it was of some interest to compute, using simple models, the decay of a conservative substance (i.e., one which behaves as if dissolved within the parcel, and does not enter into other than the physical cycle).

In the models described below it was assumed that a substance was dissolved within a water parcel which follows simple trajectories through Puget Sound. Three trajectories of increasing complexity were considered:

In the first model the water parcel follows a trajectory through the Main Basin's circulation which has been represented in schematic fashion as a circle, where the upper and lower halves of the circumference correspond to the Main Basin's upper and lower layers, respectively (Fig. 5.3). The parcel travels around the circle in a month, or the average annual temporal scale of the circulation computed earlier. As the parcel descends from the upper to the lower layer in Admiralty Inlet, one-third of its mass escapes to the Strait of Juan de Fuca, and two-thirds is refluxed into the Main Basin's lower layer; the refluxed part of the parcel then continues in another traverse of the circle. After n months or traverses, the fraction of the parcel equalling $(0.67)^n$ remains in the Main Basin (Fig. 5.4).

The second model builds on the first by attaching secondary basins to the Main Basin. The secondary basins have been represented collectively as another circle joined to the first circle, i.e., the Main Basin (Fig. 5.3). As the parcel passes the junction between the Main and secondary basins, 0.33 of its mass is diverted into the secondary basins and 0.65 remains in the Main Basin; it has been assumed that refluxing does not occur in the junction between the Main and secondary basins. The fraction 0.33 was chosen as approximately the ratio of the total transport ($1 \times 10^4 \text{ m}^3 \text{ s}^{-1}$) diverted from the Main Basin into the secondary basins to the annual average transport ($2.9 \times 10^4 \text{ m}^3 \text{ s}^{-1}$) in the Main Basin. The temporal scale in the secondary basins was taken as approximately the average of the secondary basins or five months shown in Table 5.2. While the parcel traverses the Main Basin five times, three of its daughter parcels migrate into the secondary basins. After the first five months one of the daughter parcels emerges from the secondary basins and rejoins the parent parcel in the Main Basin.

The third model has the added complexity of refluxing in the junction between the Main and secondary basins (Fig. 5.3). The refluxing was assumed to operate similarly to that in Admiralty Inlet, i.e., as a daughter parcel emerges from the secondary basins a portion escapes to the Main Basin and a fraction returns so as to repeat the trajectory in the secondary basins. For this exercise the fraction was chosen as 0.50. The actual fraction varies between the basins: a small value probably occurs at the entrance to Whidbey Basin, which lacks an entrance sill; an intermediate value may occur at the entrance to Hood Canal where the variance is comparatively low for a sill zone; and a large value may occur at the entrance to the Southern Basin where the water is mixed top-to-bottom.

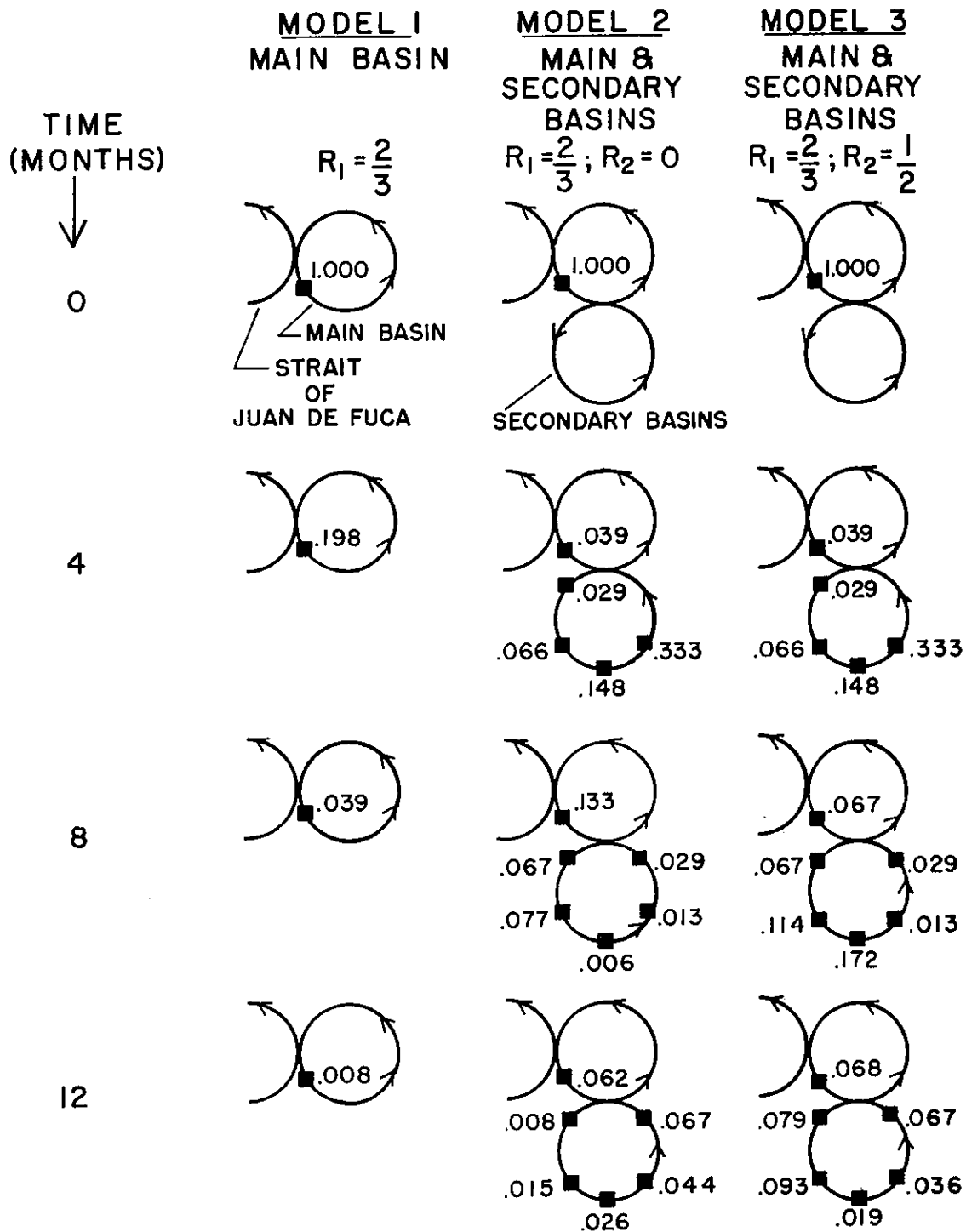


Figure 5.3. The fraction of a water parcel remaining in Puget Sound shown at four month intervals during a hypothetical year. From left to right are results for the three models: Model 1, circulation in the Main Basin; Model 2, circulation in the Main and secondary basins with no refluxing in at their junction; and Model 3, circulation in the Main and secondary basins with refluxing at their junction. The box in the Main Basin at time = 0 months (top) represents the water parcel; at later times the boxes represent fractions (numbers) of the original parcel remaining in Puget Sound's basins. Refluxed fractions: R_1 , the fraction (0.667) in Admiralty Inlet; and R_2 , the fraction (0, or 0.50) in the junction between the Main and secondary basins.

Figure 5.3 shows the positions of the parcel and its daughters at selected times in the three models. Figure 5.4 shows the fraction of the parcel which remains in Puget Sound during a year. It can be seen that, with the addition of the secondary basins, the decay time markedly increases compared with decay without the secondary basins. Moreover, the fraction remaining in Puget Sound at the end of a year appears sizeable and depends on the refluxing between the Main and secondary basins.

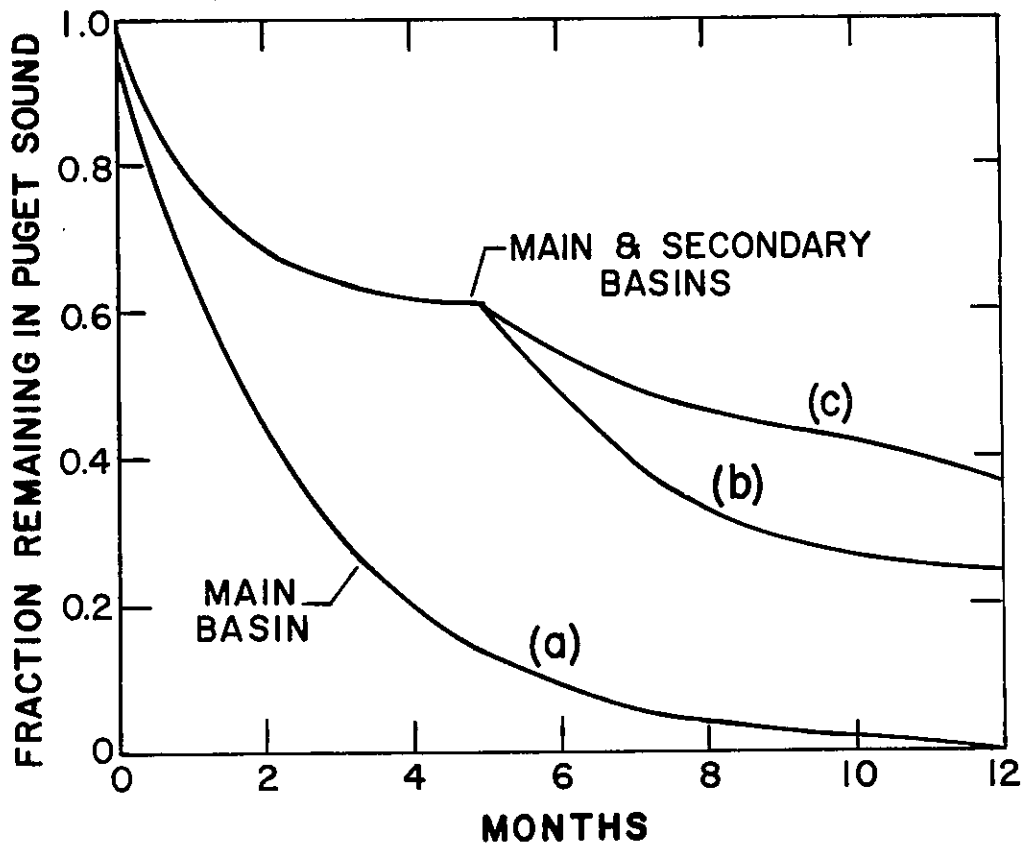


Figure 5.4. The fraction of a water parcel remaining in Puget Sound during a hypothetical year. Results of the three models are shown: a) Main Basin only with $\frac{2}{3}$ refluxing in Admiralty Inlet; b) Main and secondary basins with $\frac{2}{3}$ refluxing in Admiralty Inlet and no refluxing between the Main and secondary basins; and c) Main and secondary basins with $\frac{2}{3}$ refluxing in Admiralty Inlet and $\frac{1}{2}$ refluxing between the Main and secondary basins. The fraction shown in (b) and (c) represent the total of the amounts shown in Figs. 5.3 (models 2 and 3).

6. CONCLUSION

The observations of currents made in Puget Sound and approaches during many years (1908-1980) were combined and analyzed. The historical observations of water properties have been examined previously, but a parallel exploration of the historical current meter records had not been undertaken.

The conclusions drawn from the present analysis are summarized below.

6.1 MEAN CURRENT PATTERNS

The patterns of mean currents were examined in the Strait of Juan de Fuca and Puget Sound by constructing maps of the horizontal flow in the upper portion of the water column, and by constructing vertical profiles of mean currents in 23 sub-regions. In nearly all of the regions the mean flow was sufficiently fast that it could be detected in the historical records. The flow is two-layered in most regions, either in constrictions (Deception Pass; Balch Passage) or in channels connecting the constrictions (East Passage between The Narrows and the northern end of Colvos Passage; along the western shore of Whidbey Island between Rosario Strait and Admiralty Inlet). The flows between the constrictions extend over considerable distances (approximately 30 km), and the flow along Whidbey Island provides a comparatively direct route for the exchange of freshwater and other substances between the Strait of Georgia and Puget Sound.

6.2 VARIANCE

To examine the fluctuation of currents about the mean, we determined the distribution of variance along Puget Sound's three major branches: Main, Whidbey, and Hood Canal. The variance in the sill zones was found to greatly exceed that in the adjacent basins. In the three most energetic sill zones (Deception Pass, Admiralty Inlet, and The Narrows) the variance is approximately $10^4 \text{ cm}^2 \text{ s}^{-2}$ due mostly to tidal currents, and is sufficient to mix water vertically to near homogeneity.

6.3 TEMPORAL VARIABILITY IN THE MAIN BASIN

At one location in the Main Basin's lower layer, currents were observed during sixteen months in selected years between 1972-1977. Most (86%) of

the variance occurred with periods of several days to a month, whereas the remaining variance (14%) occurred with seasonal periods.

To explore the causes of variance, multiple regressions were computed between transport and tidal range, wind speed, and runoff. Significant correlations (at the 1% level) were found which accounted for approximately 38% of the observed variance. The regression coefficients indicated that the mean transport consists primarily of a constant value (39%) and a nearly equal contribution (40%) associated with tidal range, with small mean transports associated with wind and runoff. In contrast, most (81%) of the transport variance is associated with winds; moreover, the regression coefficient shows that winds acting at the water surface induce currents at 100 m depth equivalent on the average to 0.6% of the wind speed.

The seasonal cycle of transport in the Main Basin's lower layer was found to fluctuate between a high of $3.3 \times 10^4 \text{ m}^3 \text{ s}^{-1}$ in winter to a low of $2.5 \times 10^4 \text{ m}^3 \text{ s}^{-1}$ in autumn. The range of $0.8 \times 10^4 \text{ m}^3 \text{ s}^{-1}$ is significant at the 5% level and is equivalent to a quarter of the average annual transport of $2.9 \times 10^4 \text{ m}^3 \text{ s}^{-1}$.

6.4 VARIATIONS OF TRANSPORT AND TIME SCALES BETWEEN PUGET SOUND'S BASINS

The estimates of volume transport^a made in Puget Sound's Main and secondary (Whidbey, Hood Canal, and Southern) basins were contrasted. The contrast showed that the Main Basin's transport was an order of magnitude larger than in the entrance to the secondary basins and in two of the secondary basins (Hood Canal and Whidbey Basin; transport in the Southern Basin remains undetermined).

The regional contrast also showed that two-thirds of the transport in the Main Basin's upper layer is downwelled at the southern end of Admiralty Inlet, and returns inland in the Main Basin's lower layer. A diagram of the mean circulation in the Main Basin resembles a convective cell where the upwelling and downwelling are concentrated near the sill zones.

The temporal scale of a basin was defined as the basin's volume divided by the transport. The scales in the secondary basins ($\frac{1}{2}$ year) were found to be on the average sixfold longer than in the Main Basin (1 month). In the Main Basin the temporal scale, as computed from monthly transport estimates, varied between 27-35 days; thus the Main Basin remains quite active throughout the year.

The length of time which an instantaneous release of a conservative substance might remain in Puget Sound was estimated using several simple models. The models incorporate the temporal scales of the basins as well as the refluxing between the Main and secondary basins. For the Main Basin without secondary basins, nearly all of the substance escapes after

^aComputed separately in the upper and lower layers.

one year, whereas with the addition of secondary basins approximately a third of the substance remains in Puget Sound after a year. The mismatch in the temporal scales, as well as the refluxing in the sill zones between the basins, causes a feedback of the substance which in turn leads to a long flushing time for Puget Sound.

ACKNOWLEDGEMENTS

We thank Robert N. Dexter, Jerry A. Galt, James R. Holbrook, and Ronald P. Kopenski for valuable criticism; James R. Holbrook for kindly supplying data for the Strait of Juan de Fuca; Richard N. Cromoga, Donald M. Doyle, Paul J. Ebbesmeyer, Noel B. McGary, and Terry L. Storms for drafting the figures; and Linette G. Durham, Susan B. Stanton, and Bruce J. Titus for assisting with the computations. This work was performed under contract No. NA80RAC00074 from the National Oceanic and Atmospheric Administration.

REFERENCES

- Barnes, C.A., and E.E. Collias. 1956. Physical and chemical data for Puget Sound and approaches, January-December 1954. University of Washington Department of Oceanography. Technical Report No. 46. 259 pp.
- Barnes, C.A., and C.C. Ebbesmeyer. 1978. Some aspects of Puget Sound's circulation and water properties. In: Estuarine Transport Processes (B. Kjerfve, ed.), University of South Carolina Press, Columbia, South Carolina. pp. 209-228.
- Barnes, C.A., J.H. Lincoln, and M. Rattray, Jr. 1957. An oceanographic model of Puget Sound. Proceedings of the Eighth Pacific Science Congress III, 686-704.
- Barrick, D.E., M.W. Evans, and B.L. Weber. 1977. Ocean surface currents mapped by radar. Science 198 (4313):138-144.
- Cannon, G.A., ed. 1978. Circulation in the Strait of Juan de Fuca; some recent oceanographic observations. NOAA Technical Report ERL 399-PMEL 29. 49 pp.
- Cannon, G.A., and C.C. Ebbesmeyer. 1978. Some observations of winter replacement of bottom water in Puget Sound. In: Estuarine Transport Processes (B. Kjerfve, ed.), University of South Carolina Press, Columbia, South Carolina. pp. 229-238.
- Cannon, G.A., and N.P. Laird. 1978. Variability of currents and water properties from year-long observations in a fjord estuary. In: Hydrodynamics of Estuaries and Fjords (J.C.J. Nihoul, ed.). Elsevier Scientific Publishing Company, Amsterdam. pp. 515-535.
- Cannon, G.A. 1983. Variability of currents and water properties. To be in: Puget Sound. Oceanography of the inshore waters of Washington (D. Henry, ed.). University of Washington Press (revised and accepted).
- Collias, E.E. 1970. Index to physical and chemical oceanographic data of Puget Sound and its approaches, 1932-1966. University of Washington Department of Oceanography Special Report No. 43.

- Collias, E.E., C.A. Barnes, and J.H. Lincoln. 1973. Skagit Bay dynamical oceanography, final report. University of Washington Department of Oceanography Reference M73-73.
- Collias, E.E., and J.H. Lincoln. 1977. A study of the nutrients in the Main Basin of Puget Sound. University of Washington Department of Oceanography Reference M77-2.
- Collias, E.E., N. McGary, and C.A. Barnes. 1974. Atlas of physical and chemical properties of Puget Sound and its approaches. Washington Sea Grant Publication, University of Washington Press, Seattle, Washington. 235 pp.
- Coomes, C.A., C.C. Ebbesmeyer, J.M. Cox, J.M. Helseth, L.R. Hinchey, G.A. Cannon, and C.A. Barnes. 1983. Synthesis of current measurements in Puget Sound, Washington. Volume 2. Indices of mass and energy inputs into Puget Sound: runoff, air temperature, wind, and sea level.
- Cox, J.M., C.C. Ebbesmeyer, C.A. Coomes, J.M. Helseth, L.R. Hinchey, G.A. Cannon, and C.A. Barnes. 1983. Synthesis of current measurements in Puget Sound, Washington. Volume 1. Index to current measurements made in Puget Sound from 1908-1980 with daily and record averages for selected measurements.
- Crean, P.B. 1978. A numerical model simulation of barotropic mixed tides in the Strait of Georgia. In: Hydrodynamics of estuaries and fjords (J. Nihoul, ed.). Elsevier Scientific Publication Co., Amsterdam, Elsevier Oceanography Series #23, 283-313.
- Ebbesmeyer, C.C., J.M. Cox, J.M. Helseth, L.R. Hinchey, and D.W. Thomson. 1979. Dynamics of Port Angeles Harbor and approaches, Washington. National Oceanic and Atmospheric Administration EPA-600/7-79-252. 107 pp.
- Ebbesmeyer, C.C., and C.A. Barnes. 1980. Control of a fjord basin's dynamics by tidal mixing in embracing sill zones. Estuarine and Coastal Marine Science 11:311-330.
- Farmer, H.G., and M. Rattray, Jr. 1963. A model of the steady-state salinity distribution in Puget Sound. University of Washington Department of Oceanography Technical Report 85. 33 pp.
- Friebertshauser, M.A., and A.C. Duxbury. 1972. A water budget study of Puget Sound and its subregions. Limnology and Oceanography, 17:237-247.
- Frisch, S. 1980. HF radar measurements of circulation in the eastern Strait of Juan de Fuca near Protection Island (July 1979). Environmental Protection Agency Technical Report EPA-600/7-80-129. 133 pp.

- Geyer, W.R., and G.A. Cannon. 1982. Sill processes related to deep water renewal in a fjord. *Journal of Geophysical Research*, 87(10):7985-7996.
- Hinchey, L.R. 1979. Some estimates of net currents and transports in Hood Canal and Dabob Bay. Unpublished manuscript. 21 pp.
- Holbrook, J.R., R.D. Muench, D.G. Kachel, and C. Wright. 1980. Circulation in the Strait of Juan de Fuca: Recent oceanographic observations in the Eastern Basin. NOAA Technical Report ERL 412-PMEL 33. 42 pp.
- Larsen, L.H., N. Shi, and J.G. Dworski. 1977. Current meter observations in Colvos Passage: Puget Sound, March 1977. Department of Oceanography University of Washington, Seattle, Special Report No. 82, 10 pp. and plates.
- McLellan, P.M. 1954. An area and volume study of Puget Sound. University of Washington Department of Oceanography Technical Report No. 21. 39 pp.
- Parker, B.B. 1977. Tidal hydrodynamics in the Strait of Juan de Fuca - Strait of Georgia. NOAA Technical Report NOS-69. 56 pp.
- Rattray, M., Jr. 1967. Some aspects of the dynamics of circulation in fjords. In: *Estuaries* (G.H. Lauff, ed.), AAAS Publication 83, American Association for the Advancement of Science, Washington, D.C., pp. 52-62.
- Rattray, M. Jr., and J.L. Lincoln. 1955. Operating characteristics of an oceanographic model of Puget Sound. *Transactions of the American Geophysical Union*, 36:251-261.
- Snedecor, G.W., and W.G. Cochran. 1967. *Statistical Methods*. Iowa State University Press, Ames, Iowa. 593 pp.
- Sverdrup, H.U., M.W. Johnson, and R.H. Fleming. 1942. *The oceans, their physics, chemistry, and general biology*. Prentice-Hall, Inc., Englewood Cliffs, New Jersey. 1087 pp.
- Thomson, R.E. 1981. Oceanography of the British Columbia coast. Canadian special publication of fisheries and aquatic sciences 56. 291 pp.